The effects of part orientation and fluid flow on heat transfer around a cylinder.

By:

Darrell Rondeau

A Thesis

Submitted to the Faculty

of the

Worcester Polytechnic Institute

In partial fulfillment of the requirements for the

Degree of Master

in

Materials Science and Engineering

By

_____

May 6, 2004

APPROVED:

_____

Richard D. Sisson Jr. Advisor, Professor of Mechanical Engineering
Materials Science and Engineering Program Head

Abstract

The effects of quenchant flow around a 4140 steel cylinder have been experimentally investigated. An apparatus was developed to repeatably immerse a two inch diameter by eight inch long probe into an agitated quench tank. The probes were normalized prior to quench to relieve any residual stresses. Distortion, residual stress and hardness were experimentally measured. The results verified that there was a variation of cooling rate in respect to quenchant flow around the cylinder. The data showed that there was a higher cooling rate nearest to the quenchant flow versus a much lower cooling rate away from the flow. Computational fluid dynamics are also presented to give insight into the behavior of the quenchant flow in the tank and around the cylinder.

Acknowledgements

I would like to thank Professor Richard Sisson for his help and motivation on this project, as well his insight into the real world. I owe a great deal of gratitude to the Center for Heat Treating Excellence, for without the center this project may never have been created. I would also like to thank everyone in the graduate office for their patience and friendship while I worked on this project.

A great deal of thanks must go to the gentlemen in the machine shops here at WPI, Todd Billings, Steve Derosier, Robert Taylor, and William Weir have been a wonderful resource, and good friends.

Lastly but certainly not forgotten I must thank my family for their unconditional support and enthusiasm.

Table of Contents

List of Figures

List of Tables

1.0 Introduction

The process of quenching steel refers to the rapid cooling from an austenitizing or solutionizing temperature to a significantly cooler temperature [1]. For steel this refers to heating into the austenite phase field, typically to 845°C for 4140 steel, and then rapidly cooling to a temperature below the martensite finish temperature. The purpose of quenching steel is to produce the martensitic phase that is hard and strong, while minimizing distortion and residual stress. These steels need to be tempered after quenching to increase the toughness. Due to the demand for hardened steel parts an understanding of the mechanisms of distortion and residual stress development is necessary. Further research has been conducted at the Center for Heat Treating Excellence at Worcester Polytechnic Institute [2,3,4,5,6]

The most widely used practice of quenching is referred to as direct quenching [1]. Direct quenching involves quenching the part directly from the austenitizing temperature. This can be accomplished by immersion in different types of media (i.e. oil, water, polymer solutions, etc.). The media selected is dependant on the cooling rated desired. Agitation is also a key parameter that influences the cooling rate [7].

In commercial heat treating it is necessary to achieve the desired mechanical properties while maintaining the dimensional tolerances. The mechanisms involved in hardening and distortion are discussed in this thesis. Two aspects to note about the distortion associated with quenching are:

- Steel has a higher strength when cold than when hot
- Steel shrinks while cooling but expands during martensite formation

Coupled with distortion is residual stress development. The manner by which stress is generated during a quench is complex and the stress obtained is the net effect of the combination of several processes [8]. There are three different mechanisms that are coupled during the quenching of steel, temperature effects, phase transformations, and stress/strain development [9]. Thermal stress generation arises from the temperature gradients formed because it is difficult to cool the part uniformly. There is heat released during the work done in deformation. Phase transformations are a temperature dependant function. There is an associated heat release with phase transformation. There is a volume change during phase transformation causing stress, and the transformation kinetics are effected by stress state.

In order to understand what is going on inside the quench tank computational fluid dynamics have been employed. With the help of Michael Stratton using Fluent 6.0 it was possible to model the tank and probe setup. By using experimental data of the quenchant flow obtained with a turbine flow meter, and measured densities and viscosities of the quench fluid it was possible to determine the velocities and flow trends within the tank.

It is the goal of this project to understand how part orientation with respect to quenchant flow influences distortion, and residual stress generation in 4140 steel. Experiments were conducted using a 2” diameter x 8” long 4140 probe. The probe was heated in an atmosphere of argon and subsequently quenched normal or at 45 degrees to the surface with horizontal agitation. Along with empirical investigation of distortion, residual stress and hardness, computational fluid dynamics has been employed to determine how the flow around the part influences heat transfer.

Distortion and residual stress were measured at four points around the probe. Distortion was measured with a Coordinate Measuring Machine. The residual stress was measured using an X'Pert X – Ray Diffractometer System at Philips PANalytical, in Natick, MA. The hardness measurements were preformed both longitudinally and in the transverse direction to give insight to the formation of martenstite with respect to quenchant flow.

2.0 Literature Review

2.1 Fundamentals of Quenching

The commercial heat treating of carbon and alloy steels consists of three stages, austenitizing, quenching and tempering. For quench hardening of carbon and alloy steels austenitizing is accomplished by heating the material into the appropriate temperature range where it becomes austenitic. Once the steel is austenitic it is rapidly cooled, typically by immersion in water, oil, polymer solution, salt bath, or high pressure gas [10]. In steel the rapid cooling from the austenite phase produces a hard martensite phase. The degree of hardness and depth of hardness depend on cooling rates and the alloy of the steel. Some ferrous materials must be cooled very rapidly from their austenitizing temperatures to harden significantly because of their low hardenablility (ie. SAE 1050 steel), while some steels can quenched slowly and become fully hardened (ie. SAE 8660). [11, 12].

The stage of prime importance is quenching. In this stage is where the majority of the transformations occur. Various methods of quenching are available depending on the desired outcome. Different methods of quenching include but not limited to: Direct quenching, Time quenching, Selective quenching, Spray Quenching and Gas quenching [11].

1. *Direct quenching* is a process of direct cooling of the metal from the austenitizing temperature to ambient temperature. This is the most commonly used method for quenching. This process is also used for various metals that have undergone a solutionizing treatment [11].

2. *Time quenching* involves the cooling of the part with two or more different cooling rates. This method uses one cooling rate to cool the part below the nose of the TTT curve and then incorporates a different cooling rate to obtain the desired properties. Time quenching is normally used to minimize distortion and cracking associated with rapid cooling through the martensite transformation region [11].
3. *Selective quenching* involves cooling of specific areas of a part to produce desired properties of that section. This is accomplished by insulating the remainder of the part to shield it from the quenching medium [11].
4. *Spray quenching* uses a pressurized stream to quench the part. Cooling rates associated with spray quenching are normally very high. The velocity of the stream allows for removal of bubbles and breaks down any vapor that can be associated with the vaporization of the quench medium [11].

After quenching, tempering treatments are used to create desired mechanical properties. The process of tempering includes reheating the hardened steel to some temperature below the eutectoid temperature to decrease the hardness and/or increase the toughness. [10]

2.2 Quenching and Its Stages [13]

"Heat Treatment can be defined as an operation or combination of operations involving the controlled heating and cooling of a metal in the solid state for the purpose of obtaining specific properties"[14].

As one of the most important heat treatment processes, quenching of steel refers to the cooling from the solution treating temperature, typically 845-870˚C (1550-1600˚F),

into the hard structure-martensite [1]. Quenching is typically performed to prevent ferrite or pearlite formation and to facilitate bainite or martensite formation [1]. After quenching, the martensitic steel is tempered to produce the optimum combination of strength, toughness and hardness. For a specific steel composition and heat treatment condition, there is a critical cooling rate for full hardening at which most of the high temperature austenite is transformed into martensite without the formation of either pearlite or bainite[14].

As the steel is heated it absorbs energy that is later dissipated by the quenchant in the quenching process. It is important to understand the mechanisms of quenching and the factors that affect the process since these factors can have a significant influence on quenchant selection and the desired performance obtained from the quenching process. The shape of a cooling curve is indicative of the various cooling mechanisms that occur during the quenching process. For the liquid quenchants like water and oil, cooling generally occurs in three distinct stages, film boiling, nucleate boiling and convection stages, each of which has different characteristics. Figure 2.1 shows the cooling and cooling rate curves during the quenching process and the phenomena that occur during these three stages.

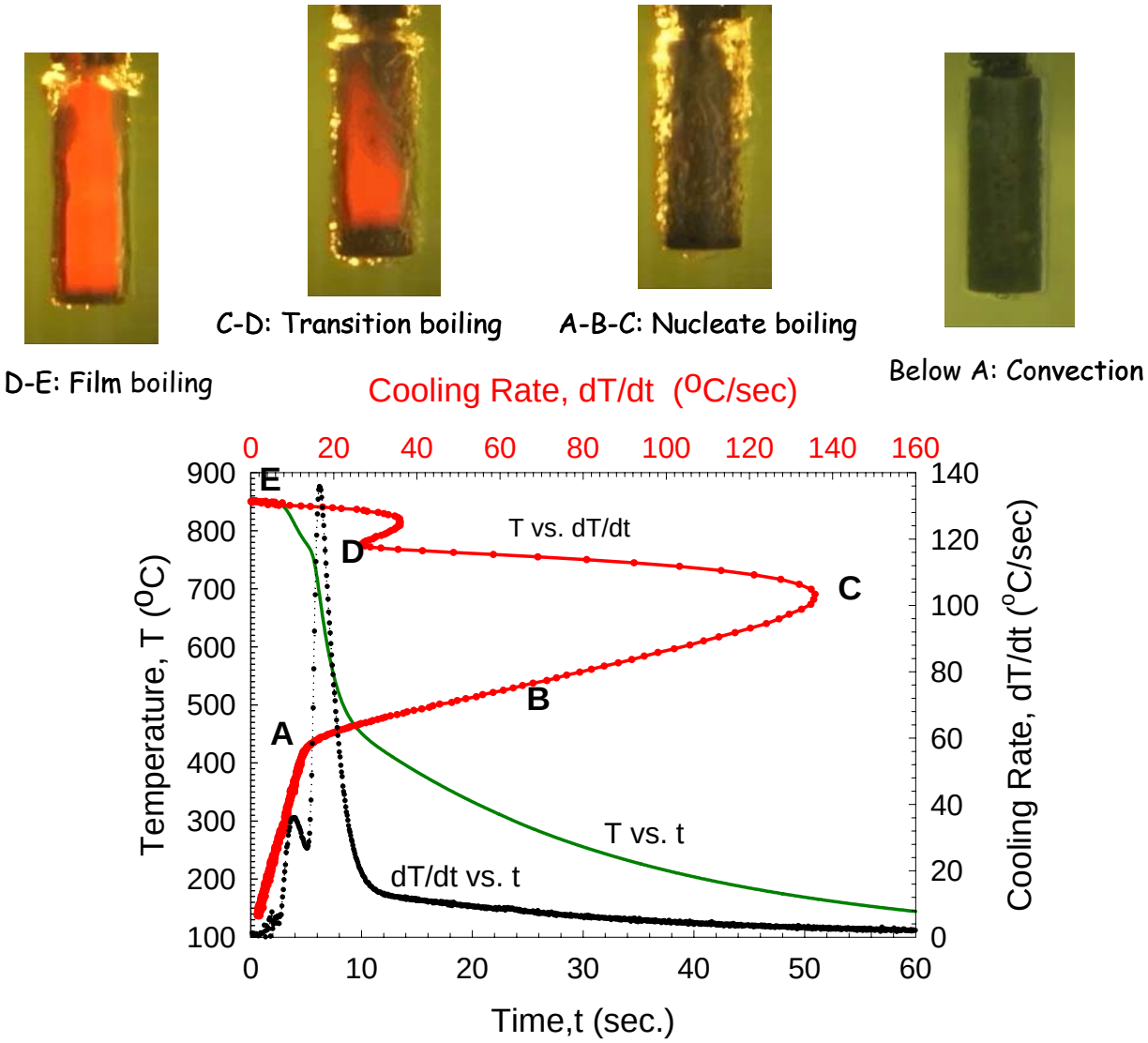

Figure 2.1: Cooling Mechanism [CHTE]

Film boiling phase

The first stage of cooling, which is denoted as D-E stage in Figure 2.1, is characterized by the formation of a vapor film around the component [1]. This vapor blanket develops and is maintained while the supply of heat from the interior of the part to the surface exceeds the amount of heat needed to evaporate the quenchant and maintain the vapor phase. This film acts as an insulator and starts to disappear when the Leidenfrost temperature, the temperature above which a total vapor blanket is

maintained, is reached. This is a period of relatively slow cooling during which heat transfer occurs by radiation and conduction through the vapor blanket. This stage is non-existent in parts quenched in aqueous solutions with more than 5% by weight of an ionic material as potassium chloride sodium hydroxide or sulfuric acid. In these cases quenching starts with nucleate boiling [1].

Nucleate boiling phase

Upon further cooling, stage C-D, or the nucleate boiling stage begins, until it reaches the maximum cooling at point C. This cooling mechanism is characterized by violent boiling at the metal surface. The stable vapor film eventually collapses and cool quenchant comes into contact with the hot metal surface resulting in nucleate boiling and high extraction rates. As the part cools the boiling becomes less violent until the metal reaches the boiling point of the quenchant.

Convection stage

Below A is the convective cooling stage, this occurs in Figure 2.1 begins when the metal cools just below the boiling point of the quenching fluid [15]. As cooling continues, the surface temperature is below the boiling point of the quenching fluid and the metal surface is completely wetted by the fluid. At this point, the cooling rate is low and determined by the rate of convection and the viscosity of the quenching fluid along with process variables such as agitation.

During quenching the duration of the vapor phase and the temperature at which the maximum cooling rate occurs have a critical influence on the ability of the steel to harden fully. The rate of cooling in the convection phase is also important since it is

generally within this temperature range that martensitic transformation occurs and it can, therefore, influence residual stress, distortion and cracking.

2.3 Distortion and Cracking

In general, the distortion occurring during quenching depends on the size and shape of the bar, bar composition and the characteristics of the quenchant employed [7]. Regular part shapes with ratios greater than 1:4 and large parts with thin cross sections are more prone to distortion than parts where uniform cooling is much more obtainable. Parts with groves, holes or other features that would change the cooling rate in specific areas are also more prone to distortion.

The composition of the part is also crucial in whether or not distortion will occur. Steels with high carbon concentration or high alloy steels that have a high hardenability are also more prone to distortion. On a similar note, steels with a high austenitizing temperature and low martensite start (Ms) temperature tend to aggravate distortion [7].

Cracking occurs when the localized strain exceeds the failure strain in the material [7]. The tendency for cracking typically decreases as the Ms temperature increases. This is due to a higher degree of ductility at increasing temperatures allowing for more strain to be allowed. Though this helps to prevent cracking, distortion is still possible. To understand distortion and cracking it is important to understand the thermal stresses and strains involved in the cooling of various parts. Section 2.4 will cover this in detail.

2.4 Thermal Stress and Strain Generation

In quenching, different parts of the component undergo different cooling rates; therefore differential thermal expansion and phase transformations within the component are sources for stresses [16]. Sedighi has written that there are three interacting physical

processes that take place in the material, temperature change, phase change and stress-strain change. These interactions can take place in six ways show in Figure 2.3.

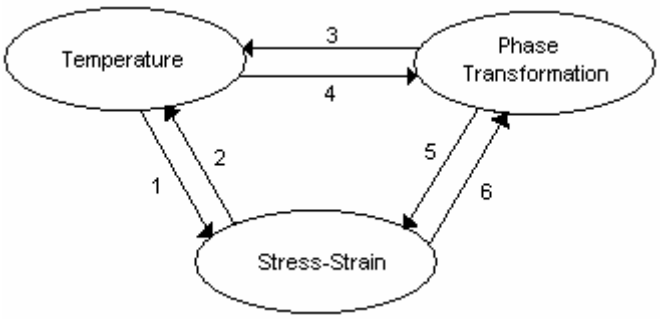

Figure 2.2: Coupled effects in quenching [9, pg 50]

1. *Thermal Stress* is the stress that arises from differential rates of thermal contraction within the component.
2. *Heat release due to the work done in deformation* is the result of plastic deformation of the material.
3. *Temperature dependant phase transformation* describes the time and temperature dependant kinetics of phase transformation.
4. *Heat release with phase transformation* arises from enthalpy variation between phases.
5. *Phase transformation effects on stress state* are divided into two effects:
    a. *Volumetric dilatation* with phase transformation causes volumetric changes due to the different densities of the phases.
    b. *Transformation plasticity* is an irreversible deformation behavior of a transforming specimen under a load state with an equivalent stress lower than the yield stress [17].
6. *Stress dependence of phase transformation* is the effect of the stress state on transformation kinetics.

Assuming uniform cooling, when a cylindrical part is immersed in a quenchant from the austenization temperature thermal gradients are formed. First the surface is cooled which initially places it in tension due to the shrinkage associated with cooling. The center of the part is still hot at this point and is therefore placed in compressive stress. As the part is further cooled and approaching ambient near the surface the tensile stresses are relaxed as the center cools down. Assuming that there is no plastic flow

during these steps the resultant stresses would be zero across the part. However this is a poor assumption because at higher temperatures the yield stress is very low and plastic flow will occur. Under these circumstances the unloading referred to above is followed by a stress reversal, so that the residual axial stress at the end of a quench would be compressive at the surface and tensile at the center [8]. Figure 2.4 shows the effects of uniform cooling in water. Starting out with (a) uniformly hot, (b) center portion of cylinder is hot upset (in compression because it has not contracted due to cooling) during quenching, (c) center portion of cylinder is short in tension when uniformly cold. Machining of the surface allows the center portion to decrease in length [18].

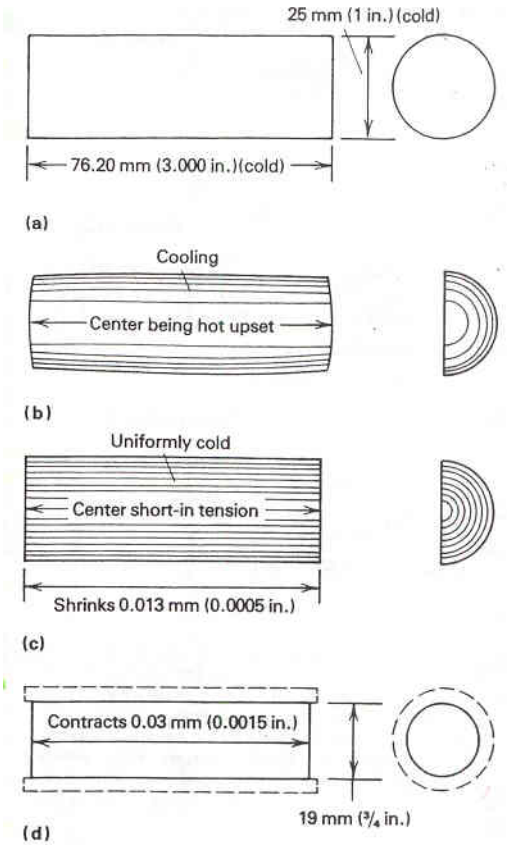

Figure 2.3: Effects of quenching a steel cylinder in water [18]

The purpose of a quench is to form specific microstructural changes. These changes are associated with an increase in volume and occur as a function of temperature and time.

The martensite transformation invariably begins at the surface and continues towards the center, unless it is prevented by diffusional process [8]. The transformation of the martensitic surface region will have a greater volume than the untransformed center. The described volumetric expansion occurring during quenching can be described by Equation 1 [19].

$$(\Delta V/V)\cdot 100 = (100\cdot V_c - V_a)\cdot(1.68\cdot C) + V_a(-4.64 + 2.21\cdot C) \quad \textbf{(1)}$$

Where $(\Delta V/V)\cdot 100$ is the change in volume in %; V_c is the % by volume un-dissolved cementite; V_a is the % by volume austenite; 100-V_c-V_a is the by volume martensite; and C is the by weight of carbon dissolved in austenite and martensite. Therefore a compressive stress will result at the surface and a tensile component will exist at the untransformed center. This equation should only be used on a plain carbon steel. Research has been conducted to determine "Carbon Equivalents" for various alloying elements [20].

Rammersdorfer *et al* calculated the thermal stresses generated during the quenching of a 50mm diameter steel cylinder that was completely transformed to martensite during a water quench.

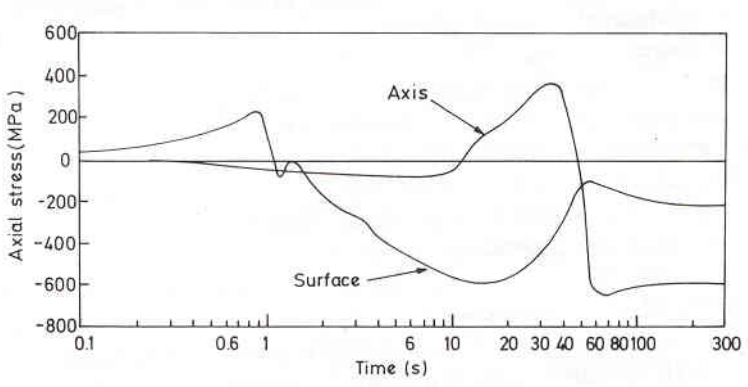

Figure 2.4: Relationship between stress and time during quenching of a fully hardened steel [21]

Two important features to highlight of Figure 2.5 is the unloading of tensile stress during martensite formation. At ~1 second the surface drops dramatically in stress value, this is when the surface reaches the Ms temperature. The center of the probe reaches the Ms temperature at ~40 seconds into the quench.

2.5 Characteristics and TTT diagram of 4140 steel [13]

According to their carbon content, the plain carbon steel can be categorized as high-carbon steel (>0.60%), medium-carbon steel (0.30-0.60) and low-carbon steels (<0.30%). [22] 4140 can be classified as the medium-carbon steels with the chemical composition of 0.38-0.43 C by weight.

AISI 4140 steel is made with chromium and molybdenum alloy additives. Chromium from 0.5 to 0.95% is added with a small amount of molybdenum (from 0.13 to 0.20%). These small amounts of these two elements increase the strength, hardenability and wear resistance of the 41xx series of alloy steels [23].

The chemical composition and typical applications of 4140 steels are listed below: AISI-SAE 4140 steel has 0.40 % Carbon, 0.58% Manganese, 0.95% Chromium, and 0.20% Molybdenum. Low alloy steels with chromium and molybdenum, because of

their increased hardenability, can be oil quenched to form martensite instead of being water quenched since the slower oil quench reduces temperature gradients and internal stresses due to volume contraction and expansion during quenching. Distortion and cracking tendencies can be minimized.

4140 is among the most widely used medium-carbon alloy steels. Relatively inexpensive considering the relatively high hardenability 4140 offers. Fully hardened 4140 ranges from about 54 to 59 HRC, depending upon the exact carbon content. Forgeability is very good, but machinability is only fair and weldability is poor, because of susceptibility to weld cracking [24].

Figure 2.5 is CCT diagram of AISI 4140, which indicates the phase transformation from austenite to martensite or bainite or pearlite depending on the cooling rate that can be achieved from specific quenchant. Such diagram is valuable since the cooling curve can theoretically be superimposed upon it to predict heat-treatment response. The steel begins to transform at the Ms Temperature and is fully hardened at the Mf temperature.

The starting and ending temperature of martensitic transformation Ms and Mf, which is quite critical for understanding of quenching process of 4140 steels, can be read from the diagram. Ms = 640^{o}F = 338^{o}C and Mf = 425^{o}F = 218 ^{o}C. Also in order to get the complete martensite and avoid the formation of pearlite or bainite, the quenchant must be able to cool the component fast enough to miss the nose of the curve for pearlite and bainite formation.

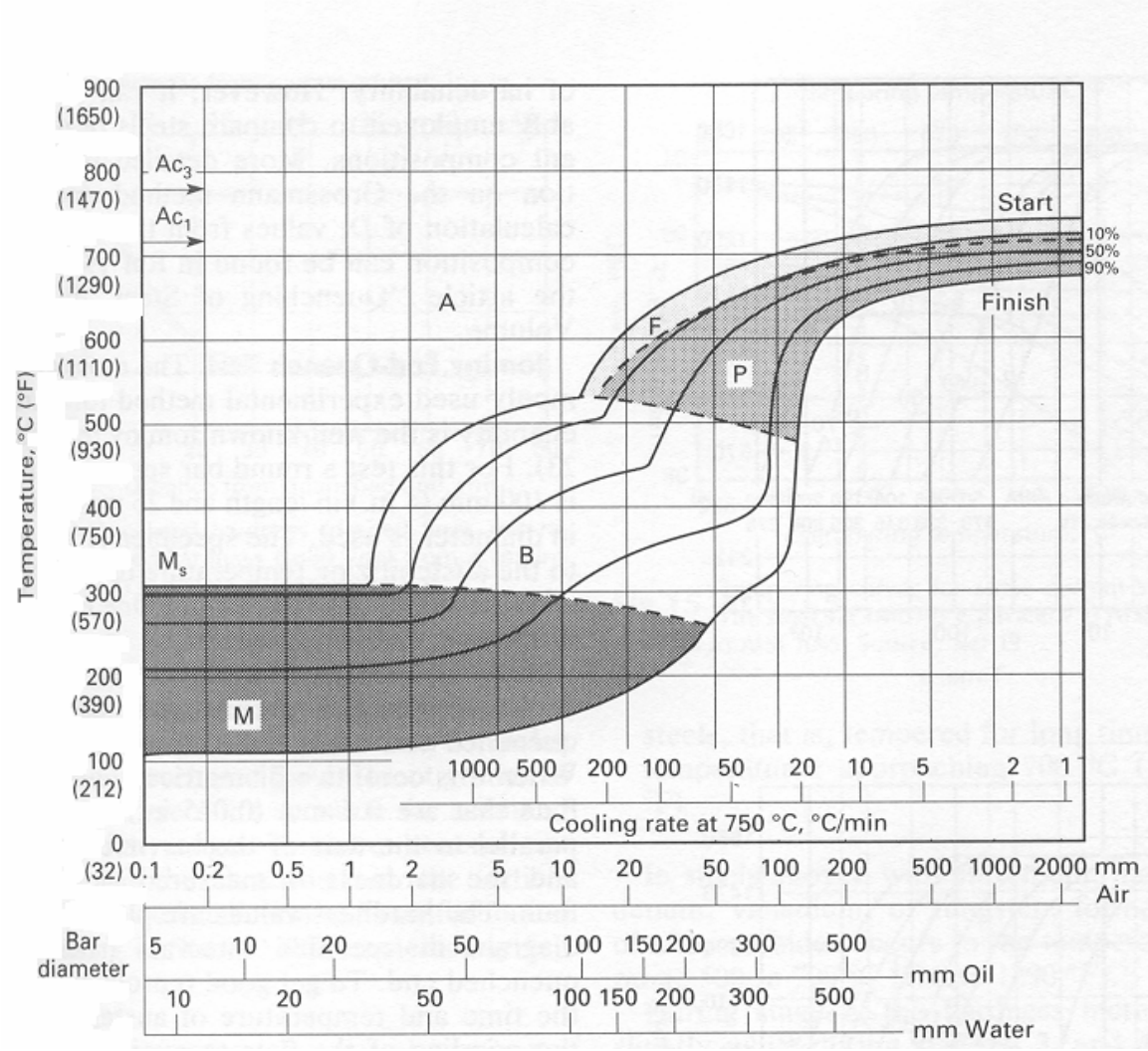

Figure 2.5: CCT diagram of AISI 4140 [1, pg. 9]

After austenitizing at 843°C and oil quenching a martensitic structure is produced and with subsequent tempering at 315°C, a tempered martensitic structure is the result. Martensite in low alloy steels consists of packets of fine units of martensite called laths that align themselves parallel to one another to form packets [23].

3.0 Paper

Quenchant flow around a 4140 steel cylinder and its effects on distortion, residual stress and hardness.

Quenchant flow around a 4140 steel cylinder and its effects on distortion, residual stress and hardness

Darrell K Rondeau, Michael Stratton, Mohammed Maniruzzaman, Katherine Macchiarola and Richard D. Sisson, Jr.
Center for Heat Treating Excellence
Materials Science and Engineering Program, Mechanical Engineering Department
Worcester Polytechnic Institute, Worcester, MA 01609 USA

Abstract

The effects of quenchant flow around a 4140 steel cylinder have been experimentally investigated. An apparatus was developed to repeatably immerse a two inch diameter by eight inch long probe into an agitated quench tank. The probes were normalized prior to quench to relieve any residual stresses. Distortion, residual stress and hardness were experimentally measured. The results verified that there was a variation of cooling rate in respect to quenchant flow around the cylinder. The data showed that there was a higher cooling rate nearest to the quenchant flow versus a much lower cooling rate away from the flow. Computational fluid dynamics are also presented to give insight into the behavior of the quenchant flow in the tank and around the cylinder.

I Introduction

The process of quenching steel refers to the rapid cooling from an austenitizing or solutionizing temperature to a significantly cooler temperature [1]. For steel this refers to heating into the austenite phase field, typically to 845°C for 4140 steel, and then rapidly cooling to a temperature below the martensite finish temperature. The purpose of quenching steel is to produce the martensitic phase that is hard and strong, while minimizing distortion and residual stress. These steels need to be tempered after quenching to increase the toughness. Due to the demand for hardened steel parts an understanding of the mechanisms of distortion and residual stress development is necessary.

The most widely used practice of quenching is referred to as direct quenching [Bates]. Direct quenching involves quenching the part directly from the austenitizing temperature. This can be accomplished by immersion in different types of media (i.e. oil, water, polymer solutions, etc.). The media selected is dependant on the cooling rated desired. Agitation is also a key parameter that influences the cooling rate [7].

In commercial heat treating it is necessary to achieve the desired mechanical properties while maintaining the dimensional tolerances. The mechanisms involved in hardening and distortion are discussed in this thesis. Two aspects to note about the distortion associated with quenching are:

- Steel has a higher strength when cold than when hot
- Steel shrinks while cooling but expands during martensite formation

Coupled with distortion is residual stress development. The manner by which stress is generated during a quench is complex and the stress obtained is the net effect of

the combination of several processes [8]. There are three different mechanisms that are coupled during the quenching of steel, temperature effects, phase transformations, and stress/strain development [9]. Thermal stress generation arises from the temperature gradients formed because it is difficult to cool the part uniformly. There is heat released during the work done in deformation. Phase transformations are a temperature dependant function. There is an associated heat release with phase transformation. There is a volume change during phase transformation causing stress, and the transformation kinetics are effected by stress state.

In order to understand what is going on inside the quench tank computational fluid dynamics have been employed. With the help of Michael Stratton using Fluent 6.0 it was possible to model the tank and probe setup. By using experimental data of the quenchant flow obtained with a turbine flow meter, and measured densities and viscosities of the quench fluid it was possible to determine the velocities and flow trends within the tank.

It is the goal of this project to understand how part orientation with respect to quenchant flow influences distortion, and residual stress generation in 4140 steel. Experiments were conducted using a 2” diameter x 8” long 4140 probe. The probe was heated in an atmosphere of argon and subsequently quenched normal or at 45 degrees to the surface with horizontal agitation. Along with empirical investigation of distortion, residual stress and hardness, computational fluid dynamics has been employed to determine how the flow around the part influences heat transfer.

Distortion and residual stress were measured at four points around the probe. Distortion was measured with a Coordinate Measuring Machine. The residual stress was

measured using an X'Pert X – Ray Diffractometer System at Philips PANalytical, in Natick, MA. The hardness measurements were preformed both longitudinally and in the transverse direction to give insight to the formation of martenstite with respect to quenchant flow.

II Experimental Plan

The experimental plan is as follows. Six probes have been quenched according to Table 3.1. Four probes were quenched in an agitated bath, and two in a stagnant bath. Of the four probes quenched in an agitated bath two have been quenched at 45° and two have been quenched vertically. Of the two probes quenched in the stagnant bath, one has been quenched at 45° and the other has been quenched vertically. The probe numbering convention is shown in the table.

Agitation (y/n)	Orientation	Number of Trials	Probe #
Y	45	2	101,102
Y	Vertical	2	103,104
N	45	1	106
N	Vertical	1	107

Table 3.1: Test matrix of CHTE Large 4140 steel probe quench orientation trials

The convention for the length of the probe has x = 0mm at the bottom and x = 200mm at the top. Another numbering convention that should be explained is how the probe is labeled in regards to quenchant flow (when applicable). Figure 3.1 illustrates the numbering convention, with position 1 being closest to the flow outlet and position 5 being on the backside, facing away from the flow outlet. Positions 3 and 7 are located 90° from position 1 and 5, and are located in a counter clockwise fashion while looking at the bottom of the probe, the bottom being the end that is not attached to the extension rod.

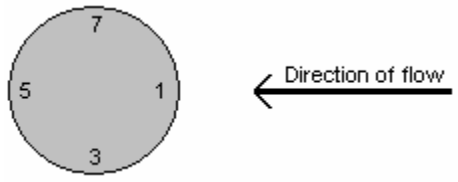

Figure 3.1: Probe position numbering convention

The measurements that have been preformed on the six quenched probes are as follows: Residual Stress, Distortion, Longitudinal Hardness, Transverse Hardness.

In parallel to the measurements made on the probes. Fluid flow measurements were preformed. In tank fluid velocities have been measured along with Computational Fluid Dynyamics of the quench tank during agitation.

III Experimental Procedure

A quench probe, and quenching system have been developed that allowed experiments to be conducted in a repeatable manner. The quench system is comprised of an atmospheric furnace, adjustable track system for insertion of the quench probe, a quench tank of Houghton T7A (22 gallons) with a detached pump, and a quench probe.

A quench probe was developed based on the Liscic/NANMAC quench probe. The probe shown in Figure 3.2 is has been made from ground 4140 rod. It is 8” in length and has a diameter of 2”. Machining has been done to drill a hole to the geometric center of the probe for thermocouple placement (For cooling results see Appendix 2), and to allow for a 1” extension rod to be inserted. The primary extension rod is 12” in length and has a fixture to position the thermocouple in contact with the center of the probe. The final extension rod is to hold the part in the tracks of the quenching system.

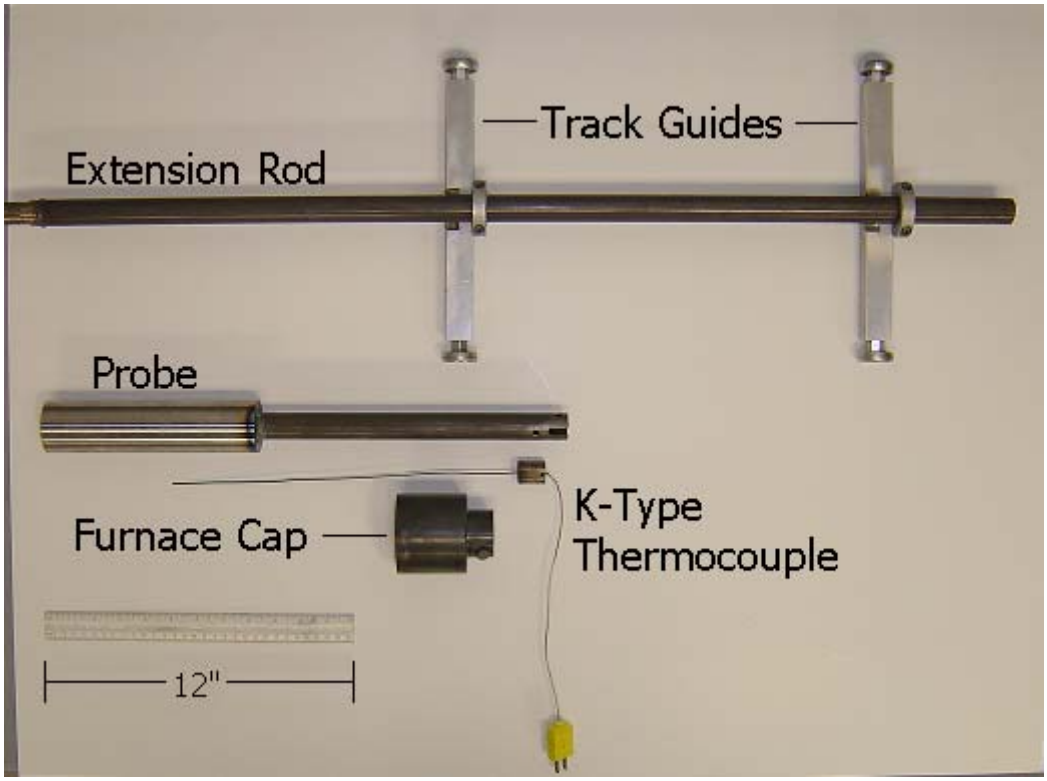

Figure 3.2: CHTE Large 4140 Quench Probe

The atmospheric furnace consists of compressed argon being passed through a heat exchanger to preheat the argon to 400C. The purpose of the argon is to minimize the decarburization of the probe during the austenitizing phase. The reasoning behind the heat exchanger is to minimize the temperature gradient of the probe. The gas is then passed into a closed 304 stainless tube, that is positioned in a (ThermomLyne F21135 Tube Furnace, ThermoLyne FB1315M Box Furnace) where the probe is suspended vertically during heating.

The adjustable track system allows for immersion to happen at various angles in a repeatable manner. In this study immersion took place at 45 degrees from vertical and at vertical. To quench the probe it is removed from the furnace and manually placed in the tracks. Figure 3.3 shows the furnace set up and the Adjustable Track System, along with the Quench Tank of Houghton T7A. The tank has a pump (Supreme Mag-Drive Utility

Pump 18A) suspended at the far end that directs the flow toward the probe. The time for removal from the furnace to quench is <7seconds. During this time the temperature of the center of the probe did not drop significantly, less than 1 degree C, the temperature of immersion was between 865C and 875C.

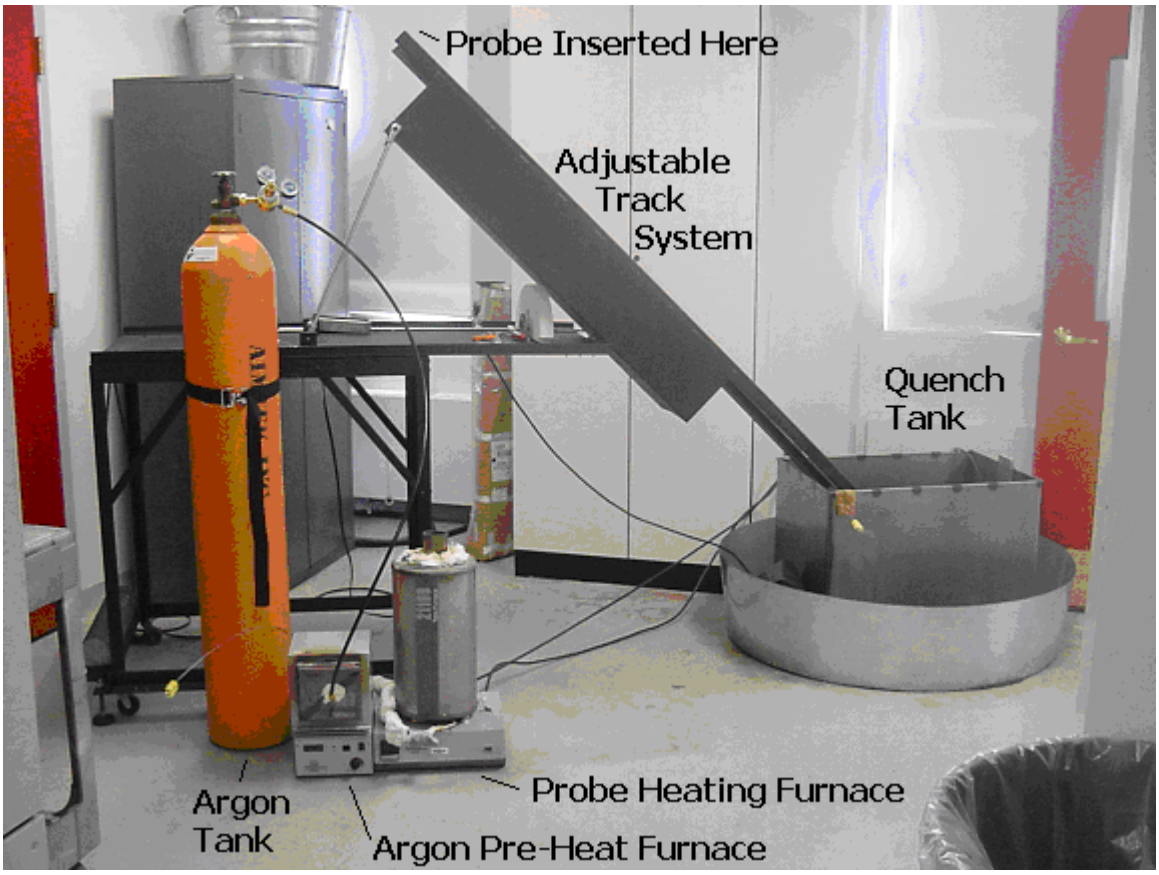

Figure 3.3: CHTE large probe quench system

Prior to the quenching heat treatment, the probe was marked at 90 degree increments, along with the above mentioned numbering convention, in order to study the effects around the circumference of the probe. Prior to quenching the probes were normalized with a furnace cool from 875C. The probes were then cleaned and roughed with 180 grit SiC paper, to provide a surface roughness similar to previous experiments at CHTE [13, pg 81].

The experiments that were conducted were subject to the following analyses: CMM profiling, residual stress measurement, and Rockwell hardness measurements (both transverse and longitudinal).

CMM profiling was accomplished using Worcester Polytechnic Institute's Coordinate Measuring Machine (Starrett HGDC 2018-16) which measures the change in height along the length of the probe. A program was written to measure the height along the length of the probe in a linear fashion. Twenty measurements were made in a line to record distortion. This data can be used to determine if any significant distortion has occurred during the quench. For each position on the probe (1,3,5,7) the profile was measured by using a line scan longitudinally along the probe.

Residual stress measurements were conducted at PANalytical using one of their Phillips X'Pert Pro XRay Diffractometers. The measurements were made at mid length of the probe. The stress measurement was conducted using a uni-axial stress analysis technique. This technique calculates the measured normal stress sigma psi and the measured shear stress tau psi. This is a classical stress analysis and is done with the Sine Squared Psi method. The normal stress is evaluated from changes in peak position with varying ψ angles [25].

Hardness values and microstructure were obtained post quenching. Longitudinal hardness measurements at positions 1,3,5,7 have been measured along with transverse hardness measurements. Transverse hardness measurements were made with a section cut out of the middle of the probe. The probe was sectioned with a horizontal band saw (DoALL C-4) using a Starrett 3-10P, 1"x0.035" Carbide Tipped blade, and a water based lubricant. The hardness measurement can be correlated to percent martensite[1, pg 80].

The Rockwell Hardness equipement (Wilson 3JR) was tested for accuracy using a series of test blocks. The accuracy of the device in the 40 – 65 RC range is ±0.5 RC.

Along with measurements conducted with the probe, fluid flow measurements have also been obtained. This has been completed using a turbine flow meter (Turbo Flo HP-302) shown in Figure 3.4. Fluent 6.0 a Computational Fluid Dynamics package was used along with the measurements obtained to understand the flow patterns in the tank.

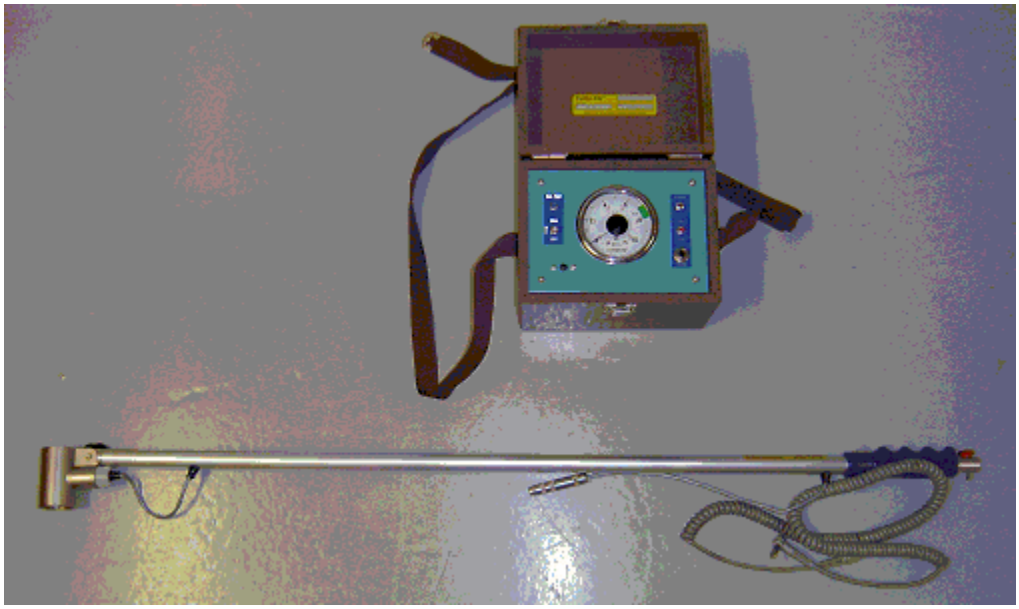

Figure 3. 4: Turbo-Flo HP-302 turbine flow meter (Scale 0 – 10 ft/s)

IV Experimental Results and Discussion

Flow Measurements Made in Tank

The results of the fluid flow in the tank are shown in Figure 3.5. This was used to determine initial velocity values in Fluent. Figure 3.5 shows the velocity as a maximum leaving the pump outlet at 7.8 ft/s at 2" from the outlet. The velocity drops to 4.5 ft/s at a position 2" from the front of the probe. Behind the probe the flow is turbulent with no real directional flow. The highest reading obtained was 0.2 ft/s at a position 5" off the back wall and 7" from the side.

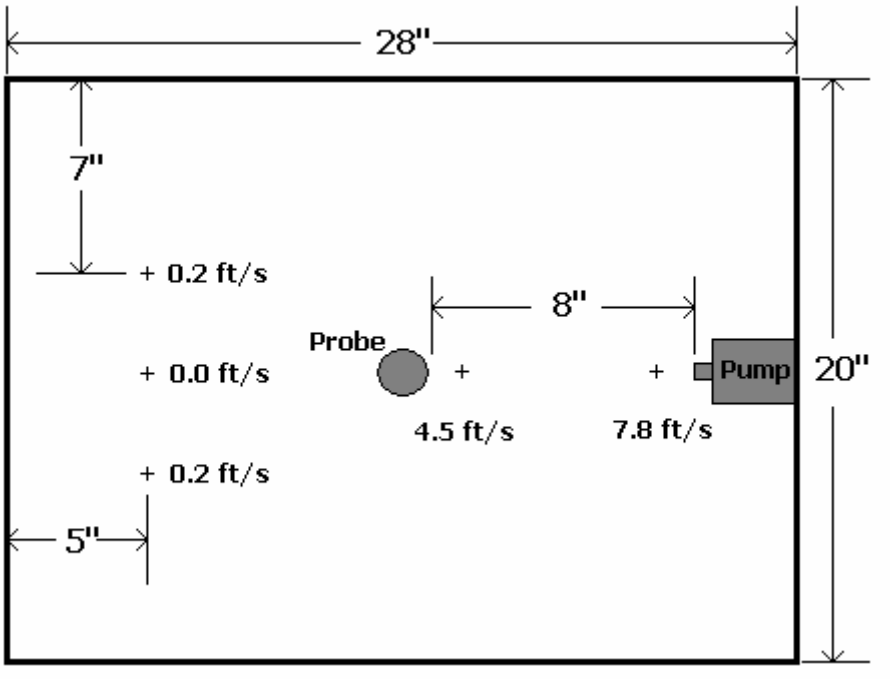

Figure 3.5: Measured Fluid Flow in the quench tank

Computational Fluid Dynamics 45° Probe

To understand the effects of part orientation in regards to quenchant flow the use of Computational Fluid Dynamics (CFD) has been employed. CFD gives insight into how the quenching fluid moves around the part, at different orientations with respect to fluid flow. The code has been drawn to scale, and uses properties found by experimental

measurement. The viscosity used for the code is $0.0685\,{}^{kg}/_{m\cdot s}$, and the density used is $0.763\,{}^{g}/_{mL}$. Figures 3.6 – 3.12 represent the fluid flow in the tank and around the probe when the orientation is at 45 degrees. Figure 3.6 is an overhead contour plot viewed at mid length of the probe. The contour plot only shows the velocity magnitude of the quenchant. The probe is positioned at the left and the pump is shown at the right, quenchant flow is from right to left.

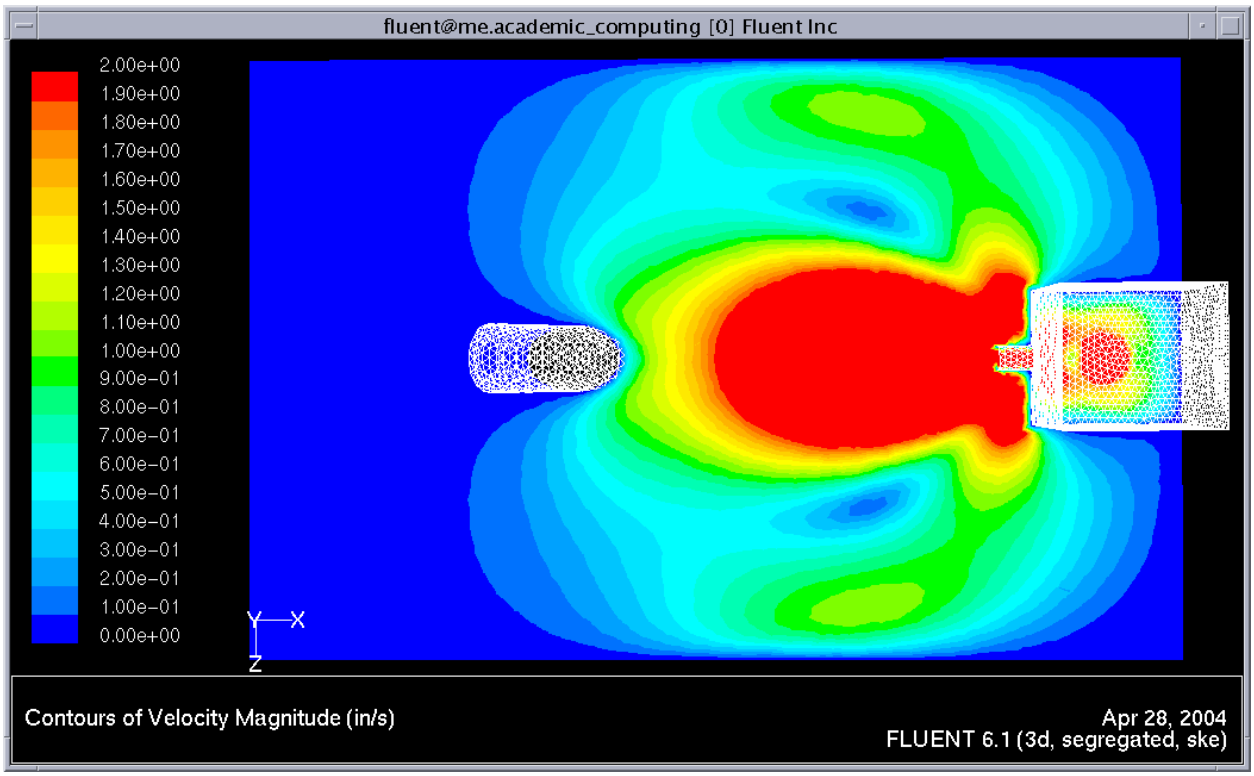

Figure 3.6: Contour plot sectioned at mid probe with a x-z plane, 45 degree probe

In Figure 3.7, which is viewed at the same orientation as Figure 3.6, the vector plot gives insight to the direction of the flow, along with the velocity. The direction is towards the probe and results in a swirling motion as the flow impacts the probe. Take notice to the minimal flow on the back side (far left) of the probe where the flow is nearly stagnant.

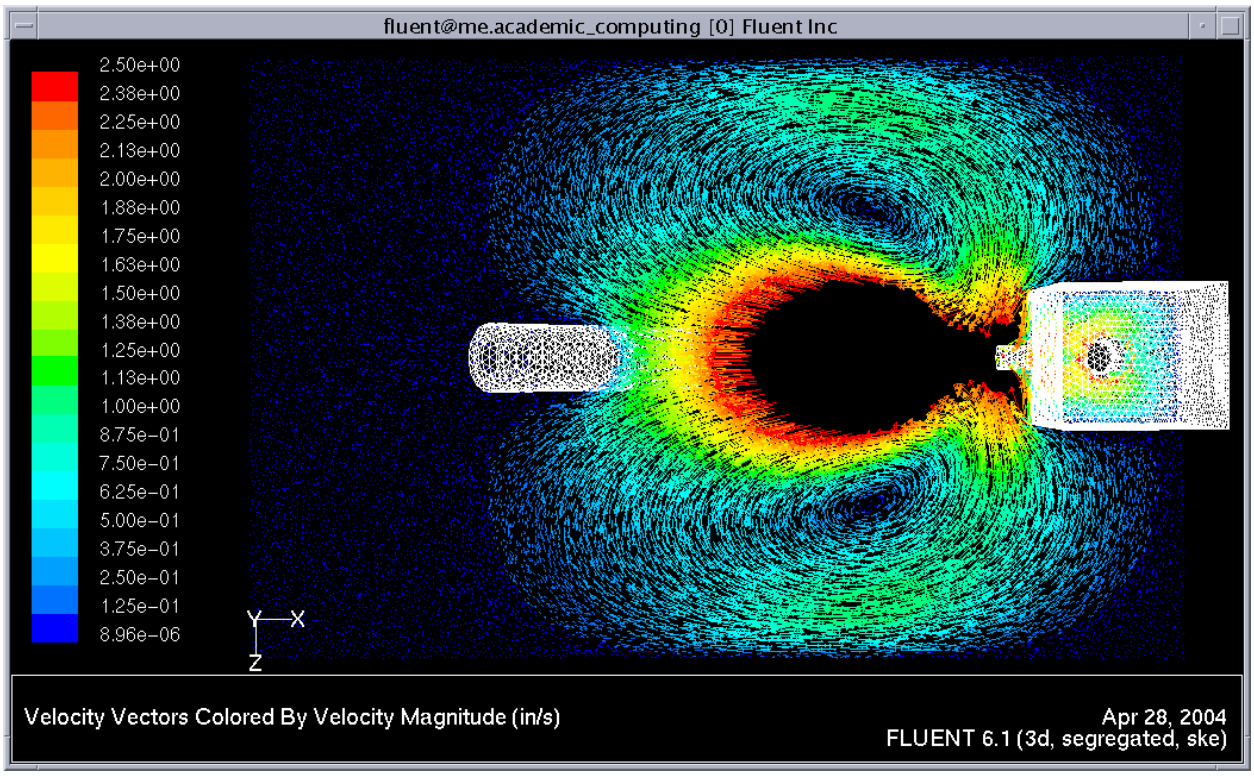

Figure 3.7: Vector plot sectioned at mid probe with a x-z plane, 45 degree probe

Figures 3.8 and 3.9 show how the flow reacts to the probe's orientation at 45°. The fluid flow impacts the probe with a slightly higher velocity at the bottom of the probe than at the top of the probe. Again it is possible to see that the flow is nearly stagnant at the backside.

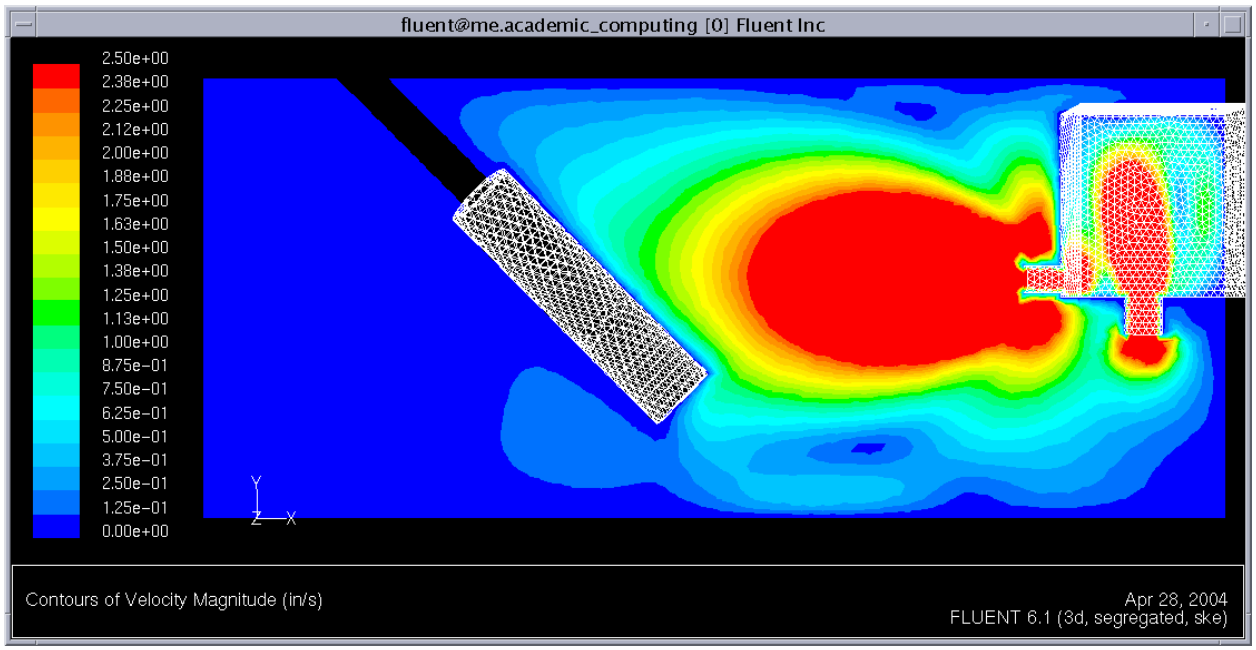

Figure 3.8: Contour plot sectioned at mid probe with a x-y plane, 45 degree probe

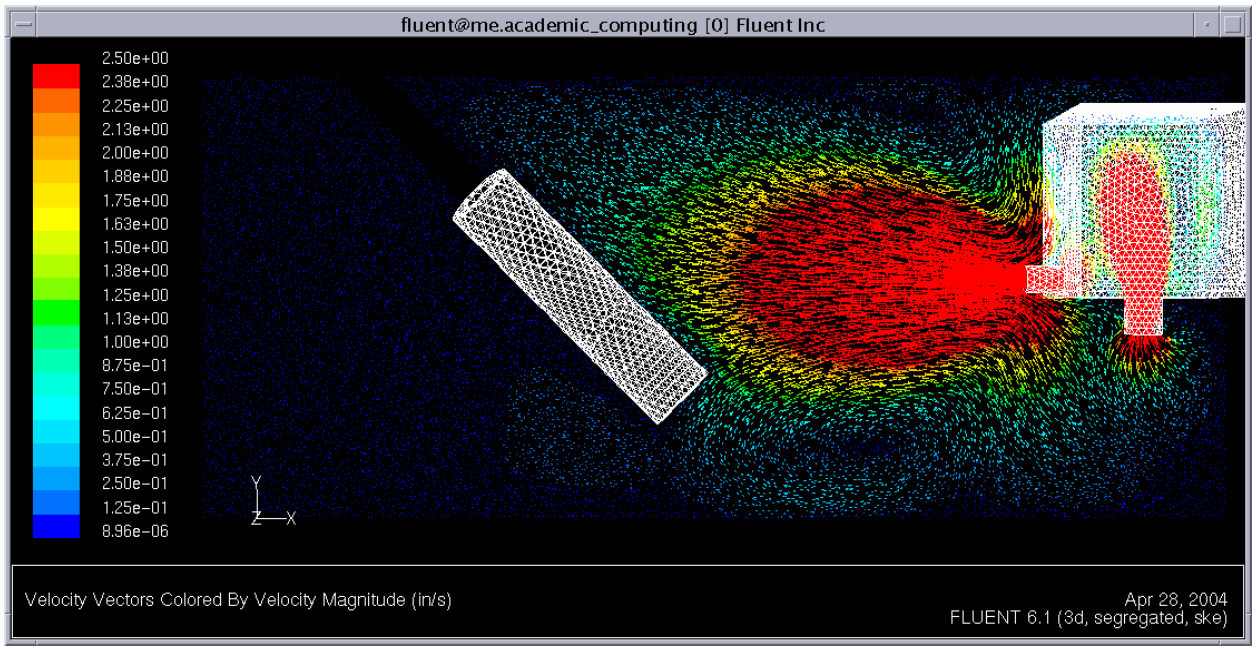

Figure 3.9: Vector plot sectioned at mid probe with a x-y plane, 45 degree probe

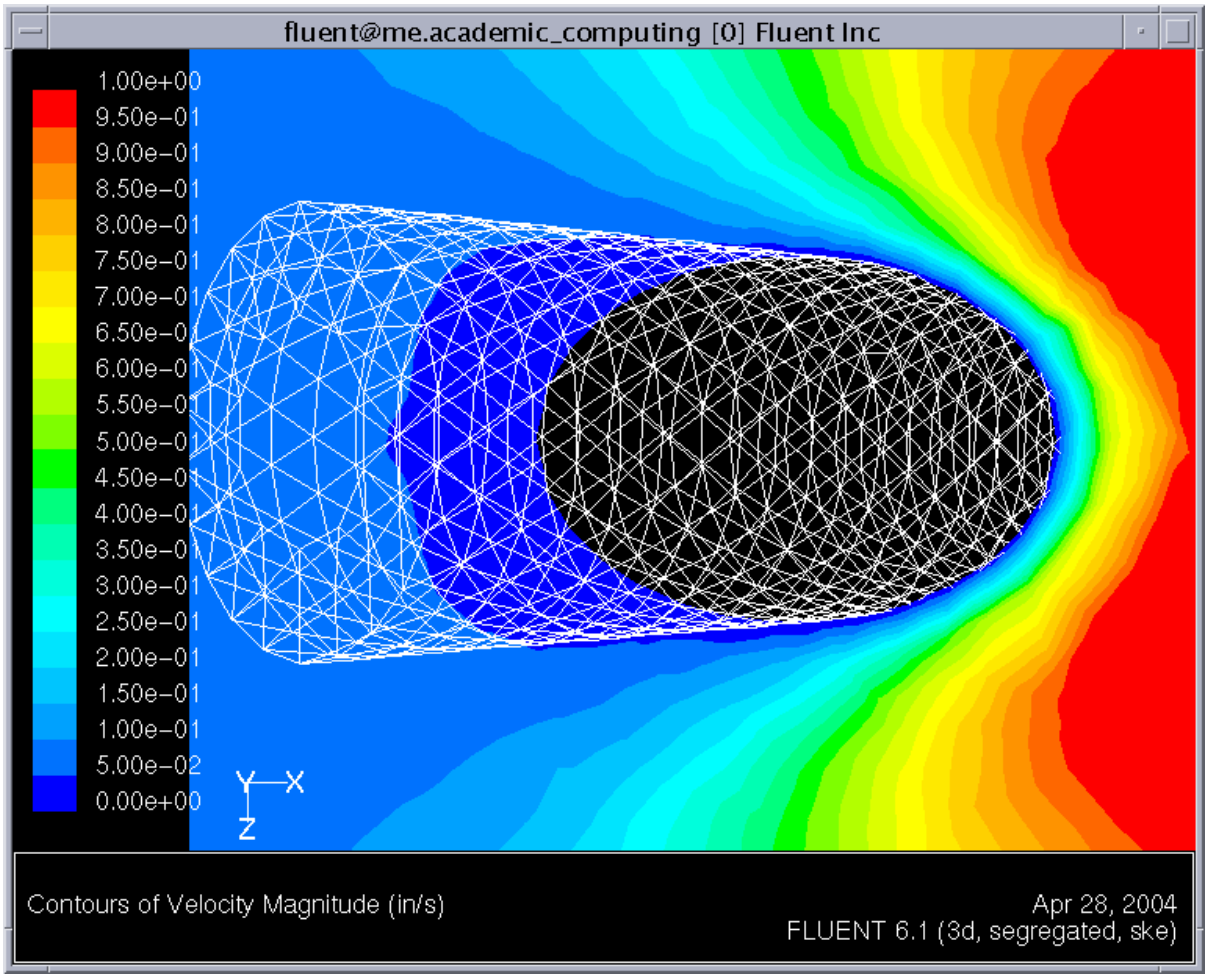

Figure 3.10: Contour plot sectioned at mid probe with a x-z plane, 45 degree, close up

Figure 3.10 is a closer view of a contour plot of the flow around the 45° probe. It is possible to see how quickly the flow breaks away from the probe and has separated before it reaches the sides where position 3 and 7 are located. This is assuming that there is a no slip boundary condition at the probe surface. Figure 3.11 actually shows how the fluid moves around the probe, and it's velocity. The fluid breaks away from the probe in a tangential fashion to a point between positions 1 and 3, and 1 and 7, leaving minimal flow at the side positions.

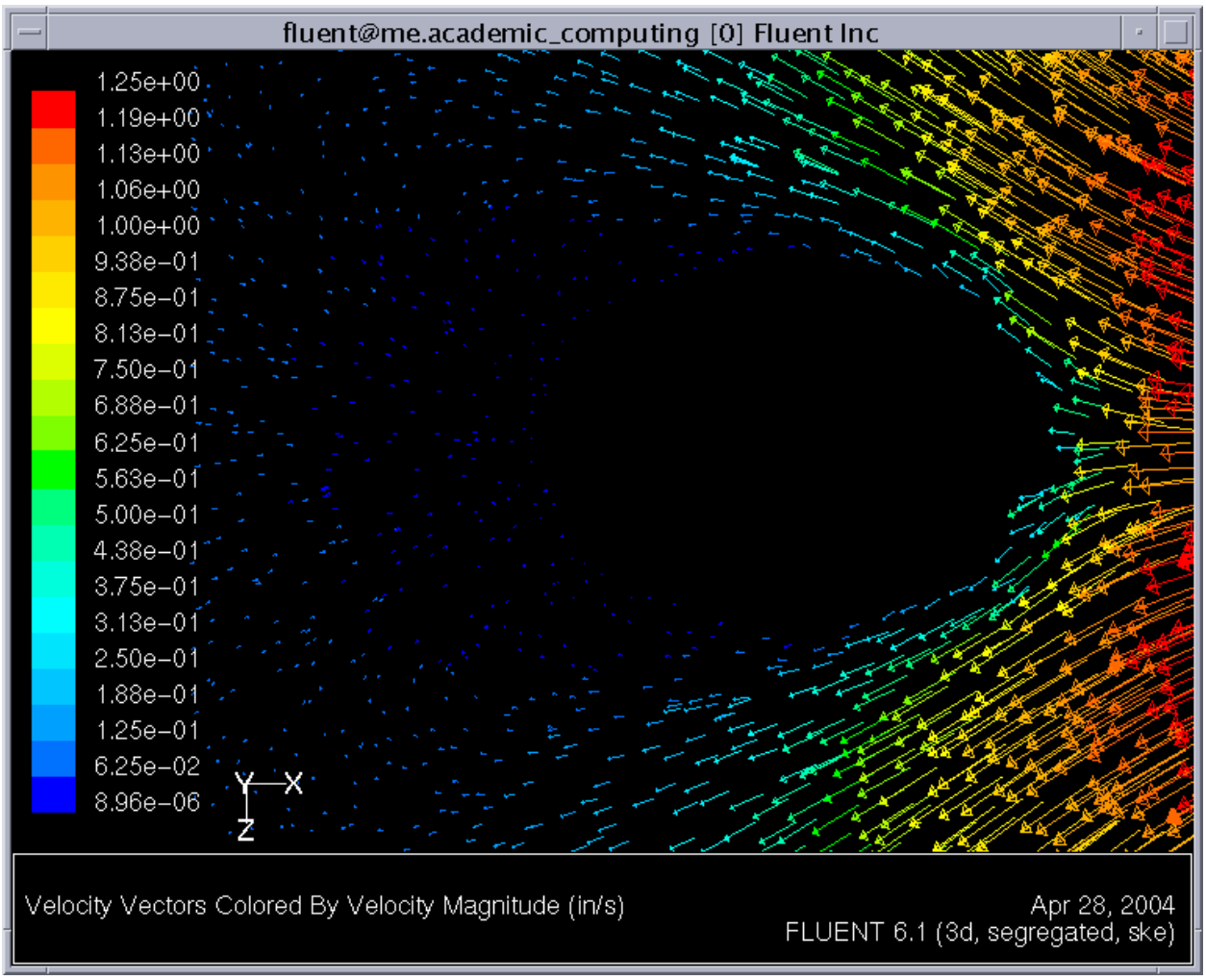

Figure 3.11: Vector plot sectioned at mid probe with a x-z plane, 45 degree, close up

Figure 3.12 shows how the flow moves up the probe. With the probe being oriented at 45° the probe can act like a ramp for the flow to move up along. Also in this Figure it is possible to see that the flow is partially deflected off the bottom of the probe. The bottom of the probe is with in the flow field and redirects part of the flow downward.

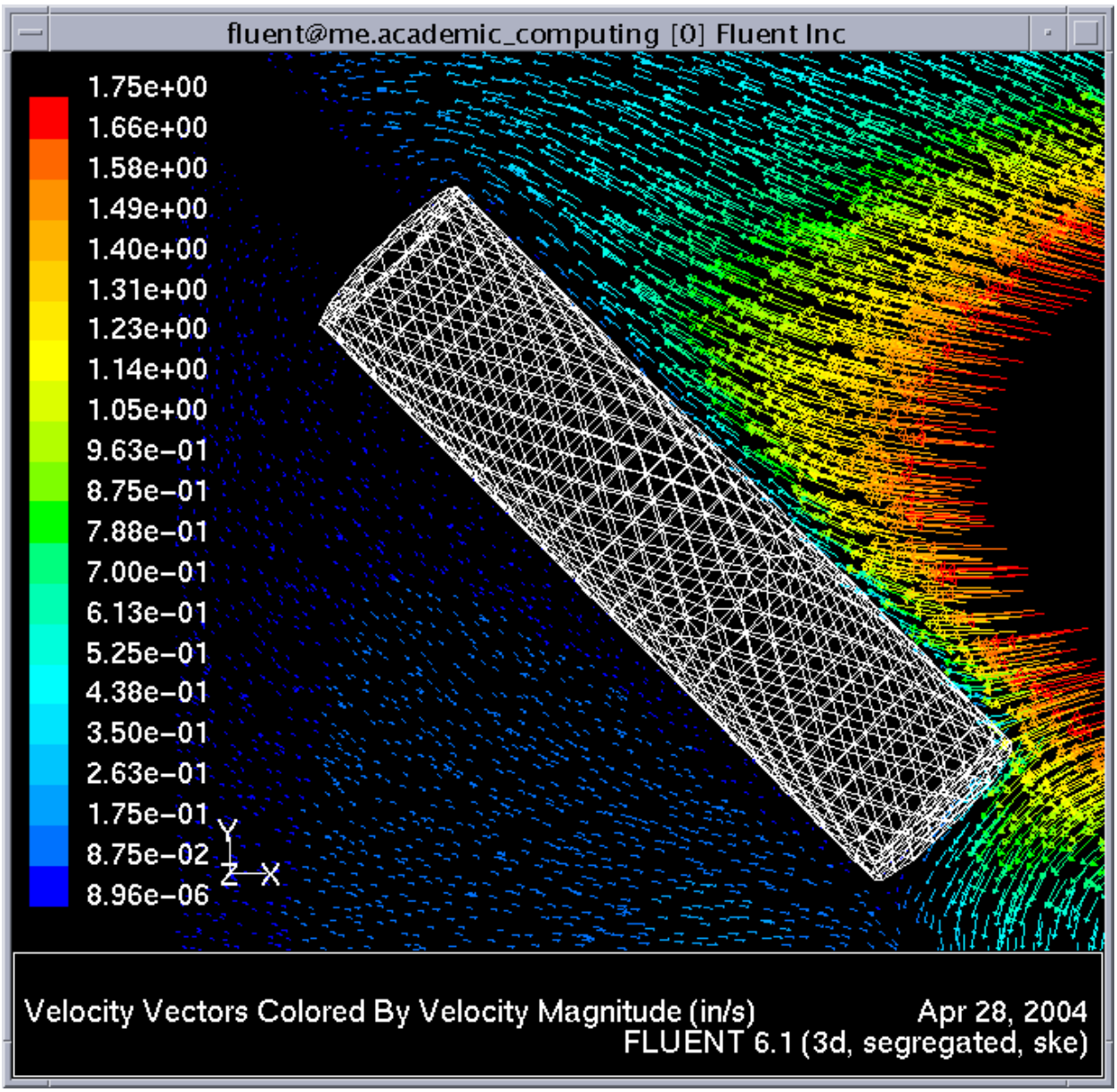

Figure 3.12: Vector plot sectioned at mid probe with a x-y plane, 45 degree, close up

Computational Fluid Dynamics Vertical Probe

Figures 3.13 – Figures 3.19 represent the fluid flow in the tank and around the proe whe the orientation of the probe is vertical. The order of the Figures is identical to that of the 45° case. Again the contour plot only gives insight to the magnitude of the velocity, whereas the vector plots show the direction of the flow. The probe is positioned at the center and the pump is located at the far right, quenchant flow is from right to left.

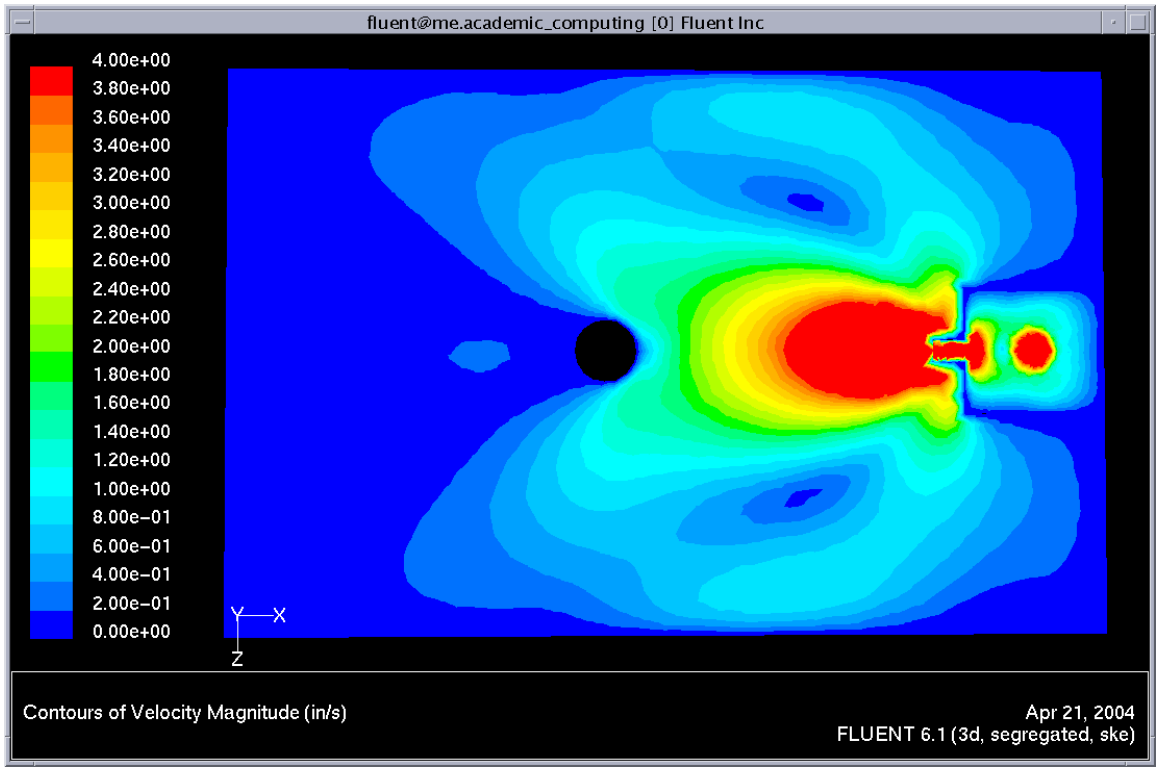

Figure 3.13: Contour plot sectioned at mid probe with an x-z plane, vertical probe

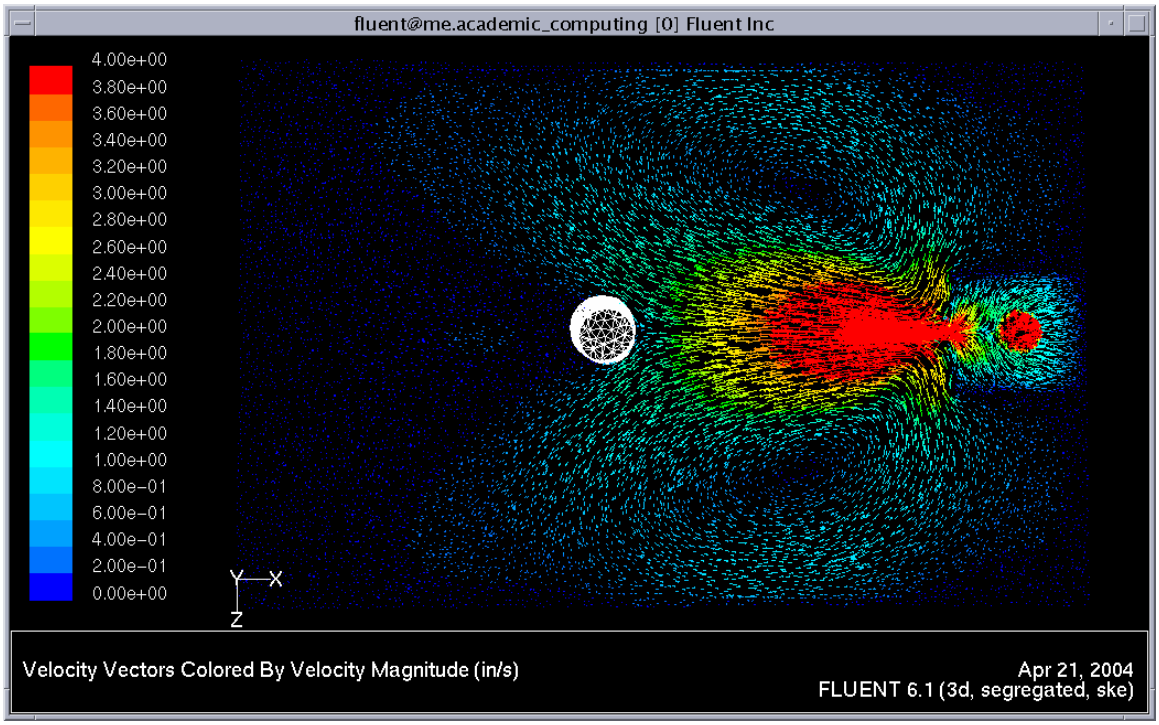

Figure 3.14: Vector plot sectioned at mid probe with an x-z plane, vertical probe

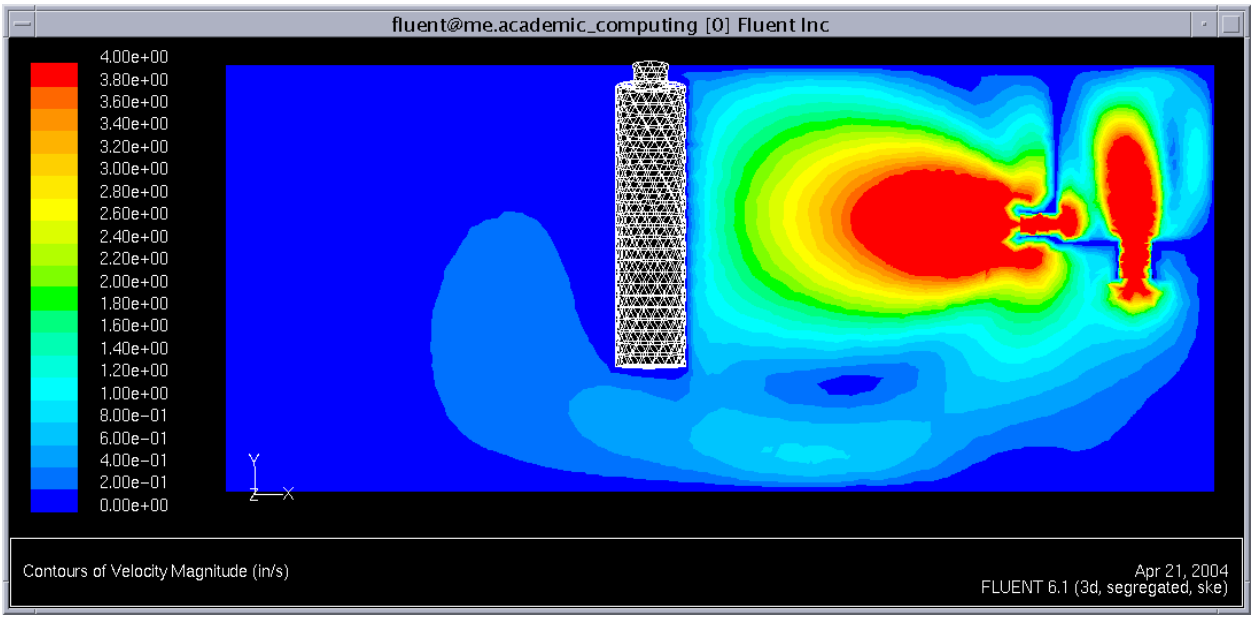

Figure 3.15: Contour plot sectioned at mid probe with a x-y plane, vertical probe

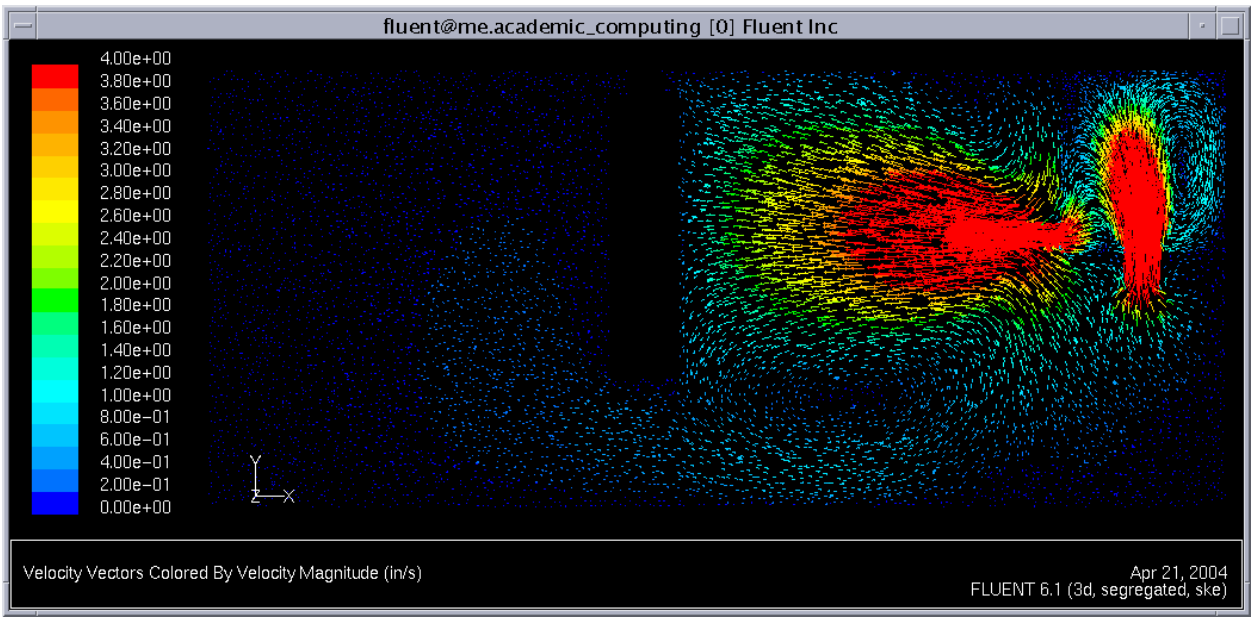

Figure 3.16: Vector plot sectioned at mid probe with a x-y plane, vertical probe

The flow patterns of the vertical case closely resemble the patterns in the 45° case. There is still a circular flow eddie as in the 45° case, and the velocities are close. The flow breaks away at a steep angle much like the 45° case as well, shown in Figures 3.17 and 3.18. One major difference is that the flow does not impact the bottom of the probe Figure 3.19, like it does in the 45° case.

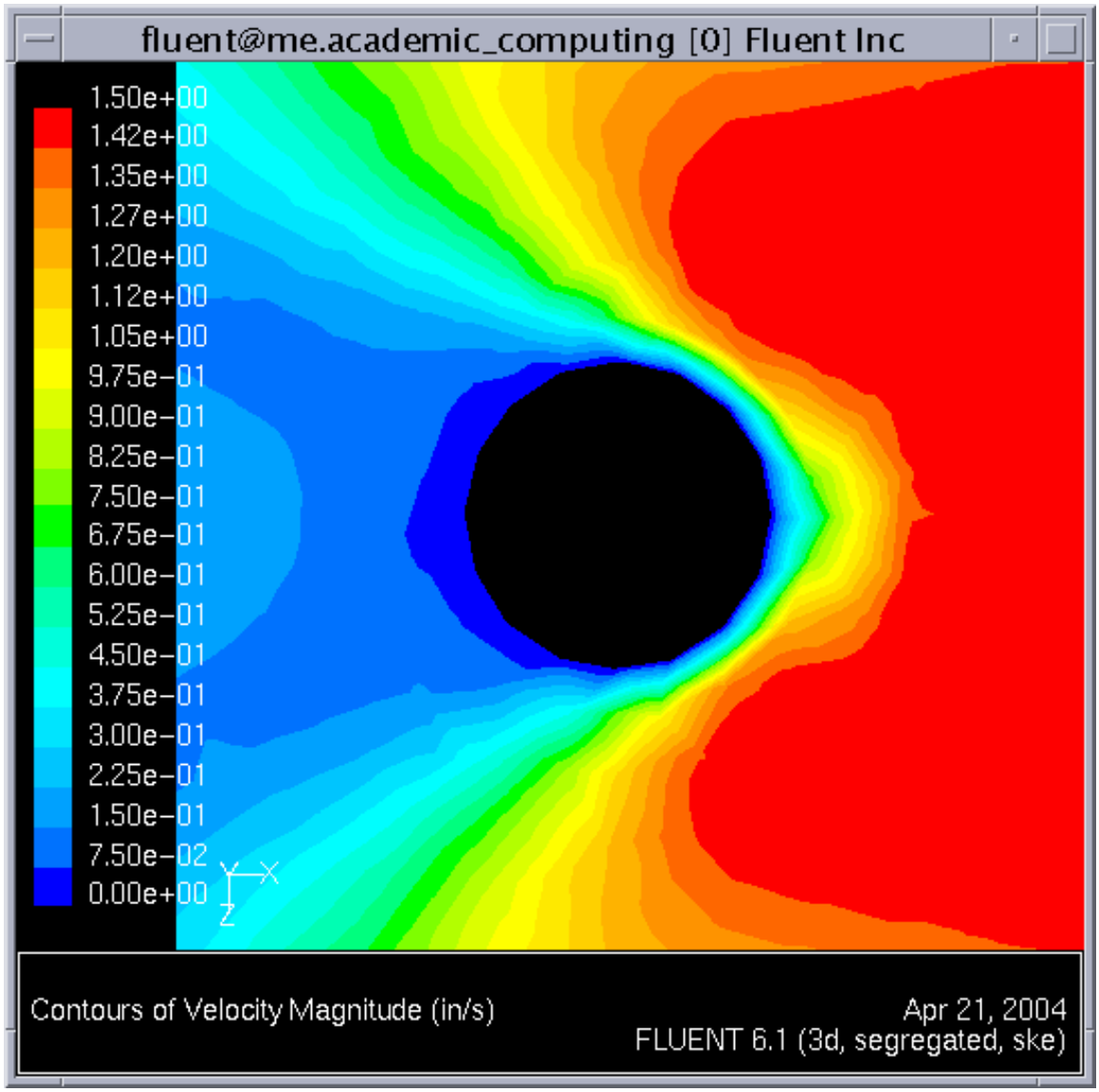

Figure 3.17: Contour plot sectioned at mid probe with a x-z plane, vertical, close up

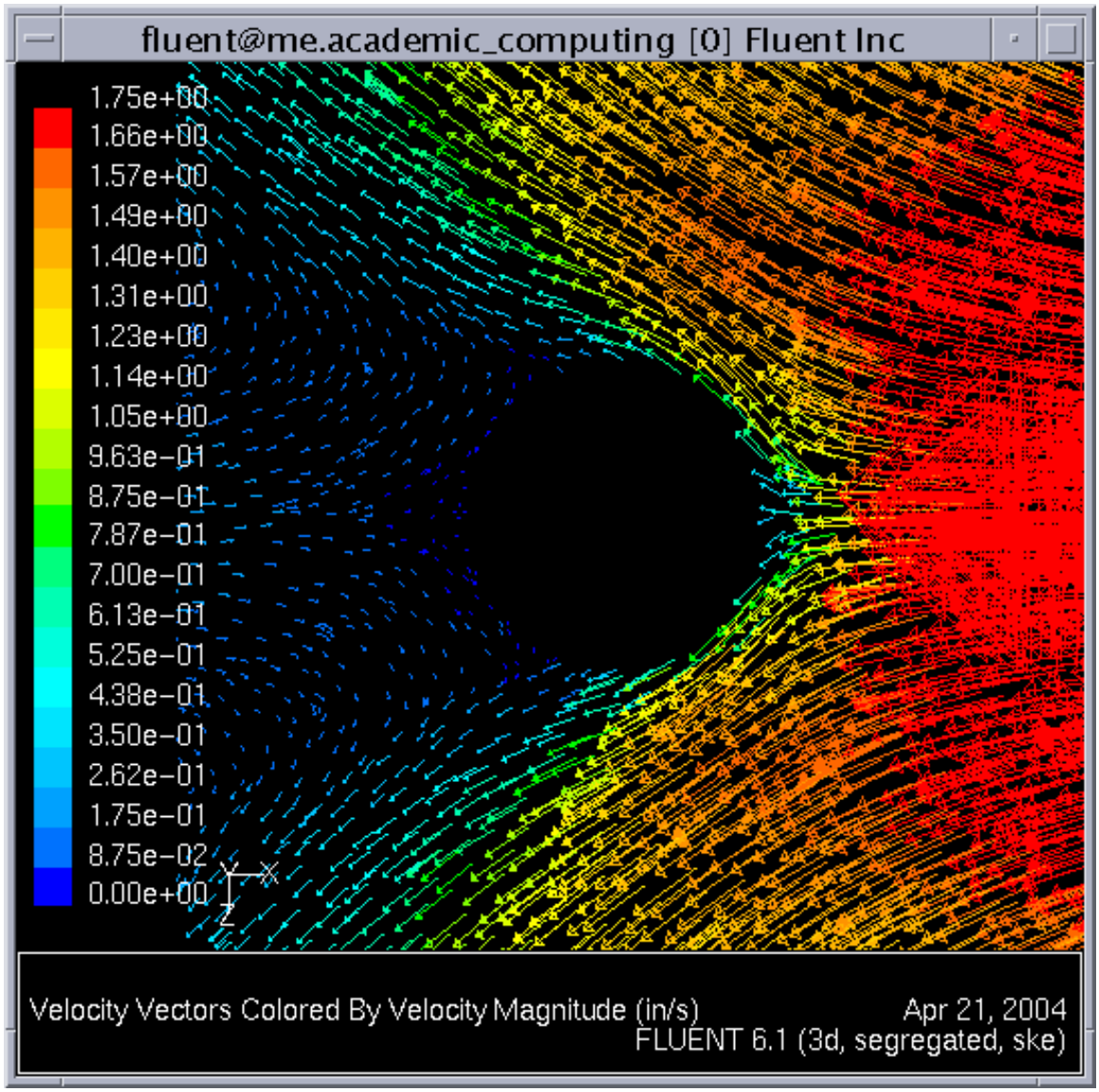

Figure 3.18: Vector plot sectioned at mid probe with a x-z plane, vertical, close up

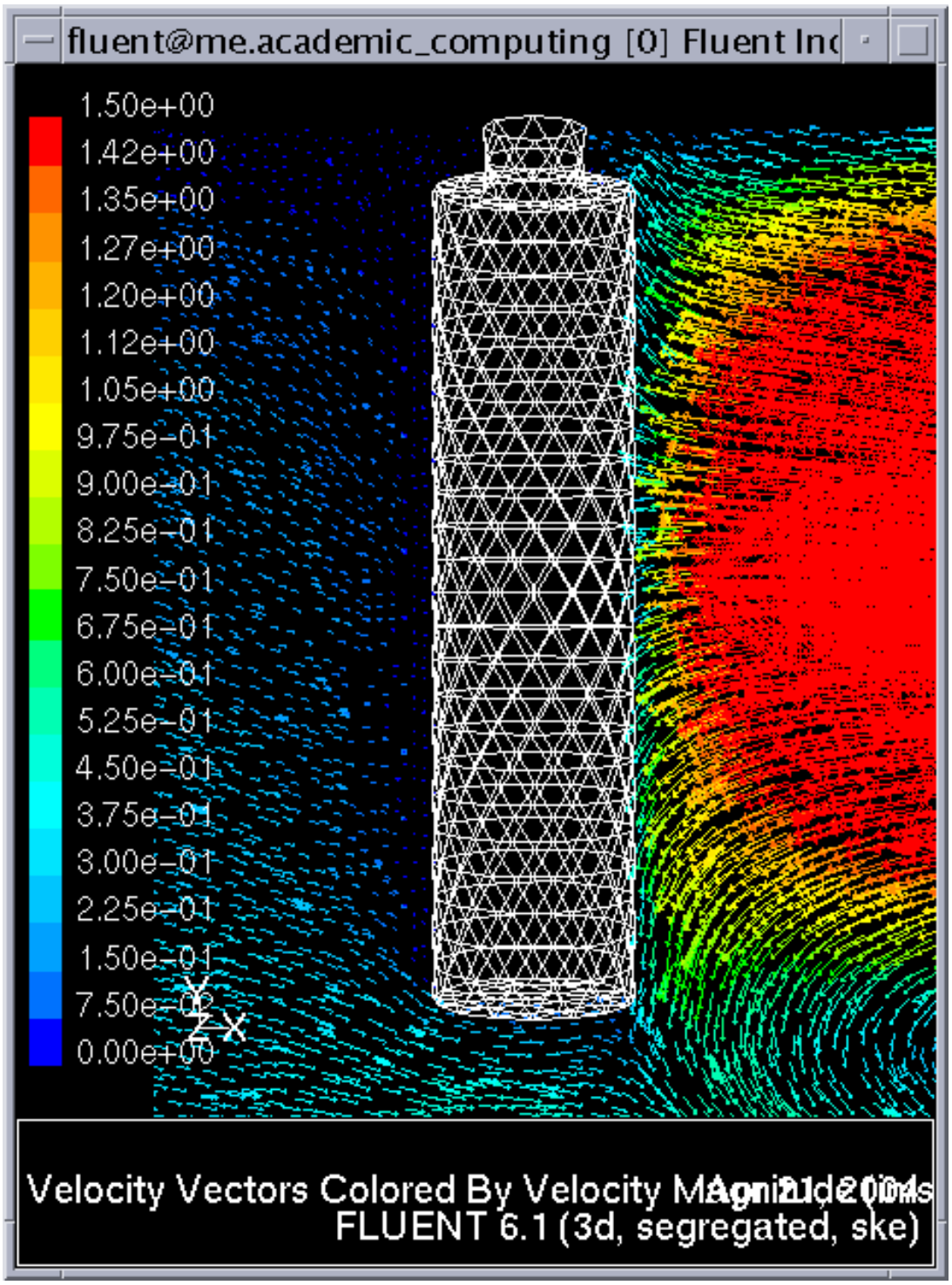

Figure 3.19: Vector plot sectioned at mid probe with a x-y plane, vertical, close up

Table 3.2 shows the velocities at mid length of the probe, right near the surface. The velocity at Position 1 is higher on the 45° case, than for the vertical case. Another major

difference is that the velocity at the sides of the probe, positions 3 and 7 are much higher for the vertical quench probe as compared to the 45° probe. Both have very low velocities at position 5.

Position	45° Quench	Vertical Quench
1	0.5	0.36
3	0.25	0.72
5	0.06	0.045
7	0.25	0.62

Table 3.2: Velocities at specified postions on the probe surface, (in/s)

Measurement of Probe Distortion

As described in the experimental plan the probes have been measured for distortion. The results are shown in Figures 3.20 – 3.25, using the same convention above for positions 1,3,5, and 7. Though the distortions are less than 0.1mm, it is possible to observe a significant trend in the distortion. In Figures 3.20 -3.23, where the quenchant was agitated according to Figure 3.1, the trend that developed shows that position 1 developed a concave bend and position 5 developed a convex bend. There is not a significant trend observed for positions 3 and 7. In Figures 3.24 and 3.25, where the quenchant was stagnant, there was no significant distortion.

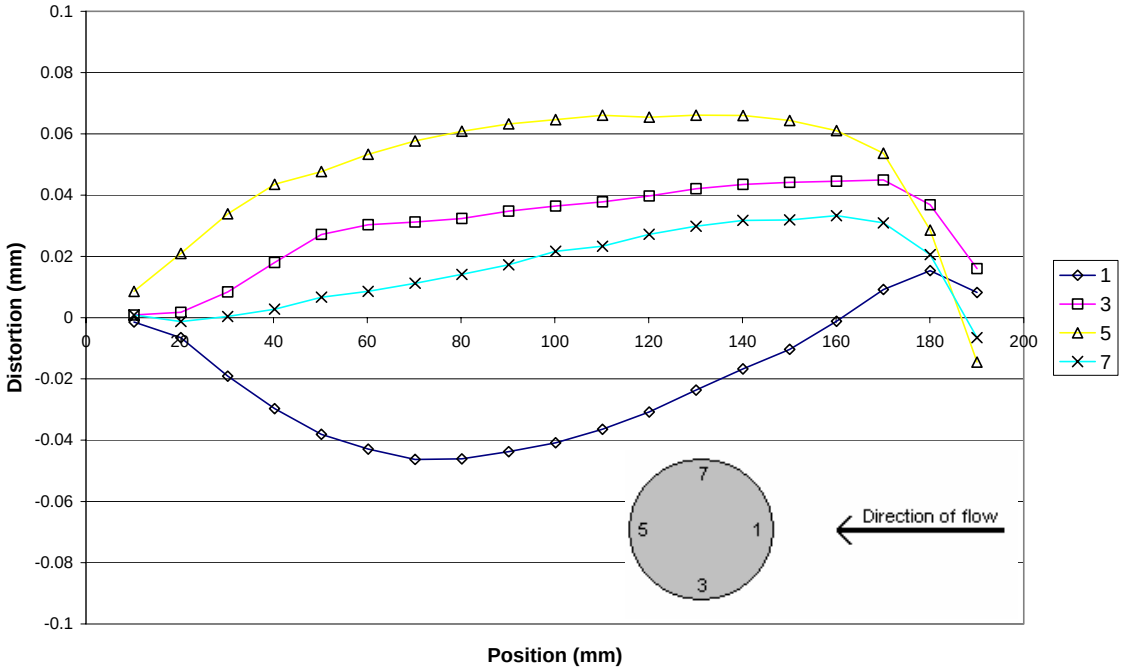

Figure 3.20: Probe 101 distortion measurement, quenched 45° in agitated Houghton T7A

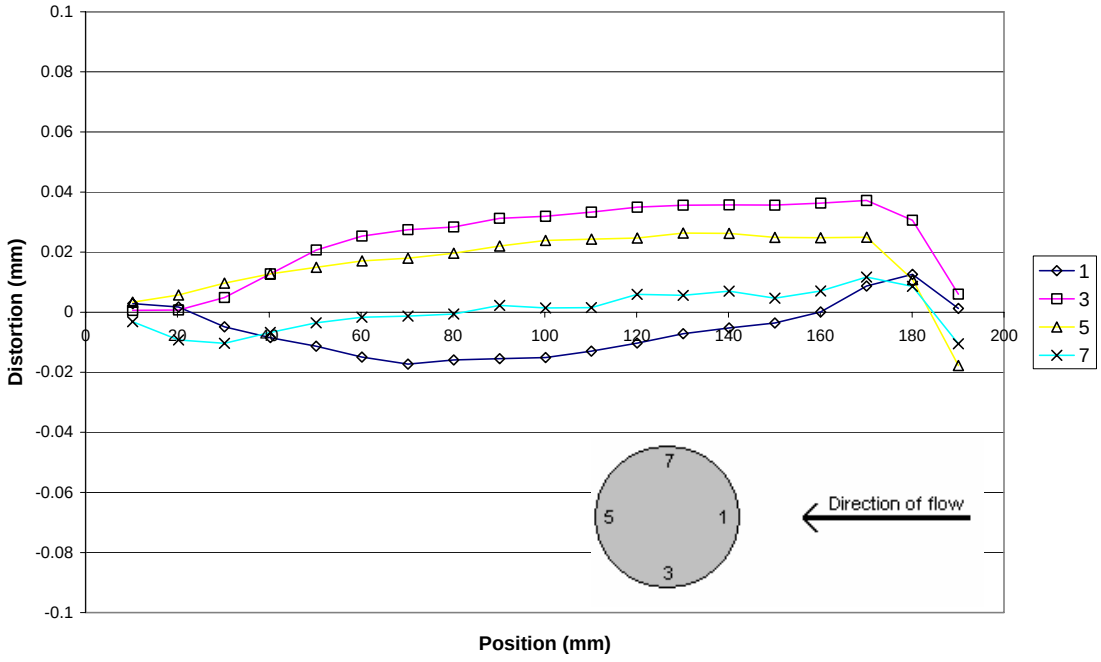

Figure 3.21: Probe 102 distortion measurement, quenched 45° in agitated Houghton T7A

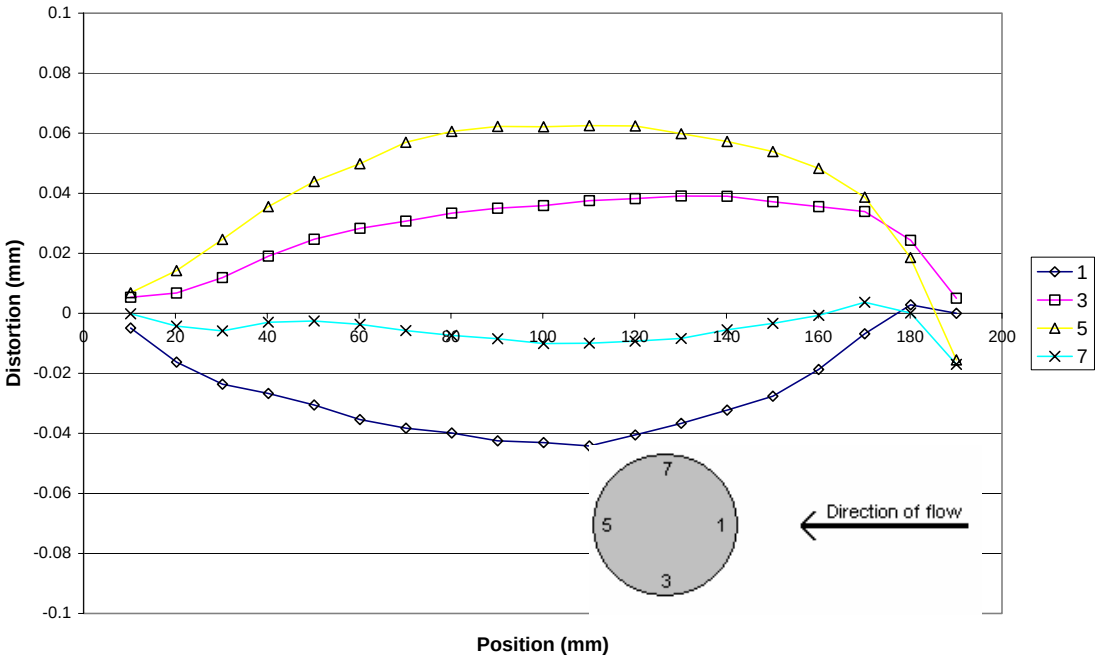

Figure 3.22: Probe 103 distortion measurement, quenched vertically in agitated Houghton T7A

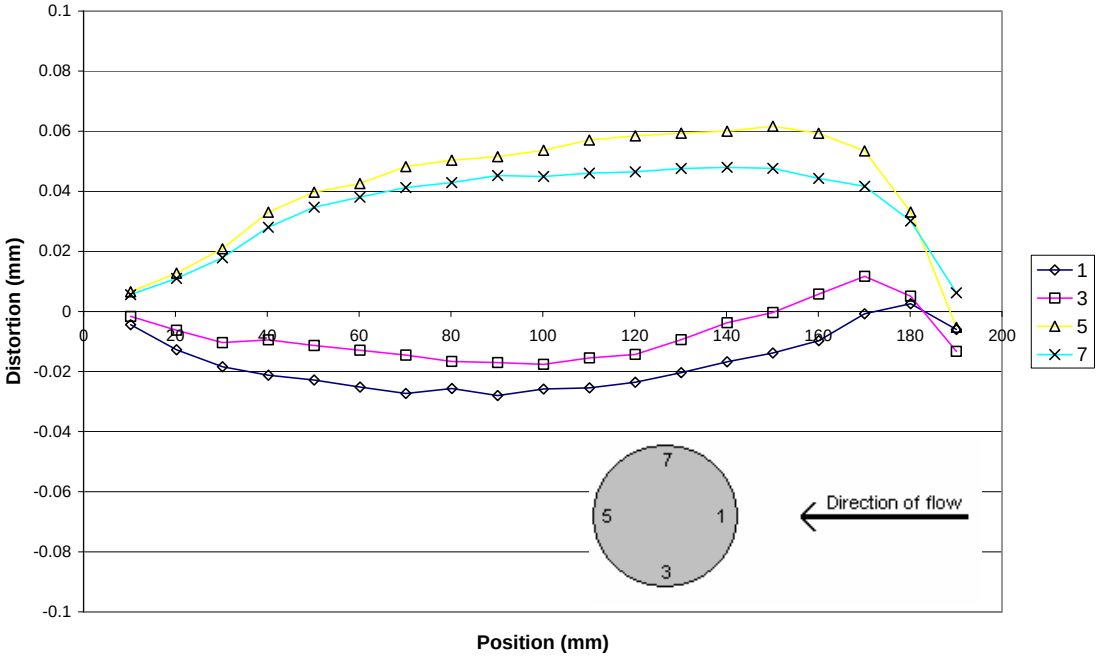

Figure 3.23: Probe 104 distortion measurement, quenched vertically in agitated Houghton T7A

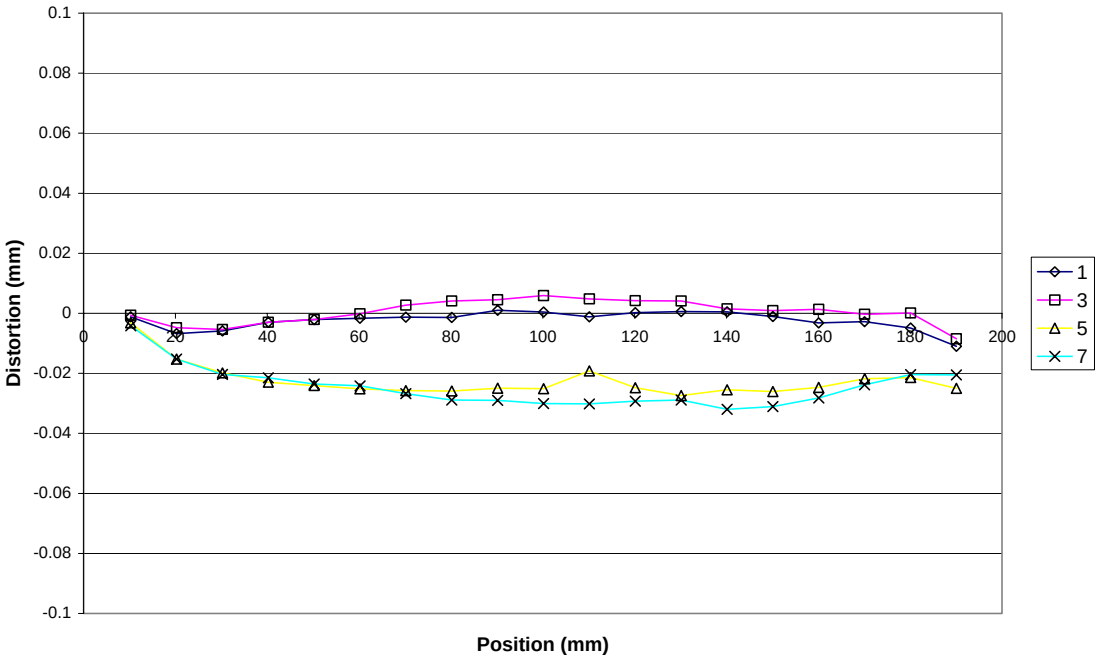

Figure 3. 24: Probe 106 distortion measurement, quenched 45° in stagnant Houghton T7A

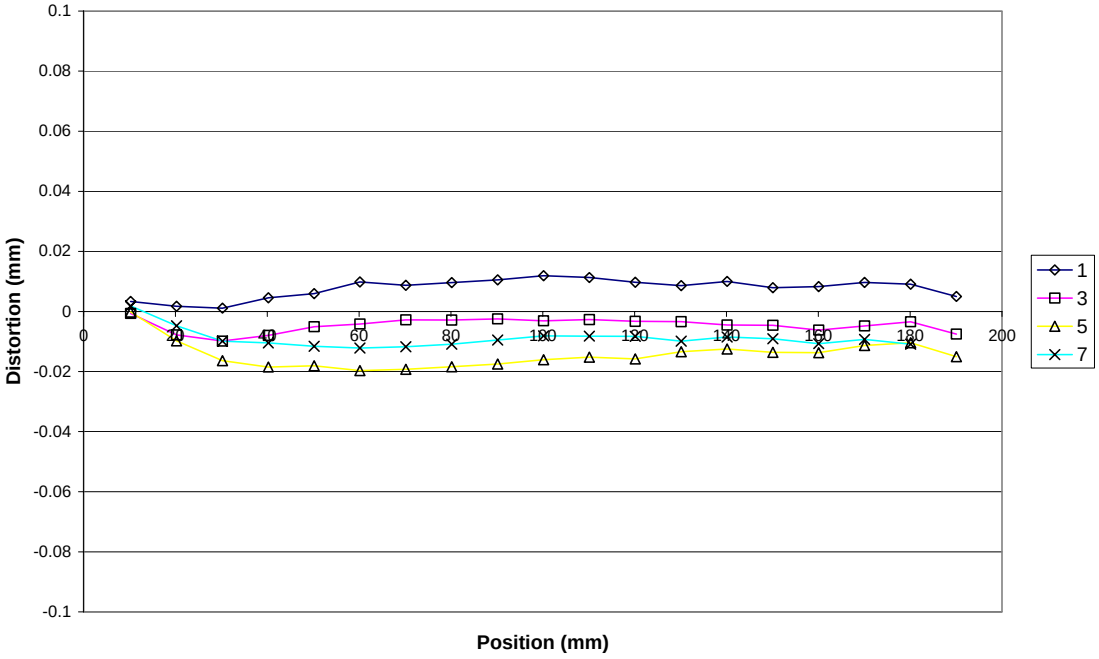

Figure 3.25: Probe 107 distortion measurement, quenched vertically in stagnant Houghton T7A

Residual Stress Values Post Quench

The residual stress was measured by X-Ray diffraction on the surface of each quenched probe. Figures 3.26 and 3.27 show the residual stress results for agitated probes and stagnant probes respectively. For the probes quenched in an agitated bath, Figure 3.8, the results show a low stress, both compressive and tensile, at position 1 and a large tensile stress at position 5. The results of positions 3 and 7 show a distinct similarity. Both have a similar range of tensile stresses. Figure 9 is the results of the stagnant quenched probes. Probe 106 was quenched at a 45^{o} immersion angle and probe 107 was quenched vertically. The results show a large tensile force around the entire surface of the probe. Probe 107 has a more uniform surface stress than that of 106. The data used to calculate the residual stress can be found in Appendix 1.

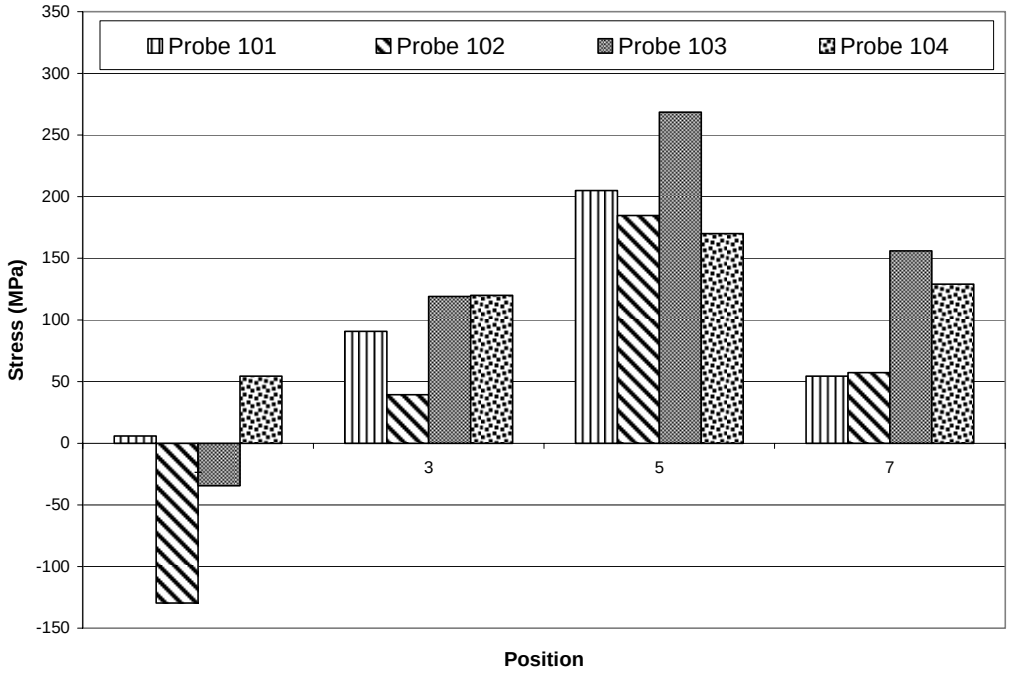

Figure 3.26: Residual Stress measured by XRD for probes 101-104

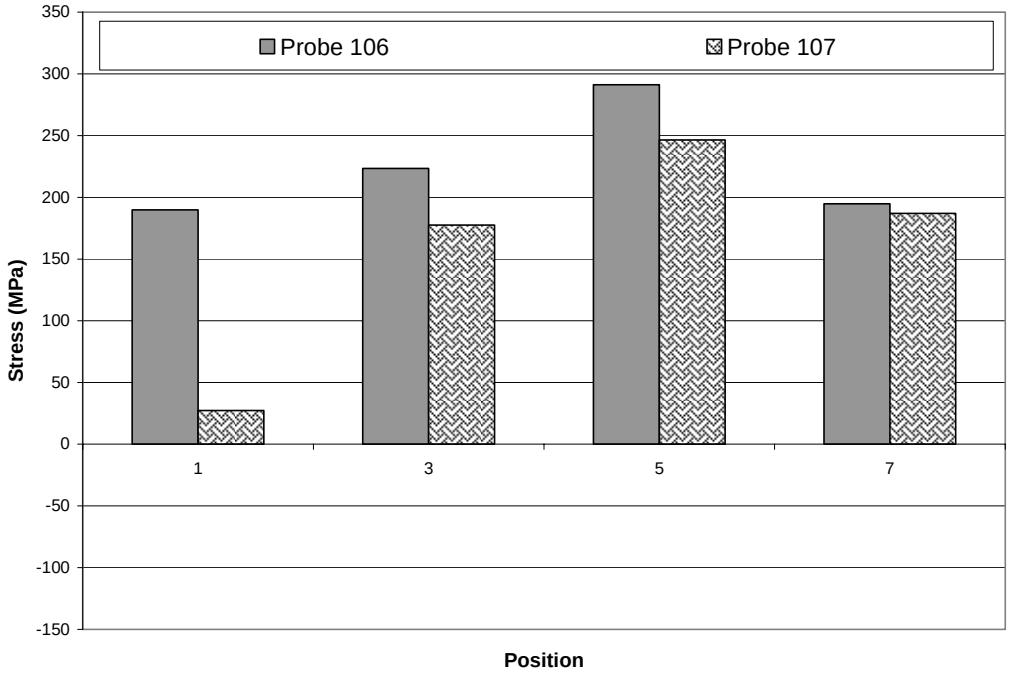

Figure 3.27: Residual Stress measured by XRD for probes 106 and 107

Table 3.3 shows the residual stress values in a tabular format. The values are in MPa.

Position	**Probe 101**	**Probe 102**	**Probe 103**	**Probe 104**	**Probe 106**	**Probe 107**
1	5.9	-129.6	-34.5	54.5	189.9	27.3
3	90.8	39.4	119.1	120	223.5	177.5
5	204.9	184.7	268.6	170	291.2	246.5
7	54.4	57.3	156	129.1	194.8	187

Table 3.3: Residual Stress values for each probe.

Longitudinal Hardness Results

The results are shown in Figures 3.28 – 3.33 in terms of Rockwell hardness and percent martensite vs. length. The same numbering convention is used as in other sections. For 4140 steel the maximum obtainable hardness is 57.1 Rockwell C. In only one case, probe 101, the surface hardness reached the maximum obtainable hardness, and only did this at position 1. The trend that developed was expected. Position 1 has a higher hardness value than position 5. One thing that was not consistent was the hardness for positions 3 and 7. In some of the probes 3 and 7 had similar hardness to that of position 1, and in the others 3 and 7 had similar hardness to position 5. Being able to relate the hardness value to the percent martensite formed gives insight into how the residual stresses are formed. Table 3.4 gives the percent martensite formed for a particular hardness in a carbon steel of 0.42 wt% C.

Rockwell Hardness (C)	Fraction Martensite
57.1	0.99
53.4	0.95
50.9	0.90
47.3	0.80
43.4	0.50

Table 3.4: Rockwell hardness correlation to fraction martensite, ASM Heat Treating Handbook for 0.42wt% Plain Carbon Steel, [1, pg 80]

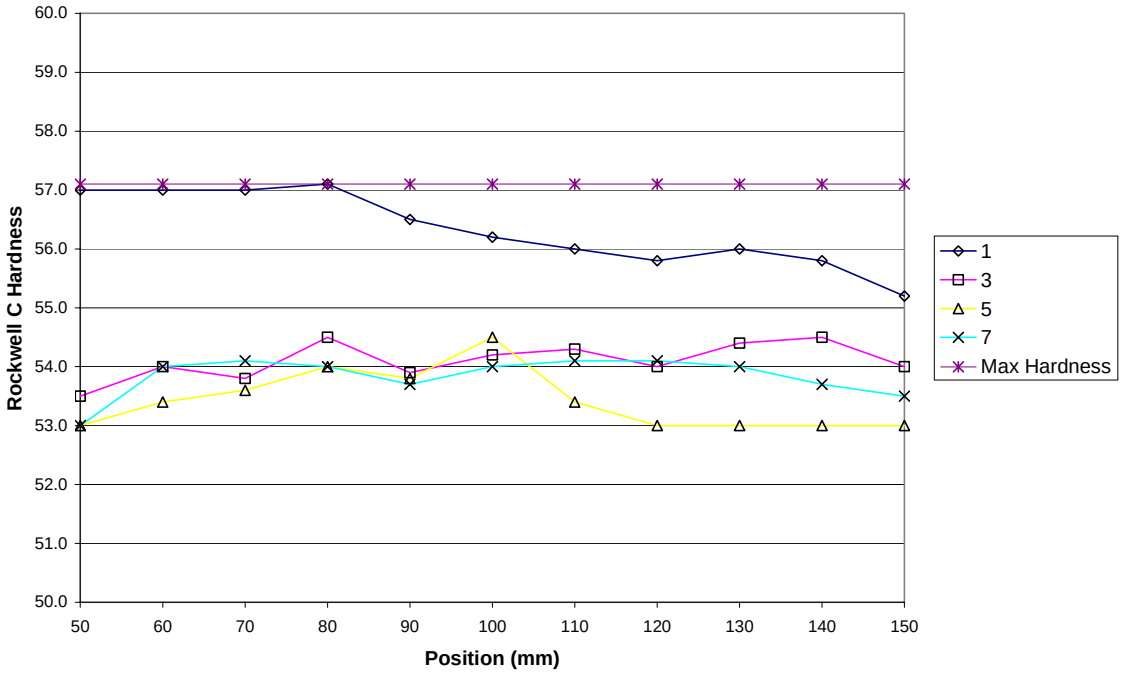

Figure 3.28: Probe 101 hardness measurement quenched at 45° in agitated T7A

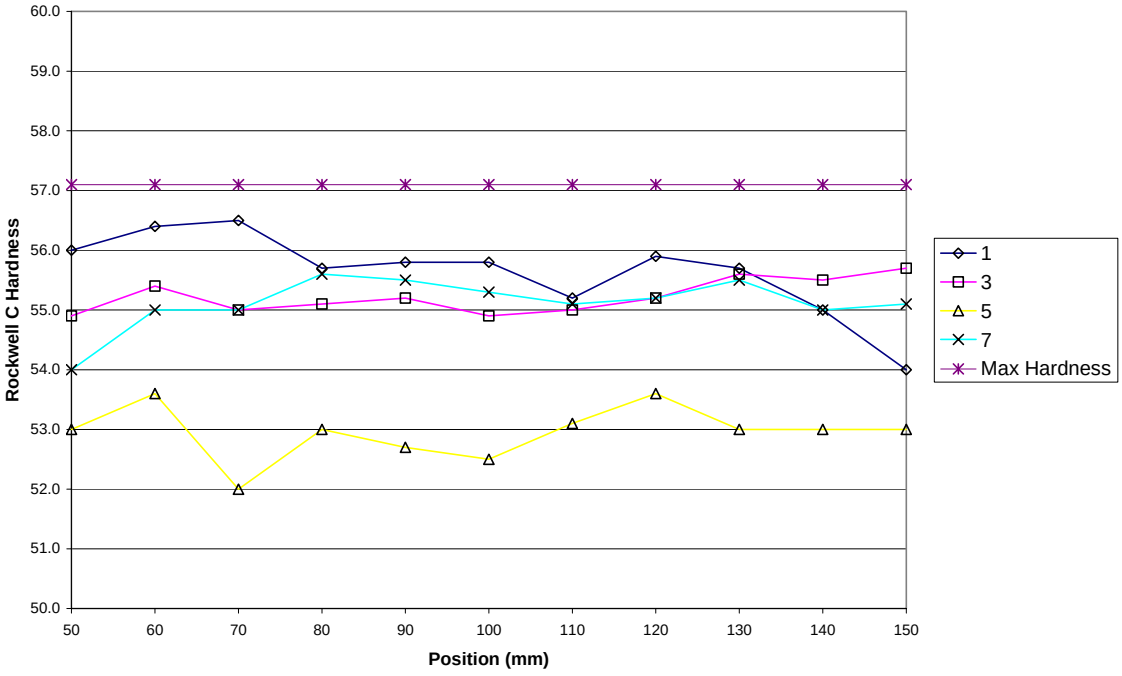

Figure 3.29: Probe 102 hardness measurement quenched at 45° in agitated T7A

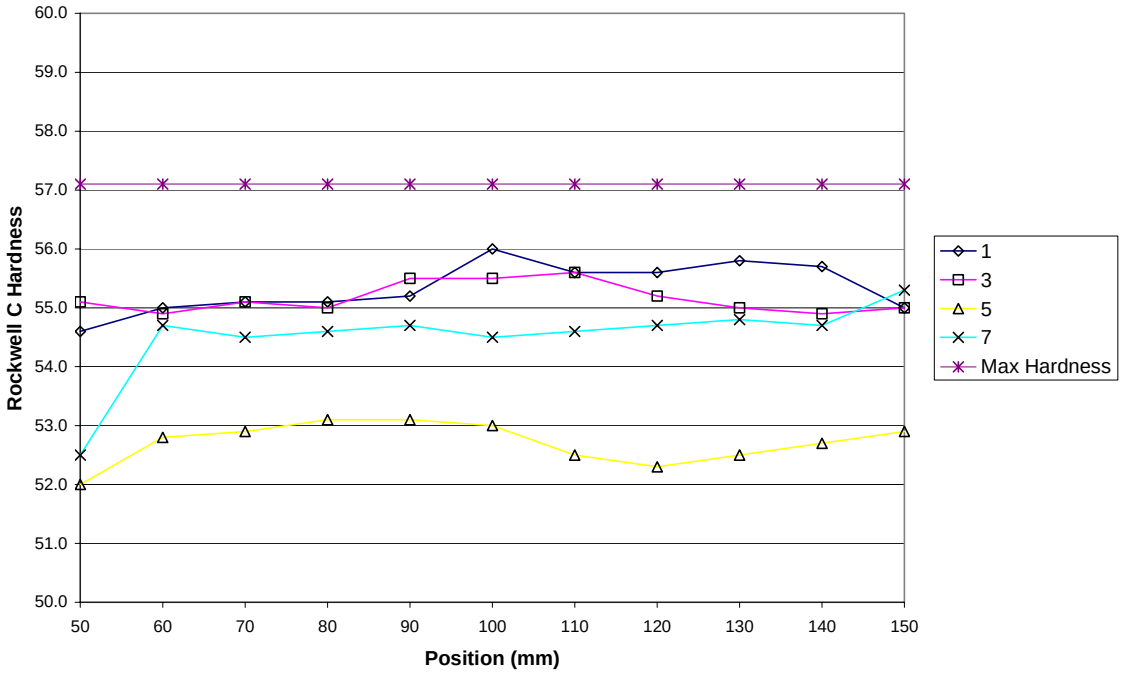

Figure 3.30: Probe 103 hardness measurement quenched vertically in agitated T7A

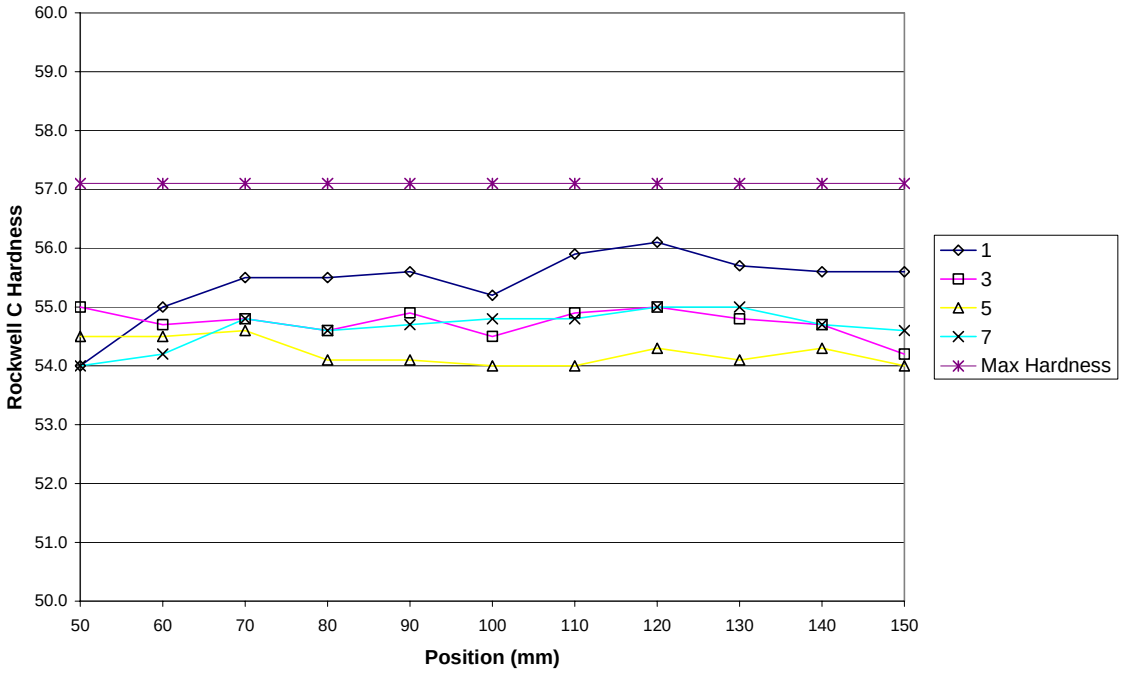

Figure 3.31: Probe 104 hardness measurement quenched vertically in agitated T7A

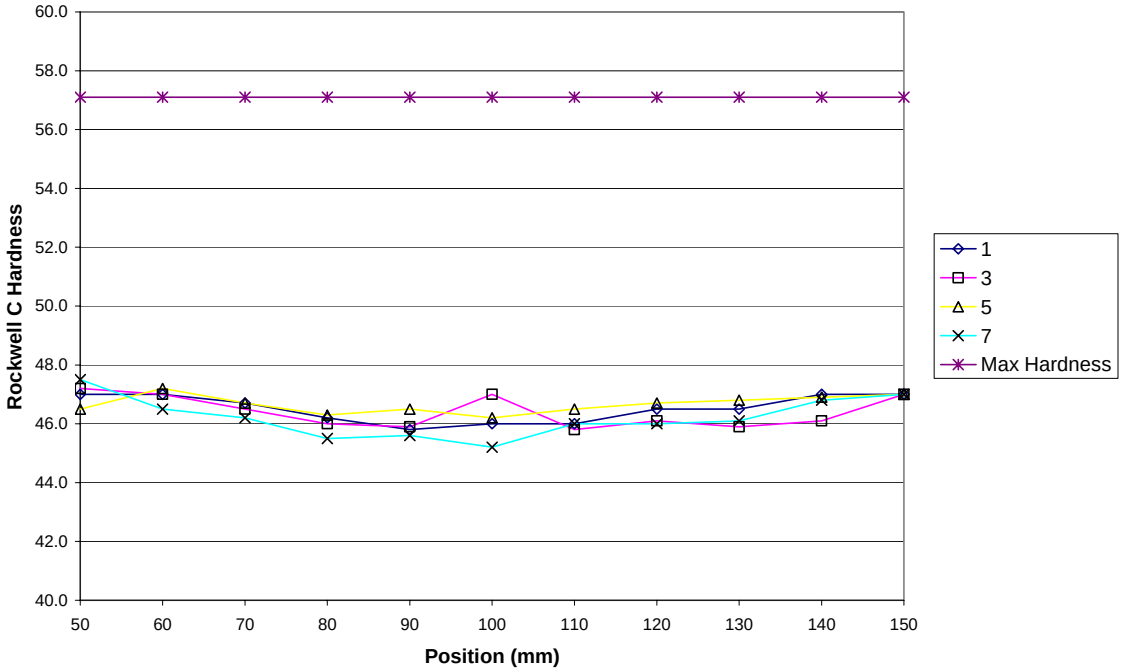

Figure 3.32: Probe 106 Rockwell hardness measurement, quenched 45˚ in stagnant T7A

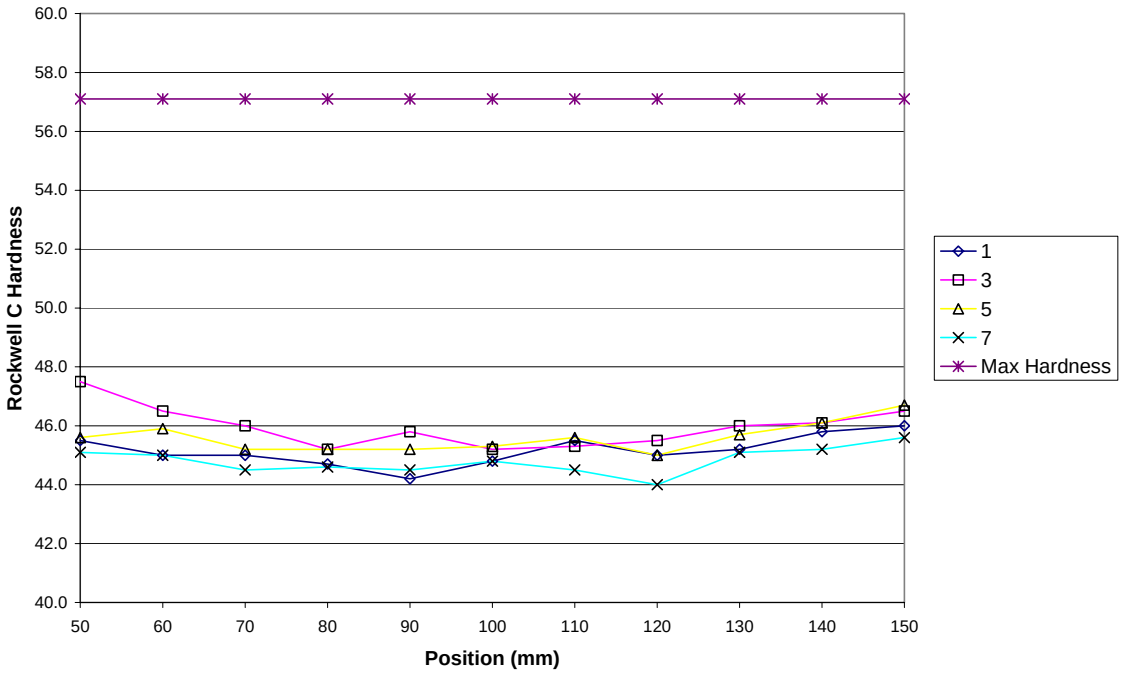

Figure 3.33: Probe 107 Rockwell hardness measurement, quenched vertically in stagnant T7A

Transverse Hardness Results

The results for the transverse hardness measurements are shown in Figures 3.34 and 3.35. Both Figures have all six probes shown. The measurements have been made at 3 mm increments starting 1 mm below the surface of the probe, continuing straight across from position 1-5 in Figure 3.34 and from position 3-7 in Figure 3.35. In Figure 3.34 from position 1 it shows that there is more hardening occurring. At a depth of 7mm from the surface position 1 the average hardness is 56.1 for all of the agitated samples vs. 54.9 at 7mm from surface position 5. Probe 6 and 7 show symmetry from one side to the other.

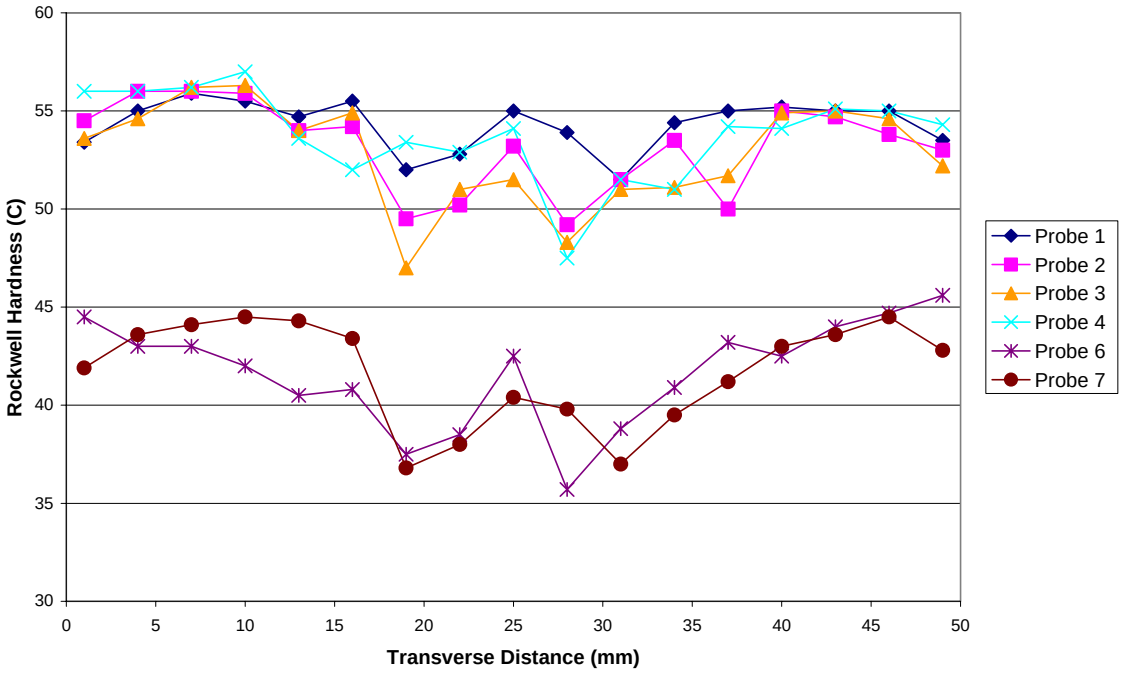

Figure 3.34: Transverse Hardness from position 1 across to position 5

In Figure 3.35 the hardness values show symmetry form position 3 to position 7 working for the outside in. Again for probes 6 and 7 there is symmetry.

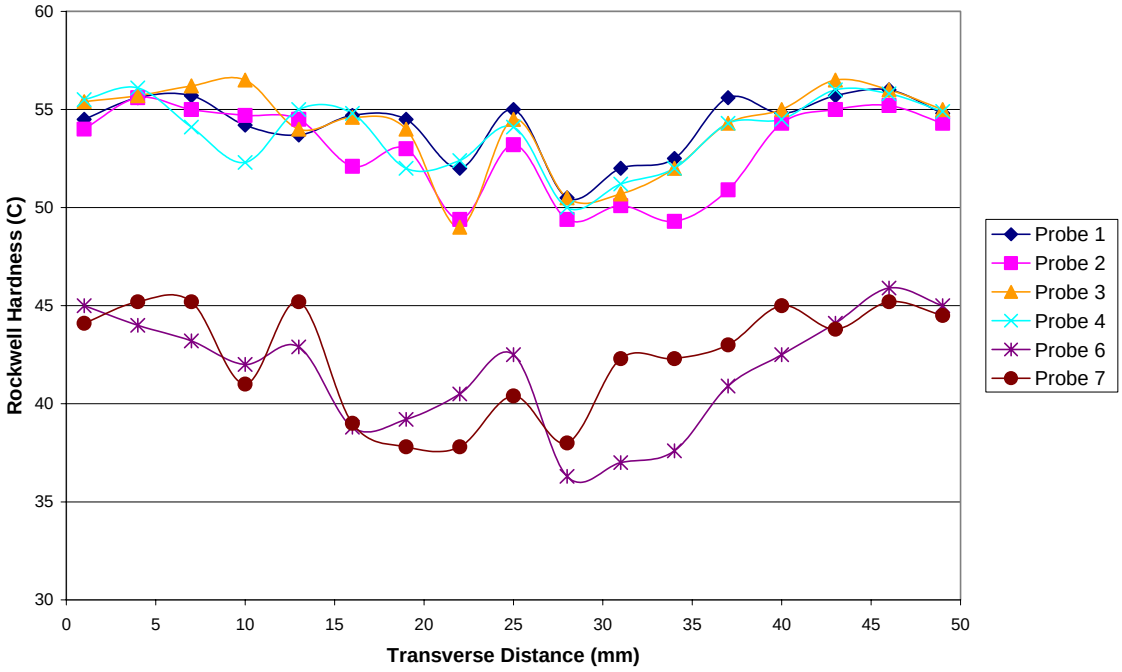

Figure 3.35: Transverse Hardness from position 3 across to position 7

Tables 3.5 and 3.6 are the raw data for the transverse hardness Figures 3.34 and 3.35 respectively.

		Probe 1	Probe 2	Probe 3	Probe 4	Probe 6	Probe 7
Position 1	1	53.4	54.5	53.6	56	44.5	41.9
	4	55	56	54.6	56	43	43.6
	7	55.9	56	56.2	56.2	43	44.1
	10	55.5	55.9	56.3	57	42	44.5
	13	54.7	54	54	53.6	40.5	44.3
	16	55.5	54.2	54.9	52	40.8	43.4
	19	52	49.5	47	53.4	37.5	36.8
	22	52.8	50.2	51	52.9	38.5	38
	25	55	53.2	51.5	54.1	42.5	40.4
	28	53.9	49.2	48.3	47.5	35.7	39.8
	31	51.5	51.5	51	51.5	38.8	37
	34	54.4	53.5	51.1	51	40.9	39.5
	37	55	50	51.7	54.2	43.2	41.2
	40	55.2	55	54.9	54.1	42.5	43
	43	55	54.7	55	55.1	44	43.6
	46	55	53.8	54.6	55	44.7	44.5
Position 5	49	53.5	53	52.2	54.3	45.6	42.8

Table 3.5: Hardness values for all probes from position 1 to position 5

		Probe 1	Probe 2	Probe 3	Probe 4	Probe 6	Probe 7
Position 3	1	54.5	54	55.4	55.5	45	44.1
	4	55.6	55.6	55.7	56.1	44	45.2
	7	55.7	55	56.2	54.1	43.2	45.2
	10	54.2	54.7	56.5	52.3	42	41
	13	53.7	54.5	54	55	42.9	45.2
	16	54.7	52.1	54.6	54.8	38.8	39
	19	54.5	53	54	52	39.2	37.8
	22	52	49.4	49	52.4	40.5	37.8
	25	55	53.2	54.5	54.1	42.5	40.4
	28	50.5	49.4	50.5	50	36.3	38
	31	52	50.1	50.7	51.2	37	42.3
	34	52.5	49.3	52	52	37.6	42.3
	37	55.6	50.9	54.3	54.3	40.9	43
	40	54.8	54.3	55	54.5	42.5	45
	43	55.7	55	56.5	56	44.1	43.8
	46	56	55.2	56	55.8	45.9	45.2
Position 7	49	54.8	54.3	55	54.9	45	44.5

Table 3.6: Hardness values for all probes from position 3 to position 7

Results Mid - Probe

The results have been presented in the previous sections. This section is intended to display the trends of those results. Table 3.7 displays the results of position 1 at mid length for probes 101 - 107. These results can be compared to that shown in Table 3.8 which displays the results for position 5 for the same probes. It is possible to see a trend in the results for all four specific measurements. Starting with distortion, for position 1

Position 1

Probe	XRD	CMM	Hardness (RC)	Flow (ft/s)
101	5.9	-0.041	56.2	0.5
102	-129.6	-0.015	55.8	0.5
103	-34.5	-0.043	56.0	0.4
104	54.5	-0.026	55.2	0..36
106	189.9	0.000	46.0	0.0
107	27.3	0.012	44.8	0.0

Table 3.7: Position 1 data for mid probe length

the results for probes 101 – 104 the distortion is negative with an average value of -0.03mm. This can be compared to that of position 5 which has an average value for

probes 101-104 of 0.05mm. Similarly the results of the residual stress have a trend between positions 1 and 5.

Position 5

Probe	XRD	CMM	Hardness (RC)	Flow (ft/s)
101	204.9	0.065	54.5	0.06
102	184.7	0.024	52.5	0.06
103	268.6	0.062	53.0	0.05
104	170.6	0.054	54.0	0.05
106	291.2	-0.025	46.2	0.0
107	246.5	-0.016	45.3	0.0

Table 3.8: Position 5 data for mid probe length

Position 1 exhibits a very low tensile stress or a compressive stress where as position 5 shows a fairly high tensile stress ~200MPa. For the hardness results position 1 has a higher Rockwell hardness for position 1 than it does for position 5. Looking at the results for positions 3 and 7 Table 3.9 and Table 3.10 respectively it is evident that the positions behave very similarly.

Position 3

Probe	XRD	CMM	Hardness (RC)	Flow (ft/s)
101	90.8	0.036	54.2	0.3
102	39.4	0.032	54.9	0.3
103	119.1	0.036	55.5	0.7
104	120.0	-0.018	54.5	0.7
106	223.5	0.006	47.0	0.0
107	177.5	-0.003	45.2	0.0

Table 3.9: Position 3 data for mid probe length

Position 7

Probe	XRD	CMM	Hardness (RC)	Flow (ft/s)
101	54.4	0.022	54.0	0.3
102	57.3	0.001	55.3	0.3
103	156.0	-0.010	54.5	0.7
104	129.1	0.045	54.8	0.7
106	194.8	-0.030	45.2	0.0
107	187.0	-0.008	44.8	0.0

Table 3.10: Position 7 data for mid probe length

V Summary of Results

- For a 2 inch diameter 4140 steel probe, the orientation in respect to quenchant flow creates a nonuniform heat transfer coefficient around the probe. The results of distortion, residual stress and hardness support this statement.

- The results of the computational fluid dynamics show that there is a mild difference between the vertical orientation, and the 45° orientation of the 2 inch diameter cylinder. There is a lower velocity at position 1 for the vertical case, versus the 45° case. For the 45° case there is also a directional flow sweeping up the probe which may increase the cooling rate during the nucleate boiling phase. Both orientations exhibit nearly stagnant flow at position 5.

- The results for distortion show that the bending that occurred during quenching was a result of nonuniform cooling as opposed to inhomogeneous phase transformation. The thermally induced stress during the initial stages of cooling exceded the yield stress of the probe at those temperatures causing plastic defromation. The martensite phase transformation may have occurred at different times during the quench, but due to the high degree of hardenablity of 4140 a nearly symmetrical transformation to martensite occurred, which can be seen in the hardness results. There was no distortion seen in the stagnant quenches.

- The residual stress is in agreement with the distortion results. For the agitated quenches (probes 101- 104) there was a tensile strain seen at position 5 and nearly

zero strain at position 1. The results for residual stress for the stagnant quenches show nearly uniform stress around the part.

- There was a higher hardness recorded at position 1 versus position 5 for the probes quenched in an agitated bath. Positions 3 and 7 showed similar results for all probes.

- The agitated probes exhibit a clear trend in distortion, residual stress, and hardness from position 1 to 5. At position 1 it is clear that there is a higher cooling rate / heat transfer rate as compared to position 5. The results of the stagnant flow show that there is really no trend, with distortion, residual stress and hardness as to be expected.

VI Conclusions

In conclusion it is apparent that quenchant flow around a cylinder does affect the properties produced. Agitation that has directional properties can affect the outcome of the quenched parts. When designing quench tanks it should be noted that the parts that are going to be quenched need to be oriented in a manner that does not favor one side versus the other.

4.0 Bibliography

[1]Bates, Charles E., Totten, George E. N.A. Clinton. *Handbook of Quenchants and Quenching Technology*. 1993: ASM International. p.70.

[2] R. Sisson Jr., M. Maniruzzaman, S. Ma, A. Varde, M. Takahashi and D. Rondeau, *Quenching - Understanding, Controlling and Optimizing the Process – II,* CHTE, WPI, Report no. 02-2, October 2002, Worcester, MA,USA.

[3] A. Varde, M. Takahashi, M. Maniruzzaman and R. Sisson Jr., *Webbased Data Mining for Quenching Analysis*, Proceedings from the 1st International Surface Engineering Congress and the 13th IFHTSE Congress, Columbus, OH, USA, 7-10 October 2002.

[4] M. Maniruzzaman, J.Chaves, C. McGee, S. Ma and R. Sisson Jr., *CHTE Quench Probe System: A New Quenchant Characterization System*, 5th International Conference on Frontiers of Design and Manufacturing (ICFDM), 619-625 (2002), USA.

[5] Chaves, J.C., *The Effect of Surface Condition and High Temperature Oxidation on Quenching Performance of 4140 Steesl in Mineral Oil*, in *Manufacturing Engineering*. 2001, Worcester Polytechnic Institute: Worcester. p. 8, 9.29.

[6] Fontecchio, Sisson. *Quench Probe and Quench Factor Analysis of Aluminum Alloys in Distilled Water,* 2002, Worcester Polytechnic Institute: Worcester.

[7]Bates, Charles E., Totten, George E. Robert L. Brennan. *Quenching of Steel*. ASM Handbook, Vol. 4 Heat Treating. ASM International. 1991. p. 67-118

[8] Fletcher, A.J. *Thermal Stress and Strain Generation in Heat Treatment*. New York, Elsevier Science Pub. Co 1989.

[9] Inoue, T., Nagaki, S., Kishino, T. and Monakwa, M. *Description of transformation kinetics, heat conduction and elastic – plastic stress in the course of quenching and tempering of some steels.* Ing.-Arch.,1982 pg 50.

[10] Bauccio, Michael. *ASM Metals Reference Book*. Third Edition, USA, 1993.

[11]Boyer, Howard E. *Quenching and Control of Distortion*, ASM International. 1988 p. 6,14

[12]Atkins, M. *Atlas of continuous cooling transformation diagrams for engineering steels.* USA, 1980.

[13]Ma, Shuhui. *Characterization of the Performance of Mineral Oil Based Quenchants Using CHTE Quench Probe System.* 2002, Worcester Polytechnic Institute: Worcester.
[14]Houghton, *Houghton On Quenching*, Houghton International. Inc.2000. p. 7.

[15] Charles E., Totten, George E. *Application of quench factor analysis to predict hardness under laboratory and production conditions*. in *The first International Conference on Quenching & Control of Distortion*. 1992. Chicago, Illinois.

[16] Sedighi, McMahon. *The influence of quenchant agitation on the heat transfer coefficient and residual stress development in the quenching of steels.* 2000. Proceedings of the Institution of Mechanical Engineers, Vol 214 Part B. pg 555-566

[17] Fischer, F.D. *Simplified calculation of temperature field in heat treated cylinder using temperature measured at one point.* J. Mater. Science and Technology., 1992.

[18] Palmer et al., *Tool Steel Simplified*, 4th ed, Chilton, 1978.

[19] Thelning, K.E., *Steel and Its Heat Treatment*, Butterworths, London, 1975. p. 584.

[20] Kunitake and Sugisawa, *Quench Cracking Susceptibility of Steel*, Sumitomo Search, 1971, p. 16-25.

[21] Rammersdorfer, F. Fischer, W. Mitter, J. Bathe. *On thermo-elastic-plastic analysis of heat-treatment processes including creep and phase changes.* Computers & Structures **13** 1981, p 771.

[22] Davis, J.R., *Metals Handbook*. 1990: ASM International. p. 197-199, 203.

[23] Smith, William F., *Structure and Properties of Engineering Alloys*. 2nd ed. 1993, New York: McGraw Hill. p.156.

[24] Unterweiser, Paul M., Boyer, Howard E. James J. Kubbs, ed. *Heat treater's guide: standard practices and procedures for steel*. 1982, American Society for Metals: Metals Park, Ohio.

[25] Cullity, *Elements of X-Ray Diffraction.* Prentice Hall, NJ, USA, 2001. pg. 450-457.

Appendix 1 (d vs. $\sin^2\psi$)

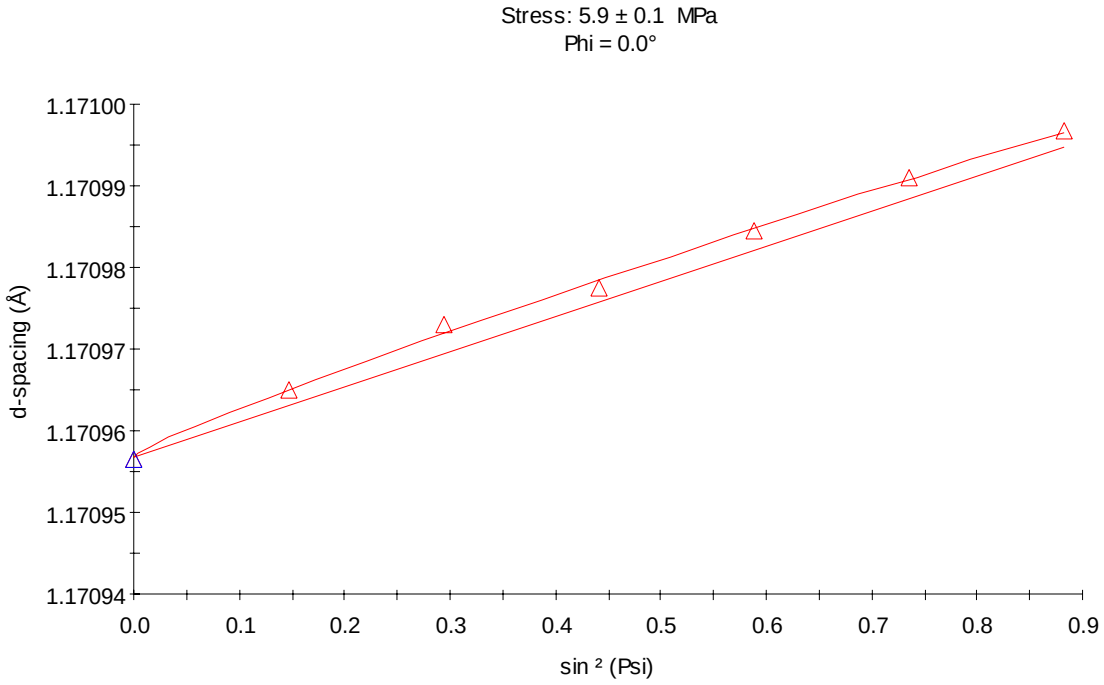

Figure A1-1, Probe 101 position 1

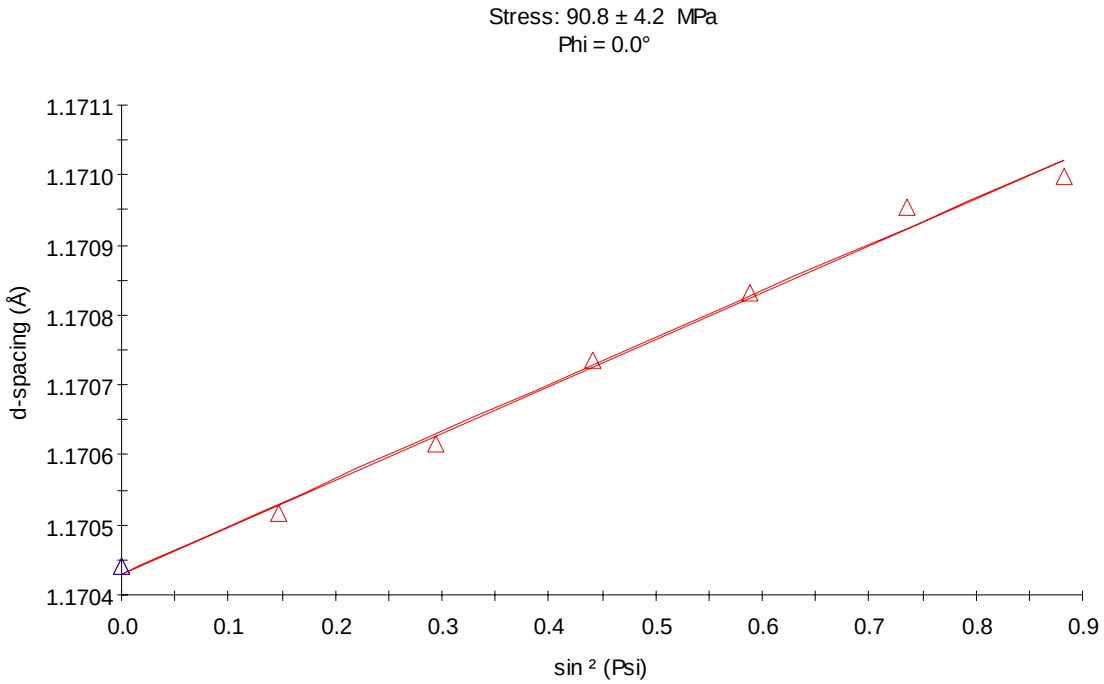

Figure A1-2, Probe 101 position 3

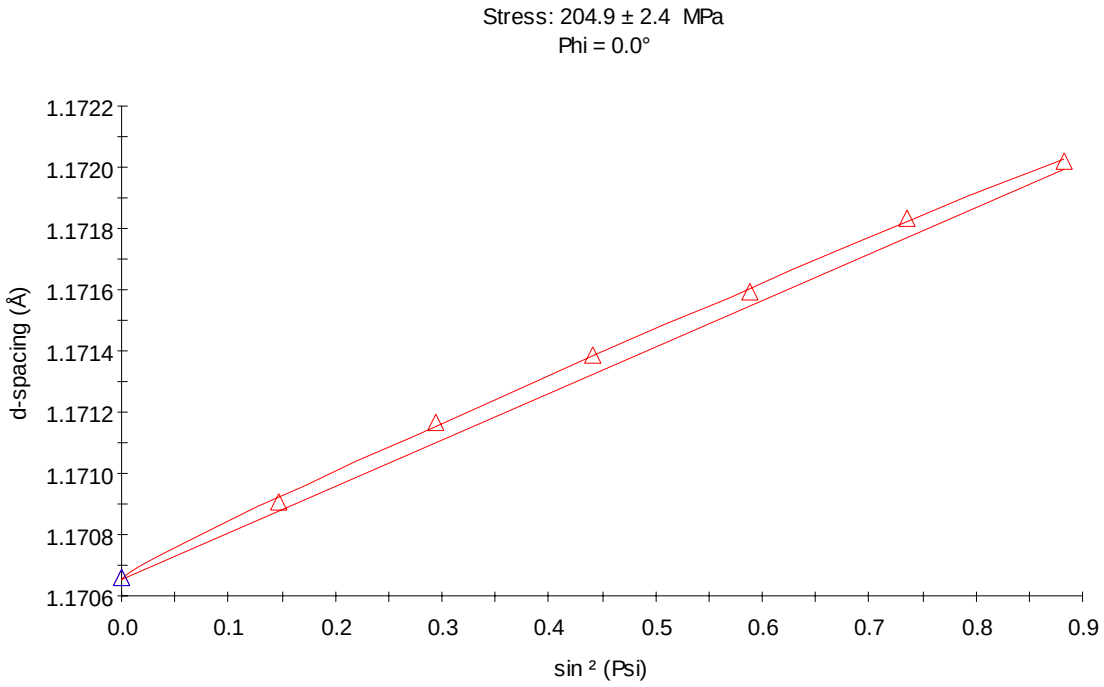

Figure A1-3, Probe 101 position 5

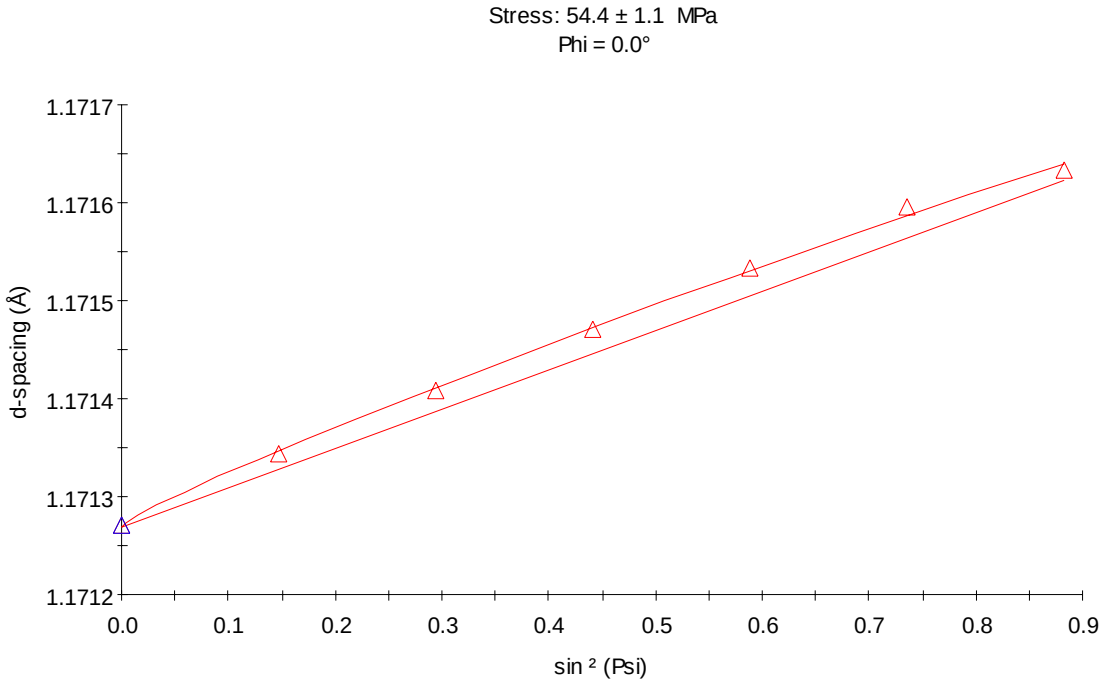

Figure A1-4 , Probe 101 position 7

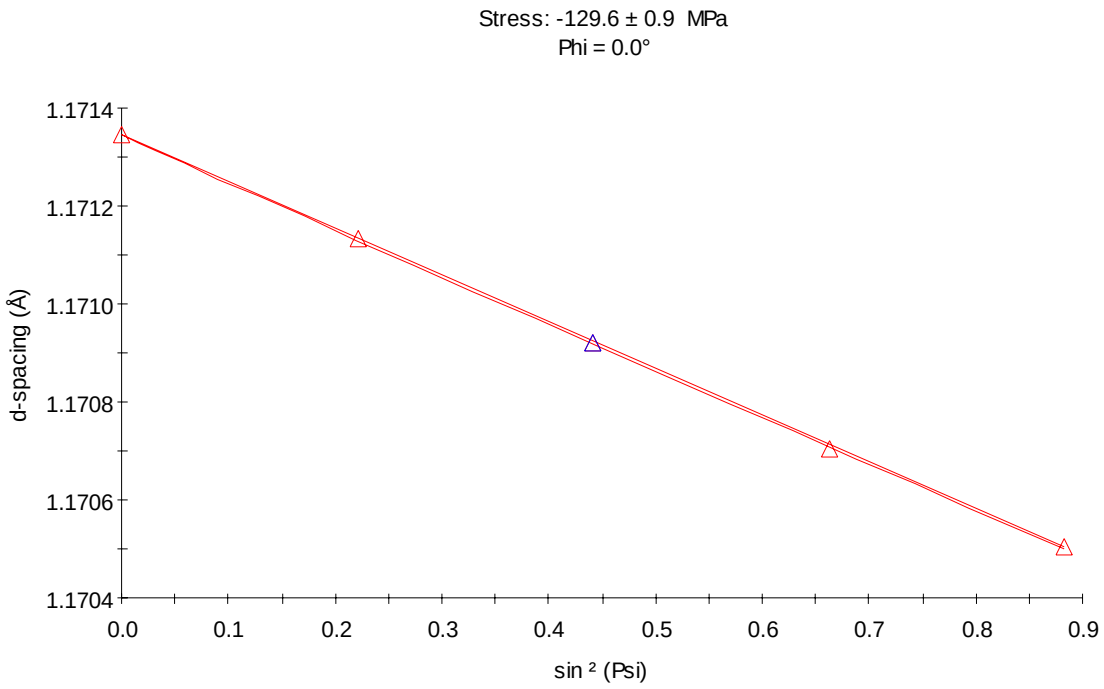

Figure A1-5, Probe 102 position 1

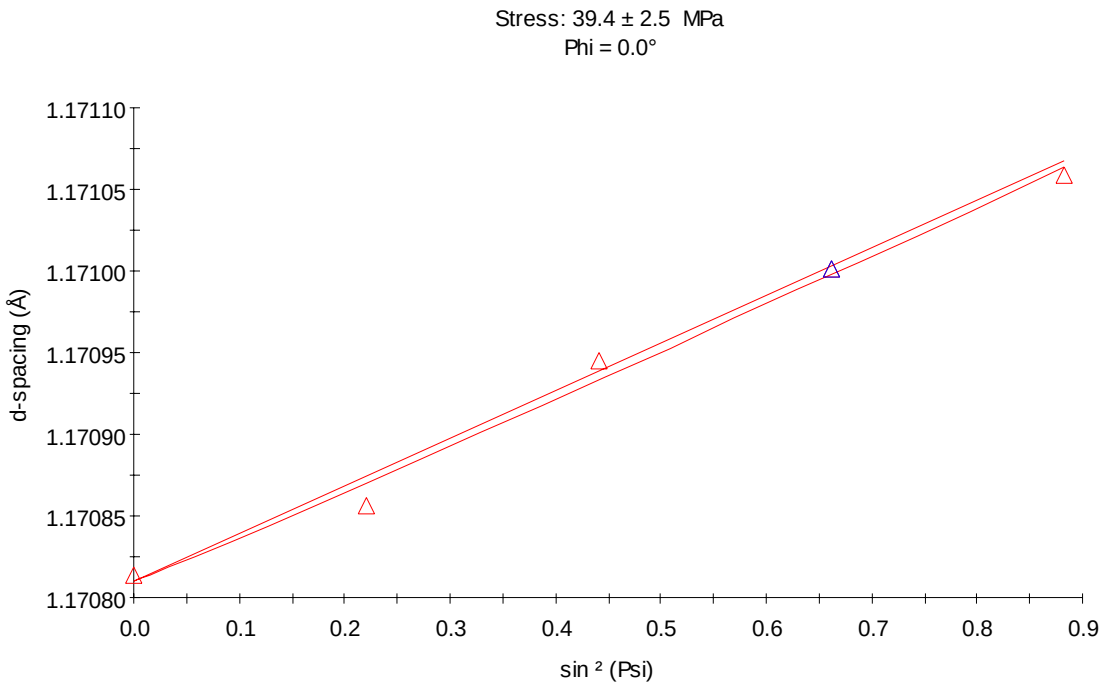

Figure A1-6, Probe 102 position 3

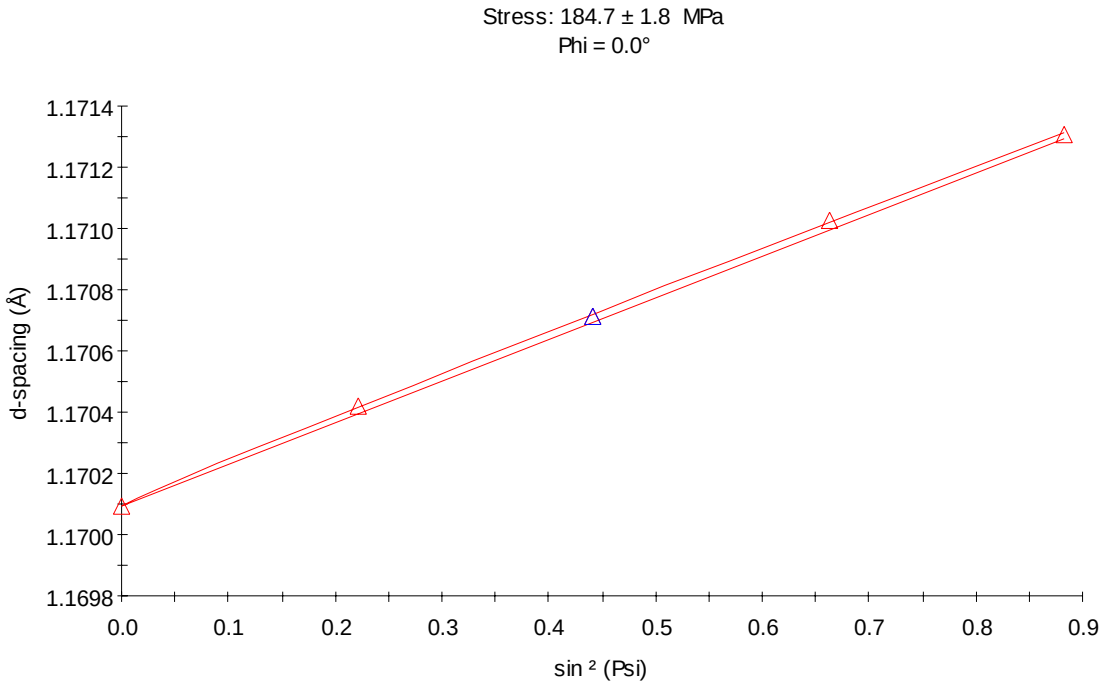

Figure A1-7, Probe 102 position 5

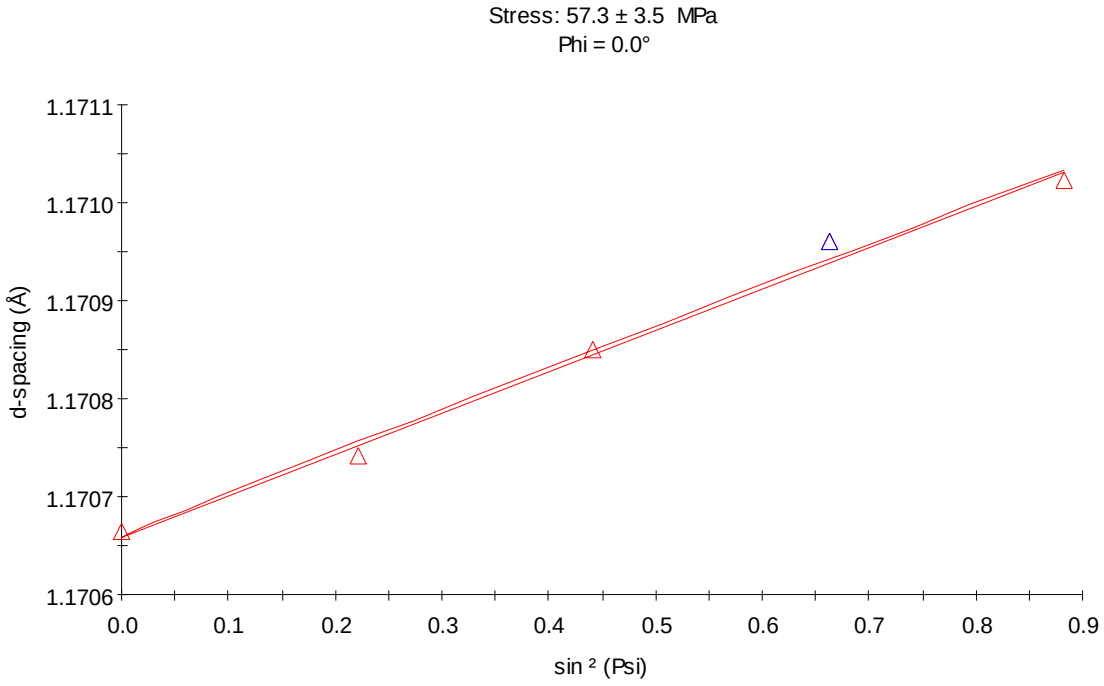

Figure A1-8, Probe 102 position 7

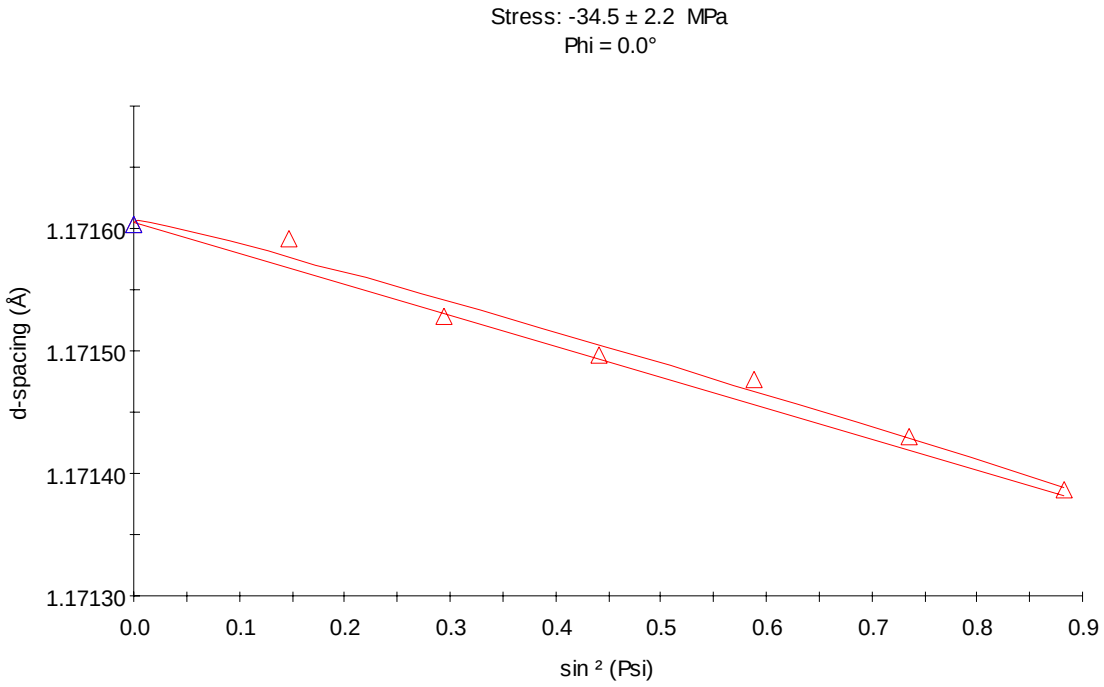

Figure A1-9, Probe 103 position 1

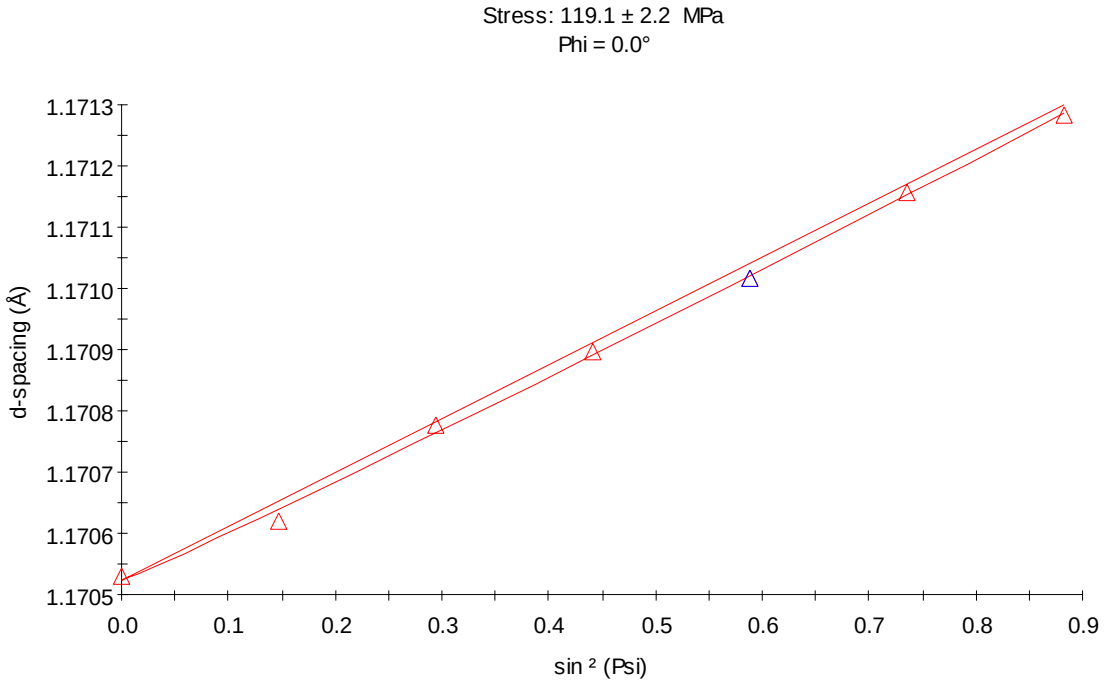

Figure A1-10, Probe 103 position 3

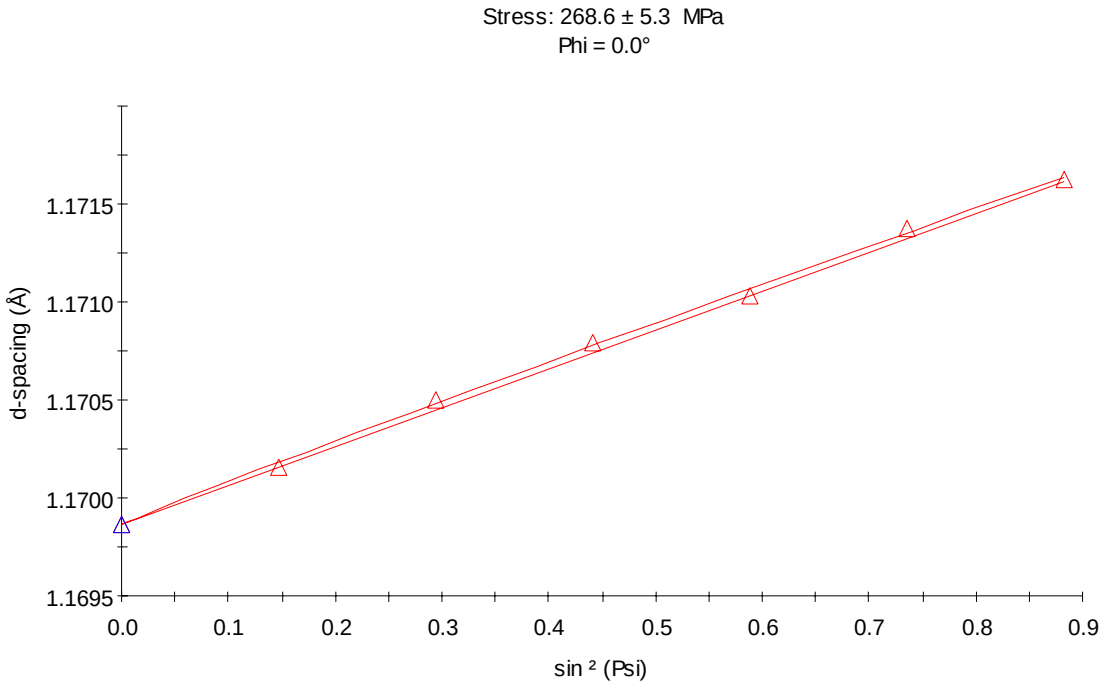

Figure A1-11, Probe 103 position 5

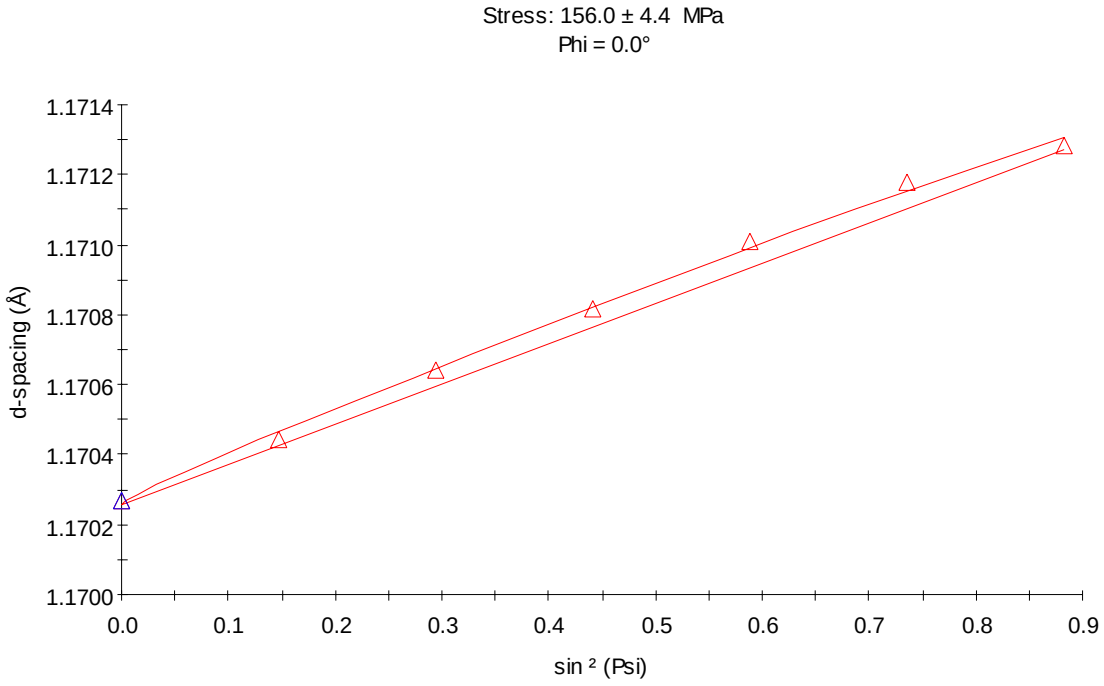

Figure A1-12, Probe 103 position 7

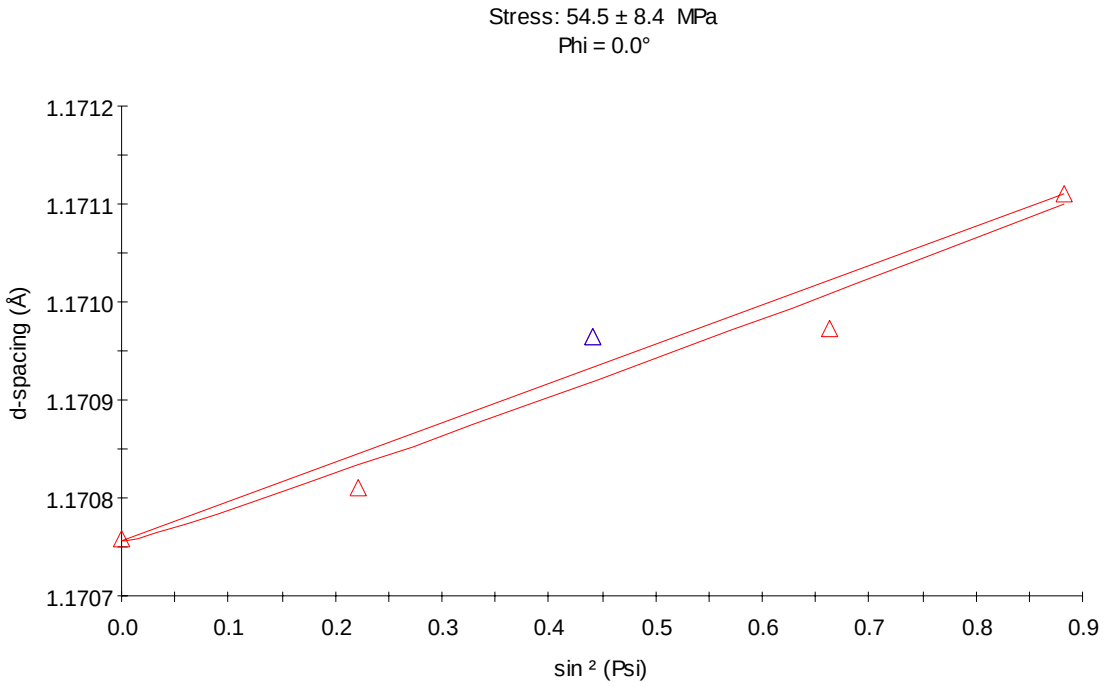

Figure A1-13, Probe 104 position 1

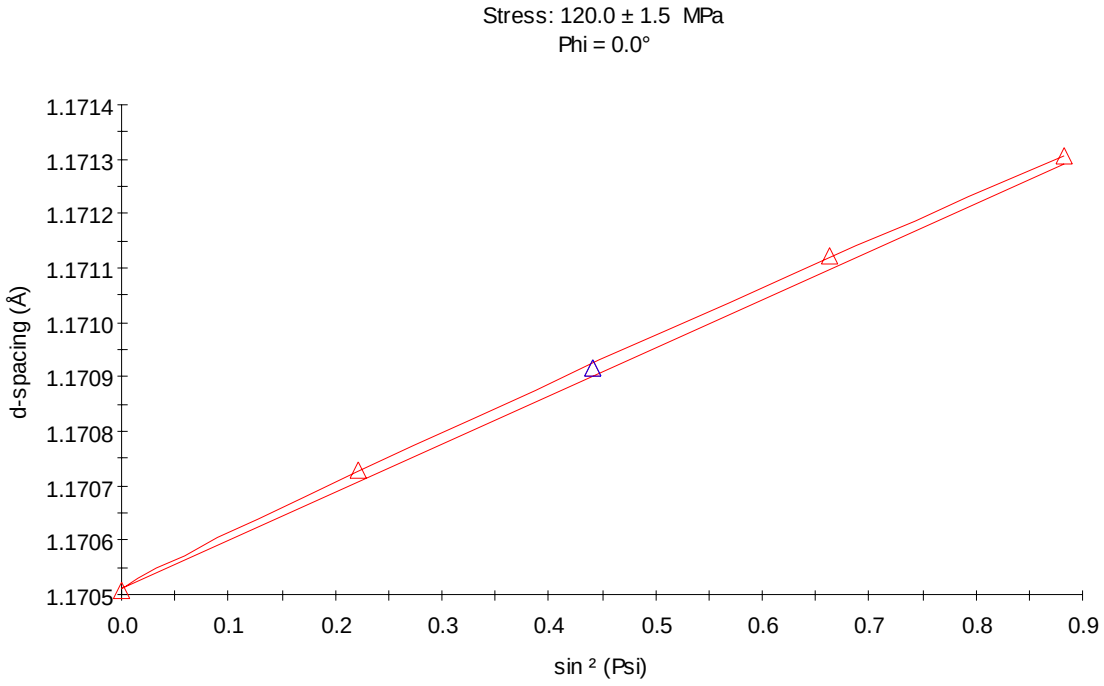

Figure A1-14, Probe 104 position 3

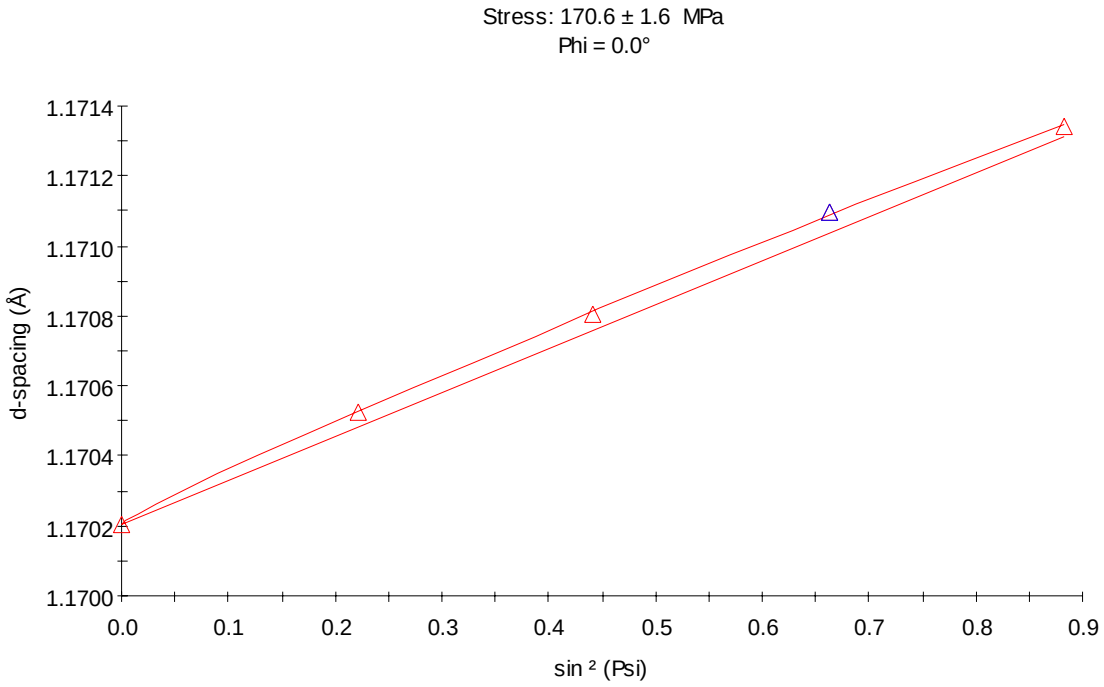

Figure A1-15, Probe 104 position 5

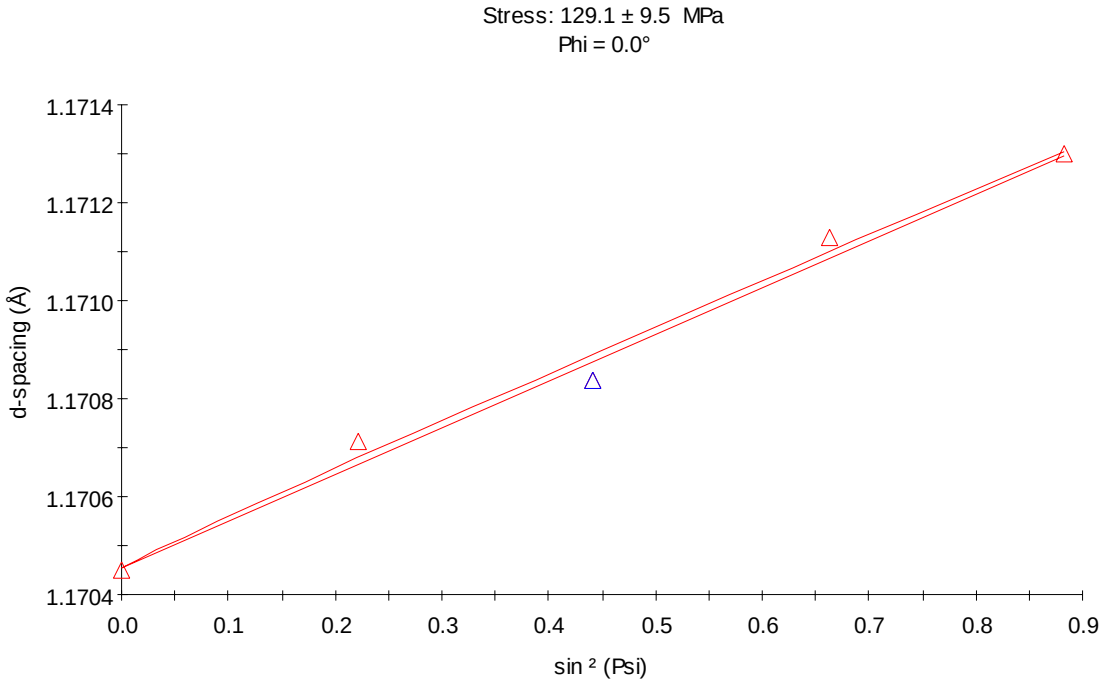

Figure A1-16, Probe 104 position 7

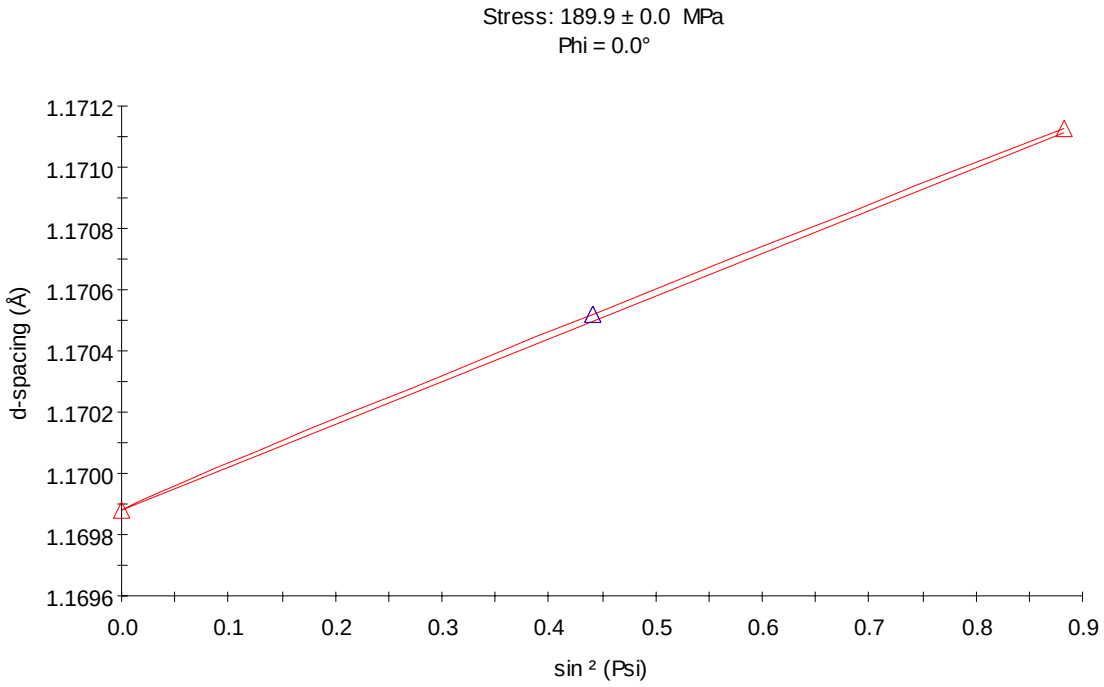

Figure A1-17, Probe 106 position 1

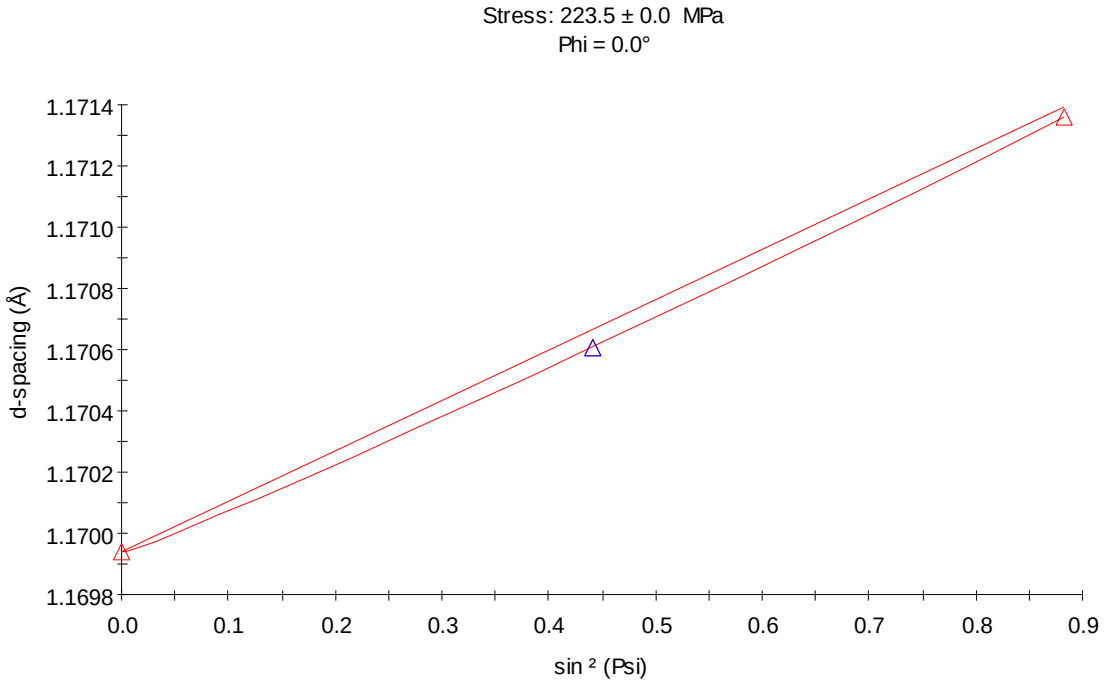

Figure A1-18, Probe 106 position 3

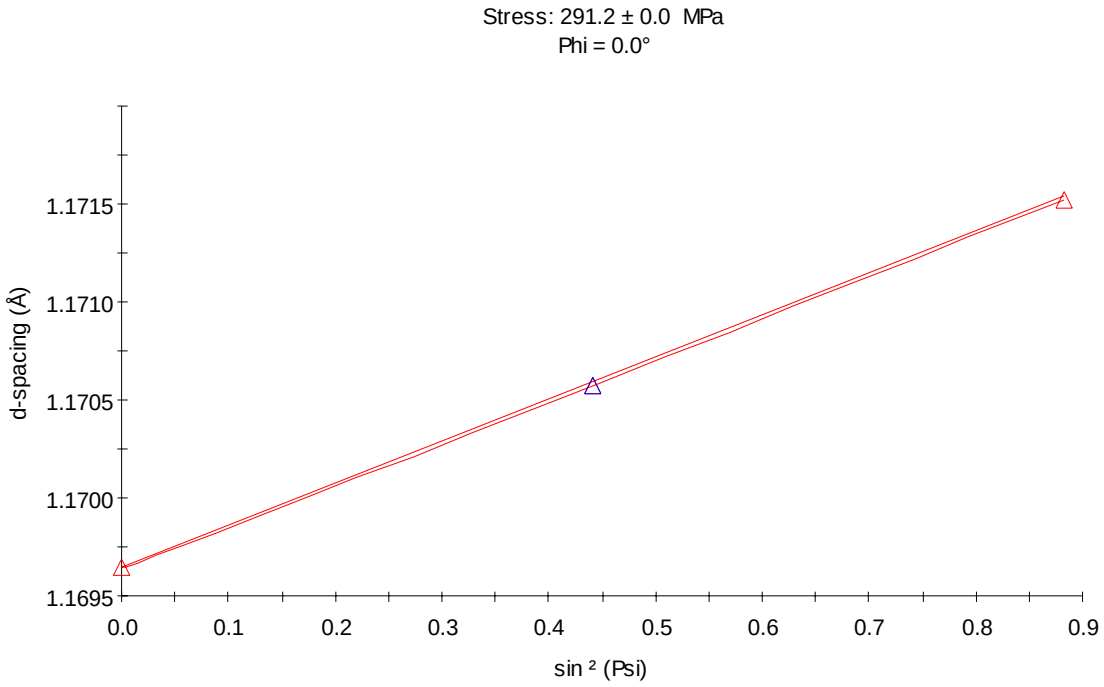

Figure A1-19, Probe 106 position 5

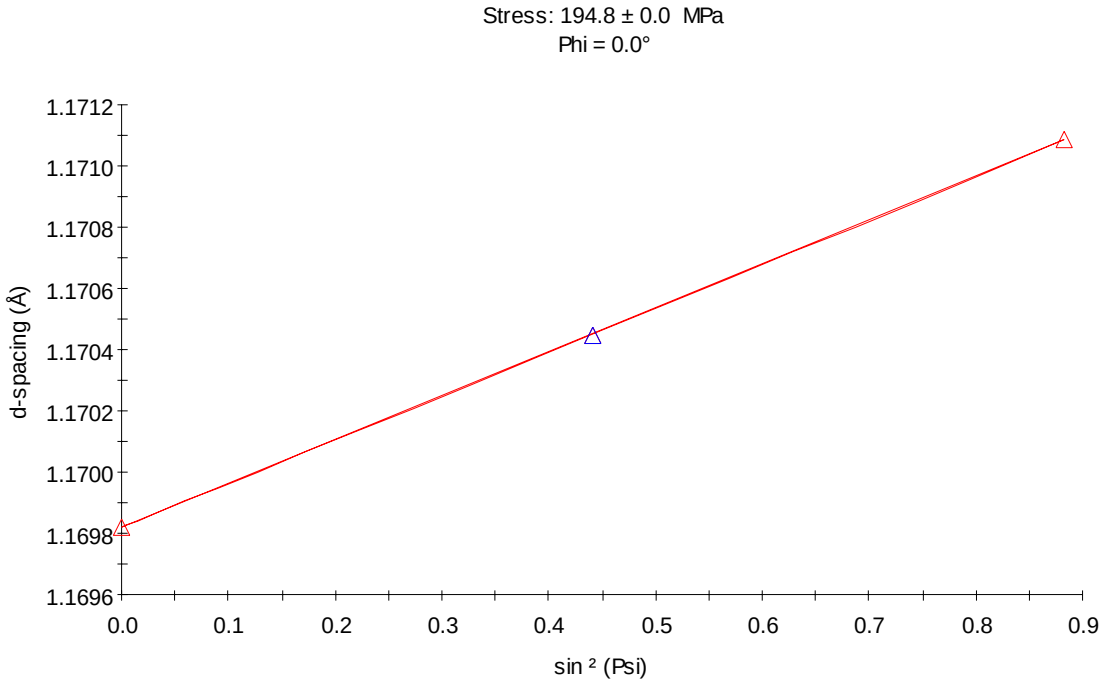

Figure A1-20, Probe 106 position 7

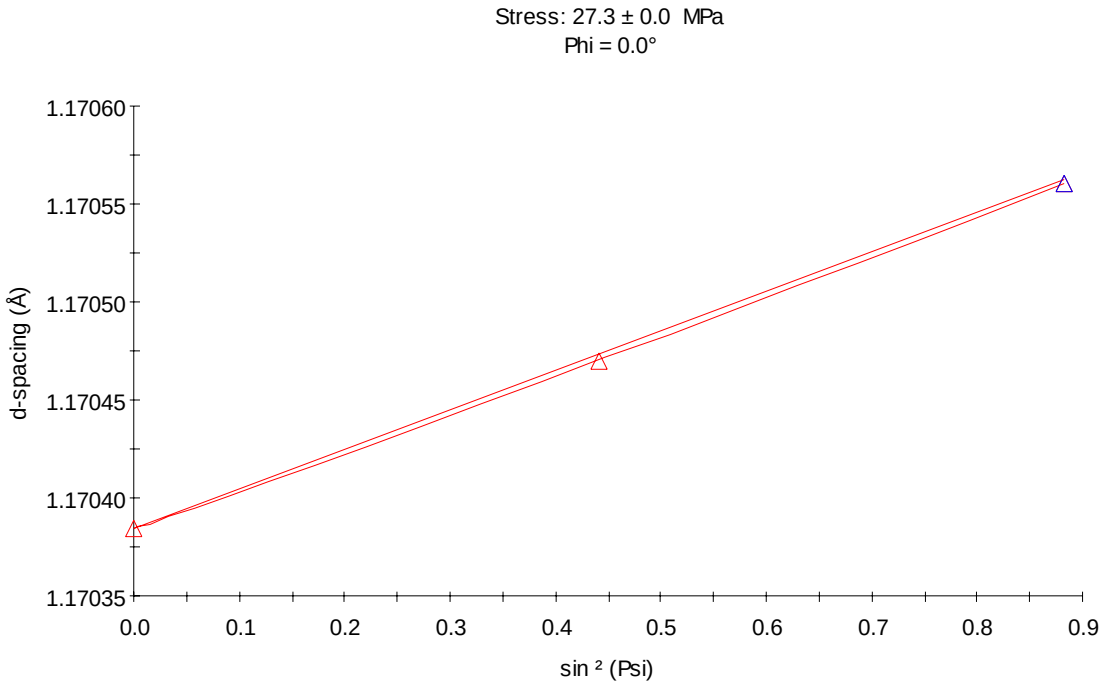

Figure A1-21, Probe 107 position 1

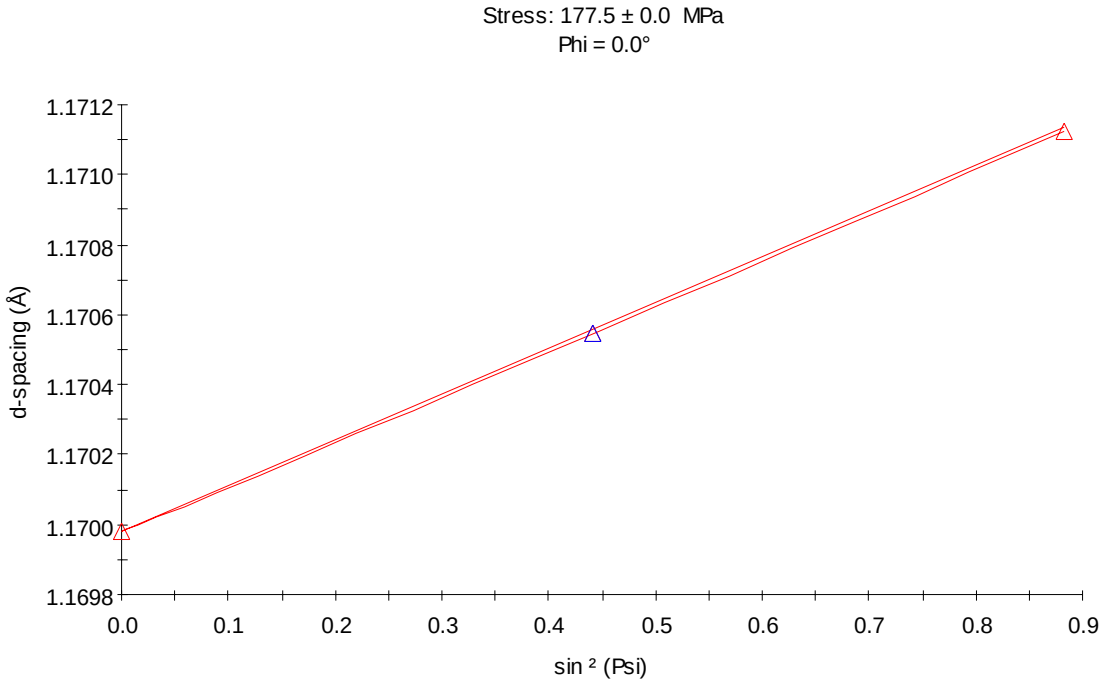

Figure A1-22, Probe 107 position 3

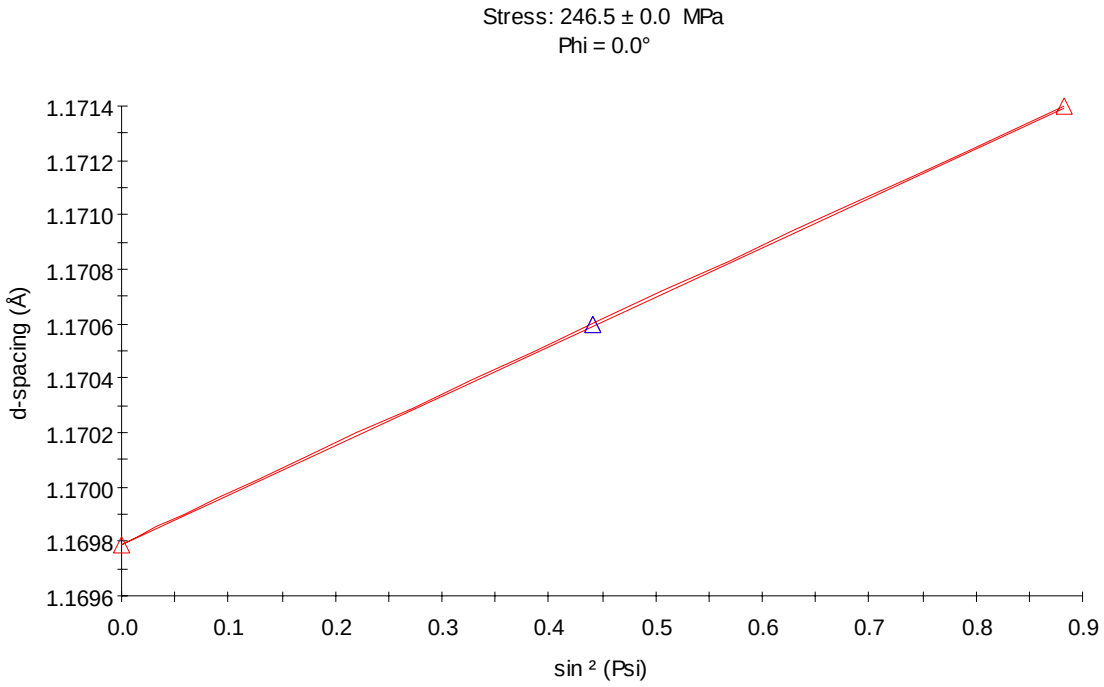

Figure A1-23, Probe 107 position 5

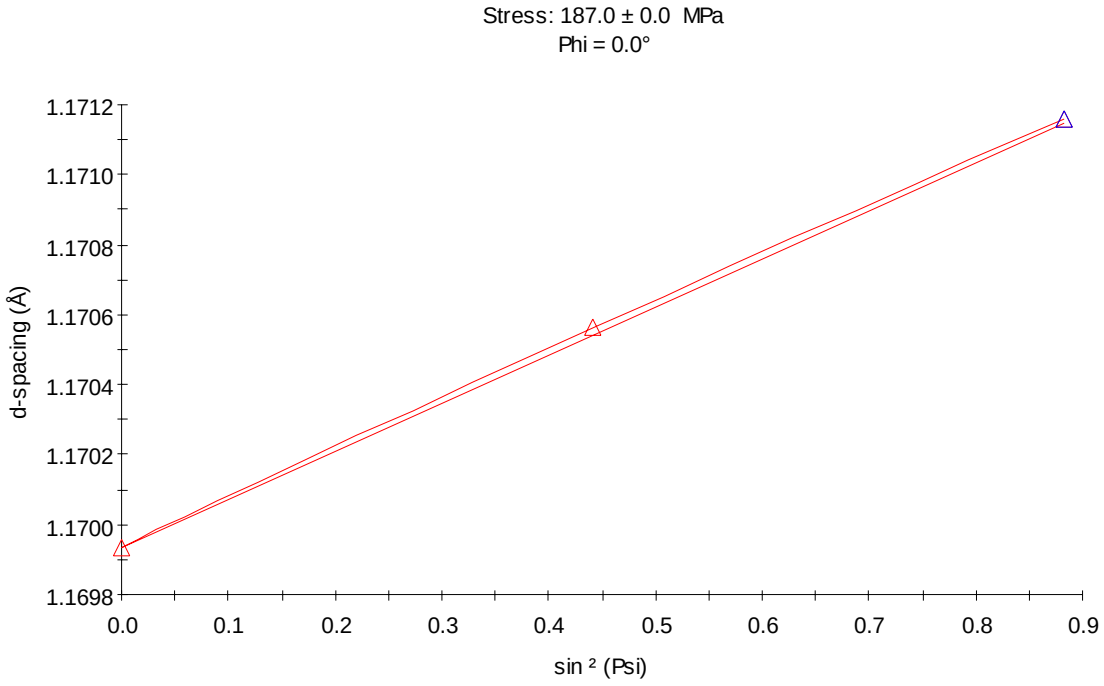

Figure A1-24, Probe 107 position 7

Appendix 2 (Cooling Data)

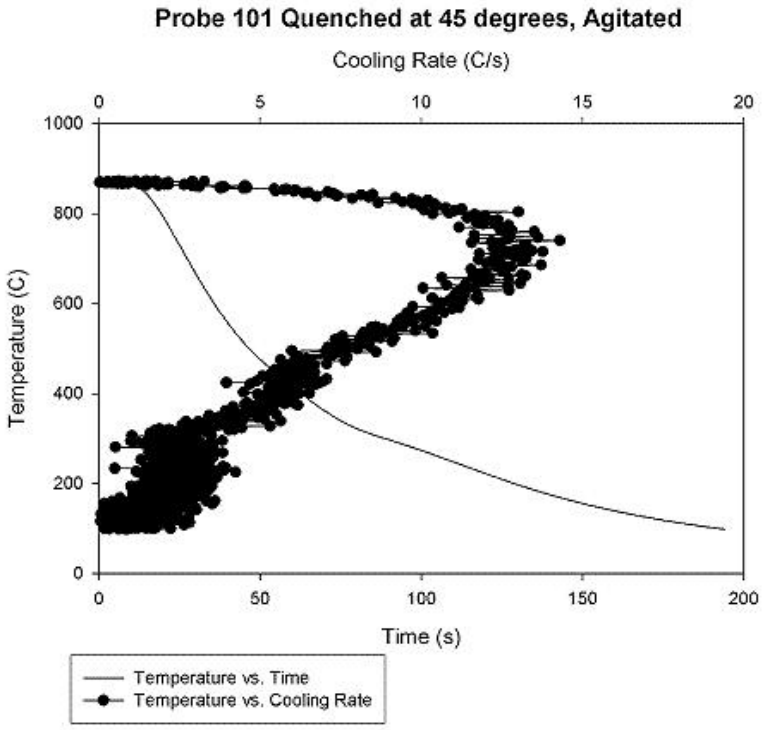

A2-1

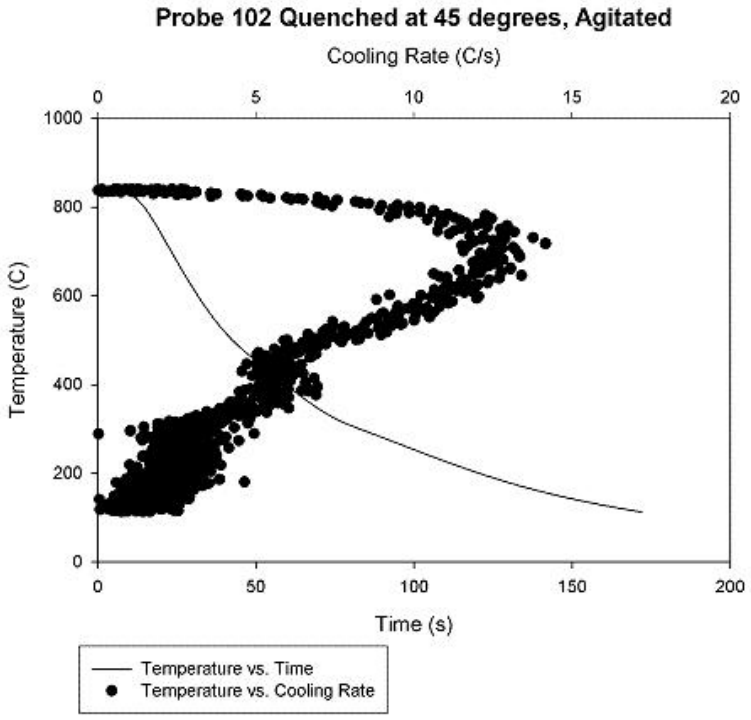

A2-2

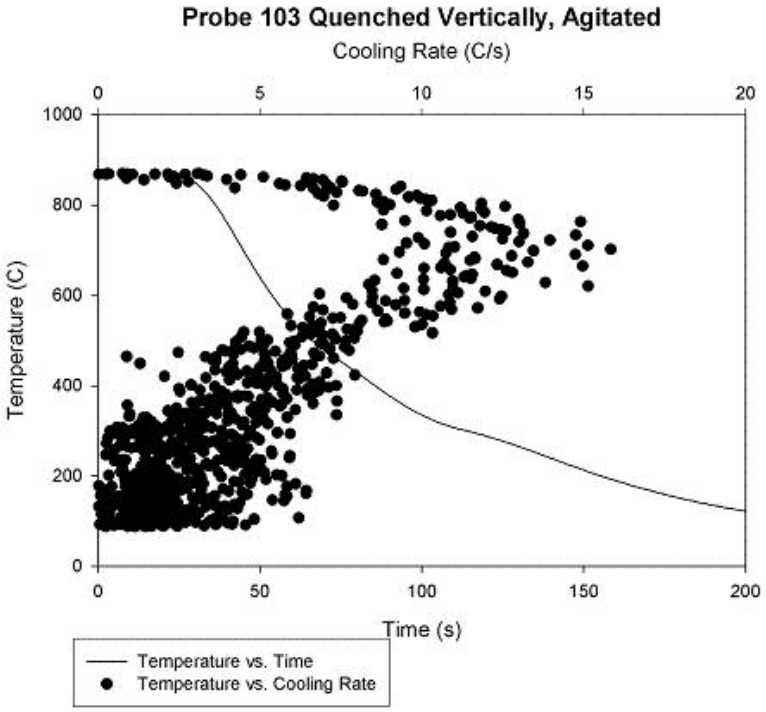
Probe 103 Quenched Vertically, Agitated
Cooling Rate (C/s)
0
5
10
15
20
1000
800
600
400
200
0
Temperature (C)
0
50
100
150
200
Time (s)
Temperature vs. Time
Temperature vs. Cooling Rate

A2-3

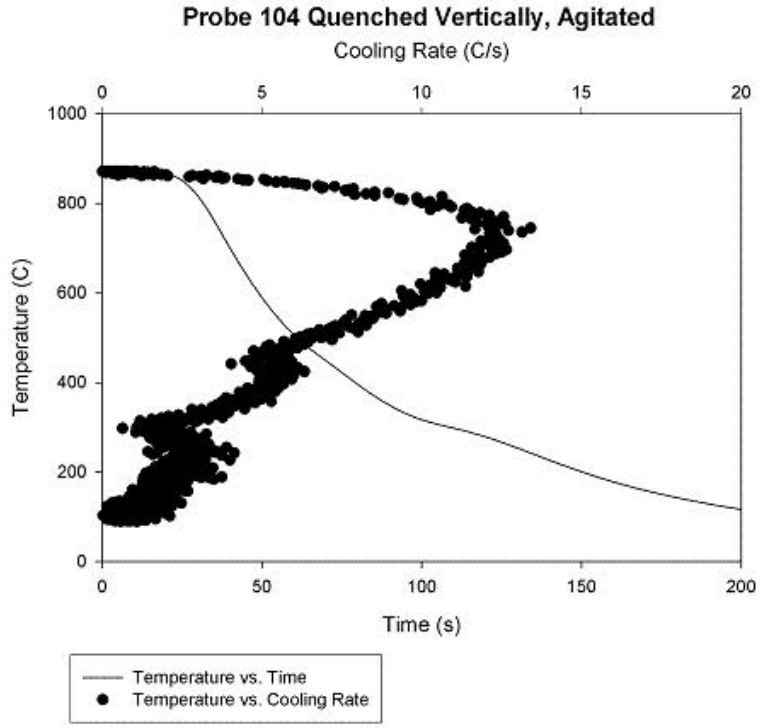
Probe 104 Quenched Vertically, Agitated
Cooling Rate (C/s)
0
5
10
15
20
1000
800
600
400
200
0
Temperature (C)
0
50
100
150
200
Time (s)
Temperature vs. Time
Temperature vs. Cooling Rate

A2-4

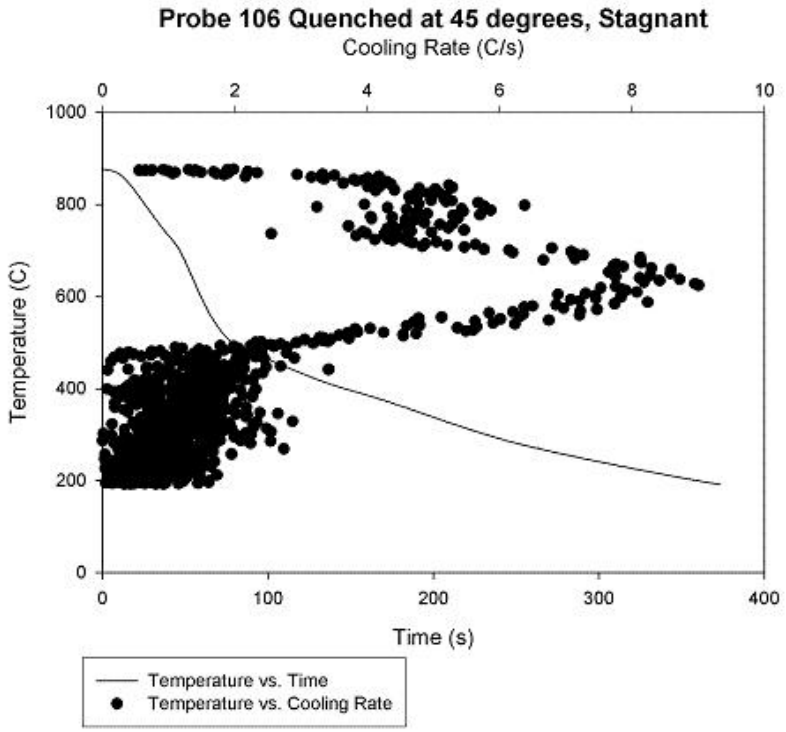
Probe 106 Quenched at 45 degrees, Stagnant
Cooling Rate (C/s)
0
2
4
6
8
10
1000
800
600
400
200
0
Temperature (C)
0
100
200
300
400
Time (s)
Temperature vs. Time
Temperature vs. Cooling Rate

A2-5

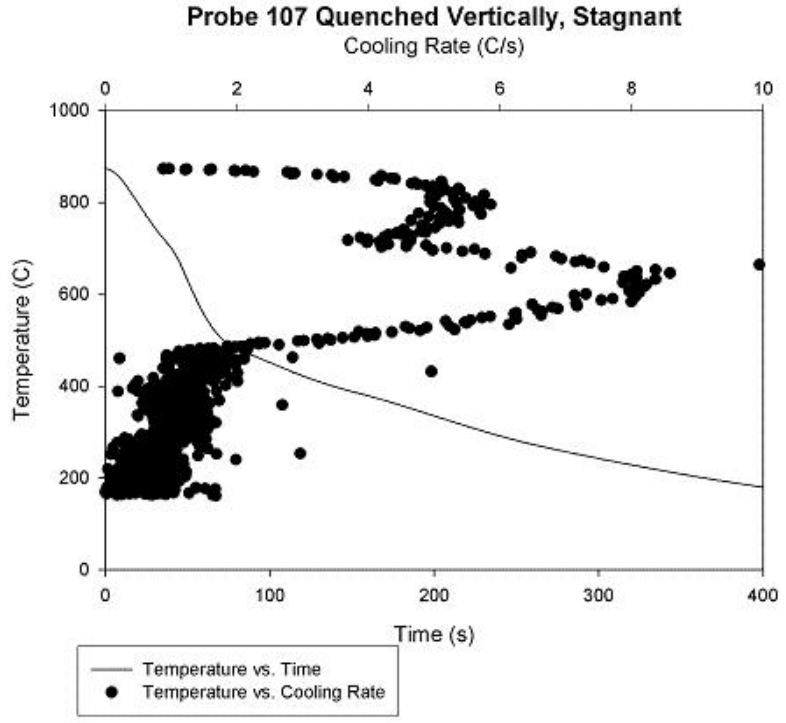
Probe 107 Quenched Vertically, Stagnant
Cooling Rate (C/s)
0
2
4
6
8
10
1000
800
600
400
200
0
Temperature (C)
0
100
200
300
400
Time (s)
Temperature vs. Time
Temperature vs. Cooling Rate

A2-6